2012

CFD and Heat Transfer Models of Baking Bread in a Tunnel Oven

Raymond Matthew Adamic
Cleveland State University

CFD AND HEAT TRANSFER MODELS OF BAKING BREAD IN A TUNNEL OVEN

RAYMOND MATTHEW ADAMIC

Bachelor of Arts

Case Western Reserve University

August, 1989

Bachelor of Mechanical Engineering

Cleveland State University

March, 1996

Master of Science in Mechanical Engineering

Cleveland State University

December, 2004

submitted in partial fulfillment of the requirement for the degree

DOCTOR OF ENGINEERING

at the CLEVELAND STATE UNIVERSITY

DECEMBER, 2012

This dissertation has been approved

for the Department of MECHANICAL ENGINEERING

and the College of Graduate Studies by

Dissertation Chairperson, Dr. Asuquo Ebiana

Department/Date

Dr. Rama Gorla

Department/Date

Dr. Majid Rashidi

Department/Date

Dr. Hanz Richter

Department/Date

Dr. Ulrich Zurcher

Department/Date

ACKNOWLEDGEMENTS

First, I would like to thank Dr. Asuquo Ebiana for being my advisor during the past eight years I have been in the Doctor of Engineering program at Cleveland State University. I thank Dr. Ebiana for being my Dissertation Committee Chairperson.

Second, I would like to thank my Dissertation Committee members for their suggestions on my research. These members are: Dr. Rama Gorla, Dr. Majid Rashidi, Dr. Hanz Richter, and Dr. Ulrich Zurcher.

I thank Patsy Donovan in the Mechanical Engineering Department for helping me with the office-related tasks.

I thank my family for their support of my academic goals.

This work was supported in part by an allocation of computing time from the Ohio Supercomputer Center.

CFD AND HEAT TRANSFER MODELS OF BAKING BREAD IN A TUNNEL OVEN

RAYMOND MATTHEW ADAMIC

ABSTRACT

The importance of efficiency in food processing cannot be overemphasized. It is important for an organization to remain consumer- and business-oriented in an increasingly competitive global market. This means producing goods that are popular, of high quality and low cost for the consumer.

This research involves studying existing methods of baking bread in a common type of industrial oven. - the single level bread baking tunnel oven. Simulations of the oven operating conditions and the conditions of the food moving through the oven are performed and analyzed using COMSOL, an engineering modeling, design and simulation software. The simulation results are compared with results obtained using MATLAB (a high-level programming language), theoretical analyses and/or results from literature.

The most important results from this research are the attainment of the temperature distribution and moisture content of the bread, and the temperature and velocity flow fields within the oven. More specifically, similar values for the temperature rise of a 0.1 m × 0.1 m × 1 m model dough/bread were attained for analytical results, MATLAB, COMSOL (using a volumetric heat source), and COMSOL (using heat fluxes from analytical calculation); these values are 41.1 K, 39.90 K, 41.45 K, and 41.46 K, respectively. Similarly, the temperature rise of the dough/bread from a 2-D COMSOL

model (using appropriate inputs for this and all models in this research) is found to be 25.39 K, which has a percent difference of - 44.4 % from the MATLAB result of 39.90 K. The moisture loss of the bread via analytical (and MATLAB) calculation is found to be 0.0423 kg water lost per hour, which is within the literature values of 0.030 and 0.25488 kg water lost per hour. The velocity flow fields within the (open) oven for the dimensional free (natural) convection COMSOL simulation show a qualitatively correct rising of the air due to the buoyancy forces imposed by the heating elements. The flow fields within the (closed) oven for the nondimensional free convection COMSOL simulation show the qualitatively correct regions of cellular flow caused by the hot (heating element area) and cold regions of the domain.

TABLE OF CONTENTS

Page

NOMENCLATURE

A	area (m^2)
A_i	area of surface i (m^2)
A_j	area of surface j (m^2)
A_s	area of surface (m^2)
A_1	area of small object (m^2)
A_1	area of surface 1 (m^2)
A_2	area of surface 2 (m^2)
B	boundary
c	heat capacity (J/kg ·°C or J/kg· K)
c	concentration of the species (mol/m^3) or (kg/m^3)
c_b	outside air (bulk) moisture concentration (kg/m^3)
c_S	humid heat of air-water vapor mixture (J/kg·K)
C	heat capacity (J/kg ·°C or J/kg· K)
C	constant of integration
C_m	specific moisture capacity
C_p	specific heat at constant pressure (J/kg ·°C or J/kg· K)
D	diffusion coefficient (m^2/s)
D_h	hydraulic diameter (m)
D_m	surface moisture diffusivity (m^2/s)
E_{bi}	black body emissive power of surface i (W/m^2)
E_i	emissive power of surface i (W/m^2)
f_0	normal stress (Pa)

F	source term (N/m^3)
F_{amb}	ambient view factor
F_{ij}	fraction of radiation leaving surface i that is intercepted by surface j
F_{ji}	fraction of radiation leaving surface j that is intercepted by surface i
g	acceleration due to gravity (m/s^2)
G	incoming radiative heat flux, or irradiation (W/m^2)
G	air mass velocity ($kg/h \cdot m^2$)
G_m	mutual irradiation, arriving from other boundaries in the (COMSOL) model (W/m^2)
G_i	irradiation upon surface i (W/m^2)
h	convective heat transfer coefficient ($W/m^2 \cdot K$) or ($W/m^2 \cdot C$)
h_C	convective heat transfer coefficient ($W/m^2 \cdot K$)
h_m	mass transfer coefficient ($kg/m^2 \cdot s$)
h_R	radiation heat transfer coefficient ($W/m^2 \cdot K$)
h_T	heat transfer coefficient ($W/m^2 \cdot K$)
H	humidity (kg H_2O vapor/kg dry air)
H_S	saturation humidity (kg H_2O vapor/kg dry air)
H_S	surface humidity (kg H_2O vapor/kg dry air)
i	an arbitrary surface
$\boldsymbol{I}$	identity matrix
j	an arbitrary surface
J	radiosity (W/m^2)
J_i	radiosity of surface i (W/m^2)

k	coefficient of heat conduction (W/m· °C or W/m· K)
k	thermal conductivity (W/m· °C or W/m· K)
k	degree of polynomial
k_c	mass transfer coefficient (m/s)
k_m	moisture conductivity (kg/m·s)
k_y	mass transfer coefficient (kg mol/s·m^2)
k'_y	mass transfer coefficient (kg mol/s·m^2 mol fraction)
k_S	thermal conductivity of the solid (W/m·C) or (W/m·K)
L	distance (m)
L	characteristic length (m)
L	residual vector
m	mass (kg)
$\dot{m}$	mass flow rate (kg/s)
M	constraint residual
M_A	molecular weight of chemical *A* (which is water) (kg/kg mol)
M_B	molecular weight of chemical *B* (which is air) (kg/kg mol)
$\boldsymbol{n}$	normal vector
N	number of surfaces in an enclosure
N_A	mass flux (kg mol of chemical *A* (which is H_2O) evaporating/s·m^2)
N_F	constraint force Jacobian matrix
p	absolute pressure (pressure above absolute zero pressure) (N/m^2)
p	node point

p_0	boundary pressure (Pa)
P	point
P	perimeter (m)
Pr	Prandtl number
q	heat flux on (COMSOL) Surface-to-Surface boundary
q	energy per unit time (W)
q	rate of convective heat transfer from gas stream to wick (W)
q	rate of heat transfer (W)
q_C	convective heat transfer (W)
q_i	radiation leaving surface i (W)
$q_{i\,j}$	radiation leaving surface i that is intercepted by surface j (W)
q_K	conduction heat transfer (W)
q_R	radiant heat transfer (W)
q_{rad}	heat transfer rate by radiation (W)
$\dot{q}$	volume heat source (W/m^3)
Q	heat source (J)
Q	energy absorbed (J)
R	drying rate (kg H_2O/ hour·m^2)
R_C	rate of drying in the constant rate drying period (kg H_2O/hour·m^2)
Ra	Rayleigh number
Ra_L	Rayleigh number at characteristic length
t	time (s)
t_0	initial time (s)

T	transpose
T	temperature (°C or K)
T	dry bulb temperature (°C or K)
T_{amb}	ambient temperature (K)
T_c	low (cold) temperature
T_f	film temperature (°C or K)
T_h	high temperature
T_i	temperature of surface *i* (°C or K)
T_i	initial temperature (°C or K)
T_{inf}	oven air temperature (°C or K)
T_j	temperature of surface *j* (°C or K)
T_0	temperature of boundary (°C or K)
T_0	initial temperature (°C or K)
T_R	temperature of radiating surface (°C or K)
T_s	temperature of surface (°C or K)
T_S	temperature of surface (°C or K)
T_w	temperature of wall (°C or K)
T_W	wet bulb temperature (°C or K)
T_0	boundary temperature (°C or K)
T_0	initial temperature (°C or K)
T_0	reference temperature (°C or K)
T_1	temperature of small object (K)

T_1	temperature of surface 1 (K)
T_2	temperature of the surroundings (K)
T_2	temperature of surface 2 (K)
T_2	temperature of enclosure (K)
T_∞	temperature of unheated fluid (°C or K)
T_∞	temperature of environment (°C or K)
$T_{m,n}^{p}$	temperature at time p at node (m,n)
$\boldsymbol{u}$	velocity vector (m/s)
u	fluid velocity in the x-direction (m/s)
u	dependent variable
U	freestream velocity (m/s)
U	degree of freedom
U	solution vector
U_0	boundary velocity
U_K	overall heat transfer coefficient (W/m^2·K)
v	air-water vapor velocity parallel to surface (m/s)
v	fluid velocity in the y-direction (m/s)
v_H	specific volume of the air-water vapor mixture (m^3/kg)
w_i	width of surface i (m)
w_j	width of surface j (m)
W_i	width of surface i divided by distance between surface i and j
W_j	width of surface j divided by distance between surface i and j
x	horizontal space coordinate in Cartesian system (m)

x_{BM}	log mean inert mole fraction of chemical *B*
X	free moisture (kg H_2O/kg dry solid)
y	vertical space coordinate in Cartesian system (m)
y	mole fraction of water vapor in the gas
y_S	mole fraction of water vapor at the surface
y_W	mole fraction of water vapor in the gas at the surface
z	depth space coordinate in Cartesian system (m)
z_M	thickness of metal (m)
z_S	thickness of solid (m)

Greek letters

$\alpha=(k/Pc_p)$	thermal diffusivity (m^2/s)
α_i	absorptivity of surface *i*
β	volumetric thermal expansion coefficient (1/K)
Δ	change
∇	differential term: $\frac{\partial}{\partial x}i + \frac{\partial}{\partial y}j + \frac{\partial}{\partial z}k$
ε	surface emissivity
ε_i	total hemispherical emissivity of surface *i*
ε_j	total hemispherical emissivity of surface *j*
ε_1	total hemispherical emissivity of surface 1
ε_2	total hemispherical emissivity of surface 2

λ	latent heat of vaporization of the water (J/kg)
λ_W	latent heat of vaporization at T_W (kJ/kg)
Λ	Lagrange multiplier vector
Ω	domain
ρ	density (kg/m^3)
ρ_i	reflectivity of surface *i*
ρ_0	reference density (kg/m^3)
ρ_∞	density of unheated fluid (kg/m^3)
φ	basis function
rho	density (kg/m^3)
τ	time (s)
σ	Stefan-Boltzman constant (5.670×10^{-8} W/m^2·K^4)
μ	dynamic viscosity (Pa·s)
ν	kinematic viscosity (m^2/s)

LIST OF TABLES

LIST OF FIGURES

CHAPTER I

INTRODUCTION

In this chapter, an introduction of the research will be outlined. First, the purpose and motivation for the research will be described, then the description of the problem will be discussed. Since this research involves bread baking in an oven, the oven will described, followed by a description of the food (bread). Finally, a review of the literature will be discussed.

1.1 Purpose and motivation

The purpose of this research is to simulate existing bread baking conditions (e.g. temperature, air velocity, moisture/humidity), and to provide a ready-made algorithm that the food processing industry can use to help optimize current baking procedures and build new processes for bread baking.

Using COMSOL (a multi-physics software) one can model the geometry and physical properties of the raw material that is either placed in a food container or directly on an oven conveyor belt. This can help the food baking industry simulate an actual food item-before, during, and after baking.

Similarly, COMSOL can be used to model the geometry and material of an actual oven. The oven may be any length, width, and height. The oven may be single or multi-level, with or without a conveyor belt, etc. This capability can help designers produce, for example, an oven best suited to factory space constraints.

Because COMSOL has fluid flow/heat transfer/mass transfer interfaces, practically any oven operating conditions can be simulated. This can, for example, help engineers determine the optimal heating conditions for whatever food may be baked in the oven. These simulations can be used to determine if the food will be cooked enough (not undercooked) and not burned (not overcooked). These computational fluid dynamics (CFD) simulations can tell workers in the field if a proposed food/food container/oven combination will work in reality. The costs of current processes in the baking industry can be reduced by performing optimum CFD simulations on existing raw materials and equipment.

Therefore, using COMSOL's geometry and physics capabilities, an engineer in the food baking industry can study what has been done in this research, and customize this work to suit his/her technical goals. This implies that a worker in this field can look at the method (algorithm) of creating the food, container and oven models in COMSOL to enable him/her solve the technical problems of baking bread in industrial ovens. For example, an engineer may want to produce a new bread product, and possibly need to adjust oven operating conditions to bake this; a COMSOL analysis will help him with this situation.

Thus the motivation for this study is to show researchers in the bread baking industry that COMSOL can be used to effectively create virtual food, container, and oven components. Furthermore, these models can be employed to improve existing processes, and be used to create new processes and products.

1.2 Description of problem

The problem involves the CFD simulation and analysis of baking bread moving on a conveyor belt through single-level tunnel oven. A one-level tunnel oven and the bread within the oven will be modeled using COMSOL; where possible, these models will be compared with corresponding MATLAB, analytical, and/or literature models.

1.3 Description of oven

Tunnel ovens are the most commonly used type of ovens in the cereal foods (bread, cake, biscuits, etc.) baking industry; this is because of a tunnel oven's high production capacity and minimal energy consumption (Baik et al., 2000 a). Schematics of two types of tunnel ovens – a gas fired band oven and an electric powered mold oven – are illustrated in Figure 1.1; from the schematics, one can see that these two types of tunnel

ovens have a number of features in common. The basic geometry of each oven is rectangular. The oven chamber may be from 1-30 meters in length, approximately 1 meter wide, and about 0.2 meter tall; Figure 1.1 is used to arrive at approximate dimensions for the model ovens in this research. Each tunnel oven is divided into multiple zones, where the top and bottom heating elements (either gas or electric) can be adjusted to meet the heating requirements of the food being baked. For example, biscuit dough can be heated gradually so that crust formation does not occur prematurely (which may lead to a biscuit that is too small in volume).

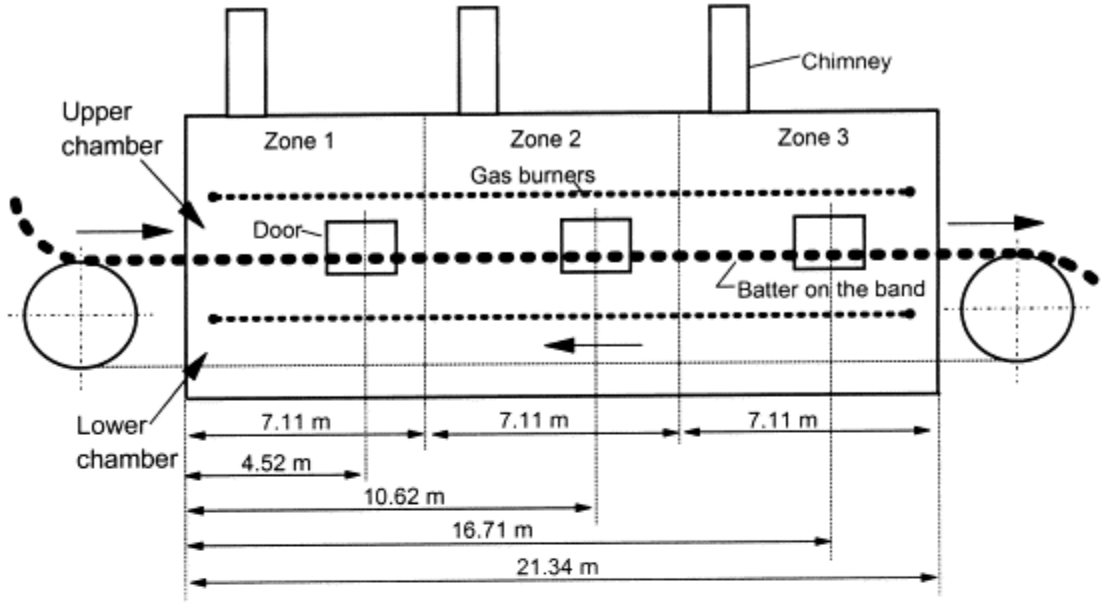

a. Gas fired band oven

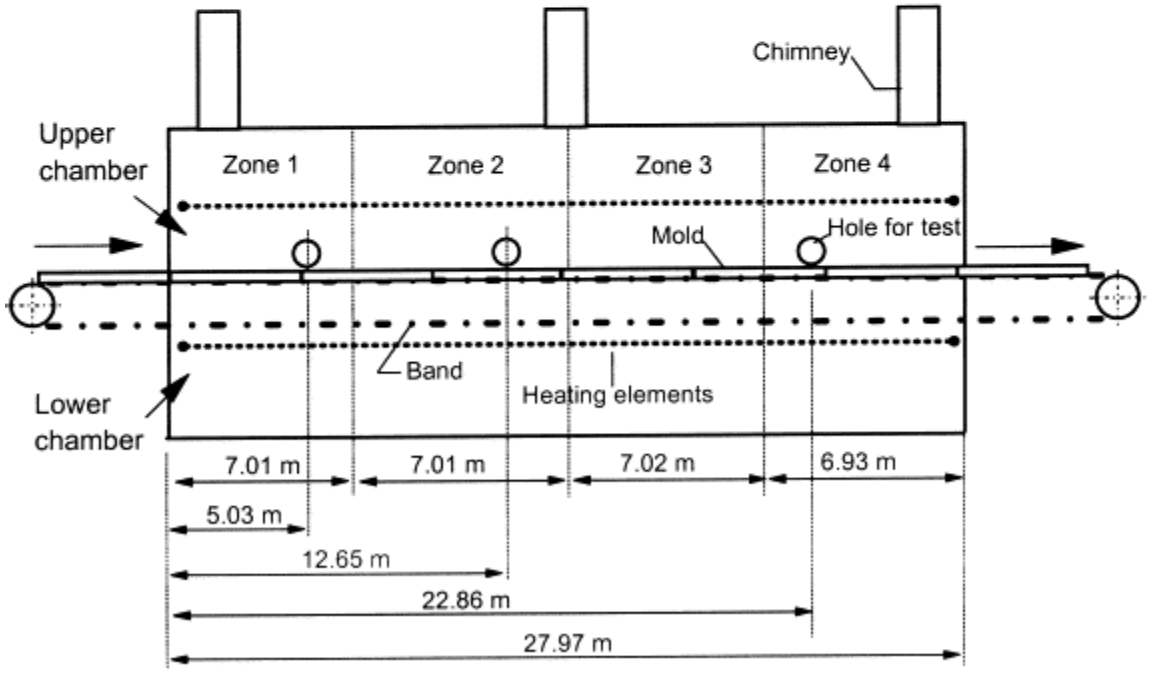

b. Electric powered mold oven

Figure 1.1: Schematics of (a) gas fired band oven and (b) electric powered mold oven (Baik et al., 2000 a).

1.4 Description of food

For one loaf of French bread, the ingredients used are: 370 g of wheat flour, 200 g of water, 6 g of salt, 6 g of sugar, 6 g of oil, and 4.5 g of dry yeast (Thorvaldsson & Janestad, 1999).

The thermal properties of dough and bread (Zhou et al, 2007) are presented in Table 1.1. It must be noted that the porosity (which can be 0.7, according to Thorvaldsson & Janestad, 1999) of bread affects its density: the higher the porosity, the lower the density.

Table 1.1: Thermal properties of dough and bread (Zhou et al, 2007)

Temperature (°C)	Density (kg/m^3)	Specific Heat ($J\ kg^{-1}\ °C^{-1}$)	Thermal Conductivity ($W\ m^{-1}\ °C^{-1}$)
28 (301.15 K)	420	2883	0.20
120 (393.15 K)	380	1470	0.07
227 (500.15 K)	340	1470	0.07

The dimensions of the bread in this research are approximations of that used by Zhou et al (2007), unless otherwise stated.

1.5 Literature review

A review of the current literature provides information on the vast use of computational fluid dynamics in the food processing industry. Some examples from Sun (2007) of the use of CFD in this industry include simulations of refrigerated compartments that store food (Cortella, 2007), simulations that analyze machines that dry food (Mirade, 2007), and simulations that involve the thermal sterilization of food (Ghani & Farid, 2007). Another example of the extensive use of CFD in this industry involves some of the different methods of heating of food: frying (Wang & Sun, 2006), grilling (Weinhold, 2008), and baking (Mirade et al., 2004, Therdai et al., 2003, 2004 a,b). Since the proposed dissertation involves the CFD simulation of the baking of food in a certain type of oven, the research was focused on this major area.

Specifically, the literature review centered on experimental and CFD work involving the baking of cereal products (such as bread, cake, biscuits, and cookies) in single-level tunnel ovens. Piazza and Masi (1997) performed experiments on cookies baked in a tunnel oven, finding that the crispness (based on a human tester's sensory perception) of a cookie is linearly related to its modulus of elasticity. Baik et al. (2000 a) studied the baking of cakes in a tunnel oven, focusing on the baking conditions (such as temperature, air velocity, and humidity). Later, Baik et al. (2000 b) focused their experimental research on the quality parameters (such as texture, pH, and surface color) of the cakes being baked in the tunnel oven. Broyart and Trystram (2003) used an artificial neural network to predict color and thickness of biscuits from the (experimentally obtained) input information of biscuit moisture content and temperature.

In a CFD study, Mirade et al. (2004) used the software Fluent to characterize the air temperature and velocity profiles in a biscuit baking tunnel oven.

An aspect of this research effort is the motion of the containers of food within the oven. Hassanien et al. (1999) point out the example of the boundary layer along material handling conveyors. In their paper, they used a boundary condition that describes the velocity of the moving plate in the solution of the governing equations.

Similar to other engineering disciplines, there are both challenges and breakthroughs in the field of industrial food baking processes. The problems encountered by researchers in this field include the uncertainties in the physical properties of the baked food, and modeling the volumetric change (expansion) of the baking food. With respect to the uncertainties in the physical properties of the food being baked, Wong et al. (2006) pointed out the importance of the temperature variation of heat capacity, density and thermal conductivity of the bread dough and that density and heat capacity were most influential on the accuracy of the simulation results. The CFD software used in their research was unable to properly simulate density variation with temperature.

Concerning the volumetric change of the baking food, Mondal and Datta (2008) suggest that computational modeling of the deformation of the food in the oven would definitely be appropriate in past CFD simulations that did not include this change. Therdai et al (2004 a) found that sandwich bread height is 85 % that of the dough height.

The breakthroughs in CFD modeling in the food baking industry include high correlation of CFD simulations with experimental measurements, and improvements in CFD simulation techniques such as parallel processing. With respect to the correlation of CFD simulation with experiments, Marcotte (2007) found that the correlation between

their CFD and experimental results of the temperature distribution in an oven was 0.92, with an average relative error of 7 %.

Concerning CFD simulation improvements, it is known that a person using COMSOL on the Ohio Supercomputing Center's (OSC) Glenn Cluster can use that software with parallel processing capability. A COMSOL mph (mutiphysics) file, thought previously to be unusable in parallel on the OSC system, was found by Larson (2010) to be usable in parallel on that system.

The uniqueness of this author's research is the extensive use of analytical computation compared with COMSOL simulations to model radiation upon bread in an industrial food processing oven; thus far, the literature review has not yielded any similar simulations. Also, the current literature search has yielded no simulations of COMSOL being compared with extensive analytical computation to model bread moisture loss within food processing ovens.

CHAPTER II

THEORETICAL FORMULATION

In this chapter, the physics relevant to food baking in a single-level tunnel oven will be examined. More specifically, the physics involved in bread baking will be outlined; this involves radiation within the oven, heat conduction within the bread and between the bread and its container (or the conveyor belt upon which the bread rests), oven natural (free) convection (both dimensional and nondimensional), oven forced convection, and moisture loss from the bread.

This chapter provides the equations that are used to effect the calculations in Chapter III, and that are the basis for the 2-D and 3-D COMSOL models in Chapters VI and VII, respectively. This chapter also presents the equations necessary for the MATLAB models in Chapter X.

2.1 Radiation theoretical formulation

The analytical and COMSOL radiation theoretical formulations are discussed in this section; the analytical calculations in Sections 3.1 are based on these formulations.

2.1.1 Analytical radiation theoretical formulation

Radiation has been found to be the dominant mode of heat transfer in the tunnel oven simulated in this research (Chhanwal et al, 2010, Mirade et al, 2004); therefore radiation is the most extensively studied mode of heat transfer in the simulations.

The radiation problem of bread baking in an oven essentially is radiation exchange between diffuse, gray surfaces in an enclosure. The following methodology of radiation formulation (including equations and figures) is derived from Incropera and Dewitt (1990). A schematic of an enclosure is shown in Figure 2.1.Surfaces *i* and *j* are arbitrary surfaces. Here, surface *i* is receiving radiation in the form of irradiation G_i from surfaces 1, 2, and *j*; radiation is leaving surface *i* in the form of radiosity J_i. The net radiation leaving surface *i* is q_i .*T*, *A*, and ε are the temperatures, areas, and emissivities of the surfaces, respectively; the terms in this figure will be subsequently described.

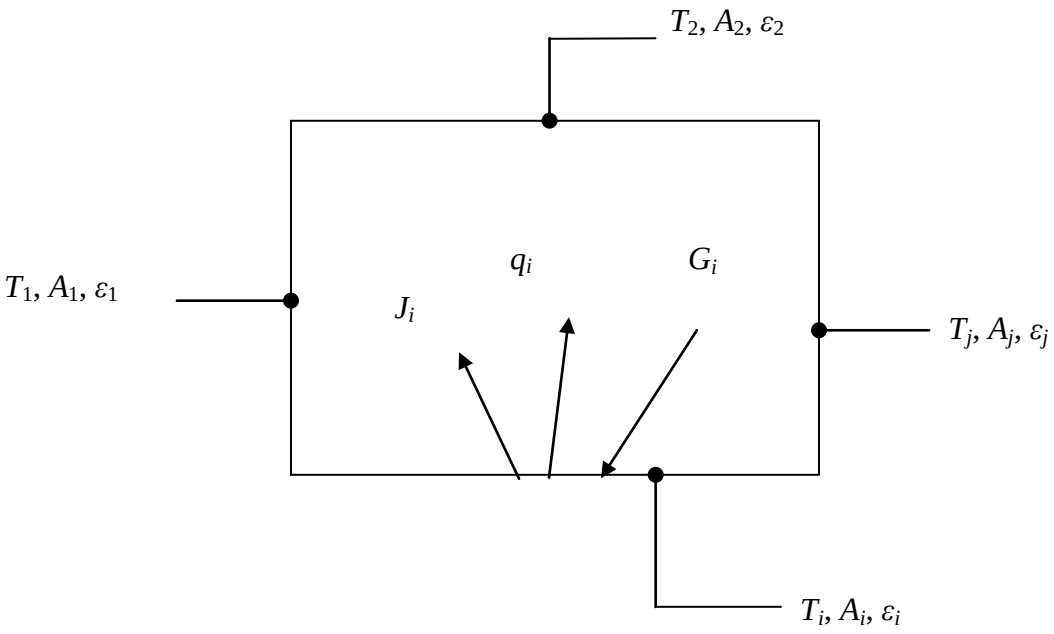

Figure 2.1: Radiation exchange in an enclosure of diffuse, gray surfaces

Diffuse means that the radiation emitted, reflected and/or absorbed by a surface is independent of direction. A gray surface is one for which the emissivity and absorptivity are independent of wavelength for the spectral region under consideration. In order to arrive at a relation describing radiation exchange between surfaces in an enclosure, the net radiation from a single surface will first be described (see Figure 2.2).

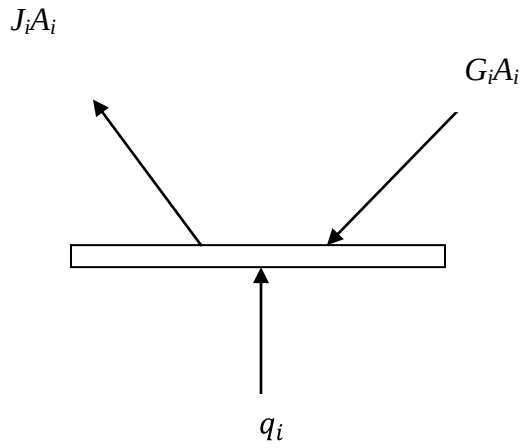

Figure 2.2: Radiative balance according to Equation (2-1)

The net rate q_i at which radiation leaves surface i involves the difference between surface i radiosity J_i , and surface i irradiation G_i :

$$q_i = A_i(J_i - G_i) \qquad (2-1)$$

where A_i is the surface area of surface i, and G_i is the radiation arriving at surface i from the other surfaces in the enclosure.

The surface radiosity is defined as follows:

$$J_i \equiv E_i + \rho_i G_i \qquad (2-2)$$

where E_i is the emissive power of surface i and ρ_i is the reflectivity of surface i.

For an opaque, diffuse, gray surface:

$$\alpha_i + \rho_i = 1 \qquad (2-3)$$

where α_i is the absorptivity of surface i. An opaque surface is one in which no radiation is transmitted through the surface.

Multiplying Equation (2-3) by G_i :

$$\alpha_i G_i + \rho_i G_i = G_i \qquad (2-4)$$

Substituting Equation (2-2) into Equation (2-1):

$$q_i = A_i(E_i + \rho_i G_i - G_i) \qquad (2-5)$$

Substituting Equation (2-4) into Equation (2-5); (see Figure 2.3):

$$q_i = A_i(E_i - \alpha_i G_i) \qquad (2-6)$$

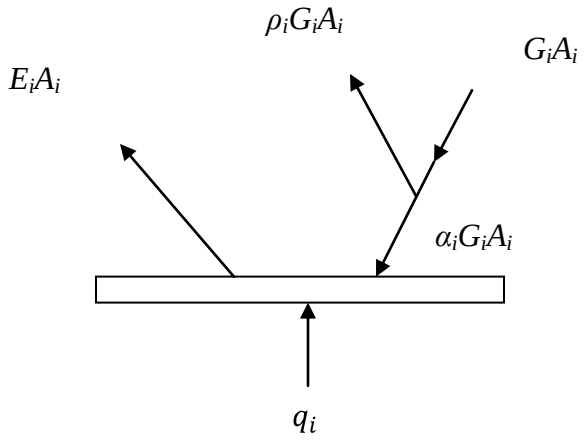

Figure 2.3: Radiative balance according to Equation (2-6)

For an opaque, diffuse, gray, surface:

$$\rho_i = 1 - \alpha_i = 1 - \varepsilon_i \qquad (2-7)$$

where ε_i is the total hemispherical emissivity of surface i. ε_i is defined as:

$$\varepsilon_i(T) = \frac{E_i(T)}{E_{bi}(T)} \qquad (2-8)$$

where E_{bi} is the blackbody emissive power of surface *i*, and *T* denotes the temperature of the surface. A blackbody surface is a perfect emitter and absorber. The equation for E_{bi} is:

$$E_{bi} = \sigma T_i^4 \qquad (2-9)$$

where σ is the Stefan-Boltzman constant.

Substituting Equations (2-8) and (2-7) into Equation (2-2):

$$J_i = \varepsilon_i E_{bi} + (1-\varepsilon_i) G_i \qquad (2-10)$$

Solving Equation (2-10) for G_i and substituting into Equation (2-1):

$$q_i = A_i \left(J_i - \frac{J_i - \varepsilon_i E_{bi}}{1-\varepsilon_i} \right) \qquad (2-11)$$

Rearranging terms on the right side of Equation (2-11):

$$q_i = \frac{E_{bi} - J_i}{(1-\varepsilon_i)/\varepsilon_i A_i} \qquad (2-12)$$

In order to utilize Equation (2-12), the surface radiosity J_i must be known. To determine this variable, it is necessary to consider the radiation exchange between the surfaces in the enclosure.

To compute the radiation exchange between any two surfaces (for example, surface *i* and surface *j*), the concept of a view factor must first be introduced. The view factor F_{ij} is the fraction of radiation leaving surface *i* that is intercepted by surface *j*. In this research a geometry the same and similar to that shown in Figure 2.4 is employed:

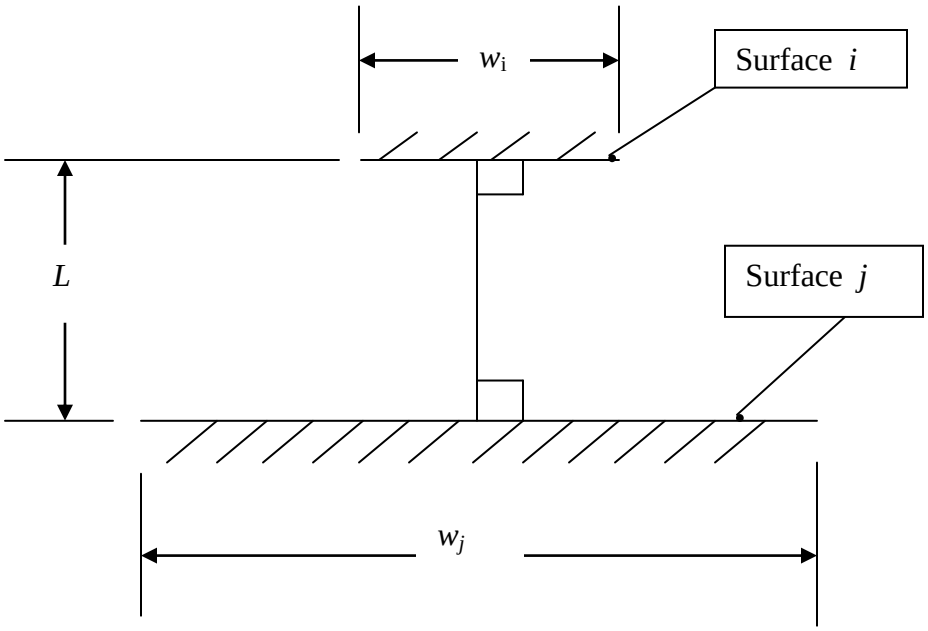

Figure 2.4: Parallel plates with midline connected by perpendicular line

Figure 2.4 shows a schematic of parallel plates with their midline connected by a perpendicular line. For the geometry shown in Figure 2.4 the view factor (from Table 13.1 in Incropera & Dewitt, 1990) is as follows:

$$F_{ij} = \frac{\left[\left(W_i + W_j\right)^2 + 4\right]^{1/2} - \left[\left(W_j - W_i\right)^2 + 4\right]^{1/2}}{2W_i} \qquad (2-13)$$

where $W_i = w_i/L$, $W_j = w_i/L$, w_i is the width of surface i, w_j is the width of surface j, and L is the perpendicular distance between the two surfaces. Equation (2-13) is

calculated from the view factor integral (a general expression for the view factor) in Incropera and Dewitt (1990). Later in this radiation theoretical formulation there will be needed a view factor summation rule for surfaces exchanging radiation in an *N*-sided enclosure (from Equation 13.4 in Incropera and Dewitt, 1990):

$$\sum_{j=1}^{N} F_{ij} = 1 \qquad (2-14)$$

Referring back to Figure 2.1, the irradiation of surface *i* can be evaluated from the radiosities of all the surfaces in an enclosure. From the definition of the view factor, it follows that the total rate at which radiation reaches surface *i* from all other surfaces, including *i* (see Figure 2.1), is:

$$A_i G_i = \sum_{j=1}^{N} F_{ji} A_j J_j \qquad (2-15)$$

At this point another important view factor relation must be introduced. This relation is called the reciprocity relation, and is:

$$A_i F_{ij} = A_j F_{ji} \qquad (2-16)$$

where A_i is the area of surface *i*, and A_j is the area of surface *j*, and F_{ji} is the fraction of radiation reaching surface *i* from surface *j*.

Substituting Equation (2-16) into (2-15):

$$A_i G_i = \sum_{j=1}^{N} A_i F_{ij} J_j \qquad (2-17)$$

Dividing both sides of Equation (2-17) by A_i and substituting into Equation (2-1) for G_i :

$$q_i = A_i \left(J_i - \sum_{j=1}^{N} F_{ij} J_j \right) \qquad (2-18)$$

Substituting the summation rule, Equation (2-14), into Equation (2-18):

$$q_i = A_i \left(\sum_{j=1}^{N} F_{ij} J_i - \sum_{j=1}^{N} F_{ij} J_j \right) \qquad (2-19)$$

Therefore:

$$q_i = \sum_{j=1}^{N} A_i F_{ij} \left(J_i - J_j \right) = \sum_{j=1}^{N} q_{ij} \qquad (2-20)$$

Combining Equations (2-12) and (2-20) results in:

$$\frac{E_{bi} - J_i}{(1-\varepsilon_i)/\varepsilon_i A_i} = \sum_{j=1}^{N} \frac{\left(J_i - J_j \right)}{\left(A_i F_{ij} \right)^{-1}} \qquad (2-21)$$

Once the surface radiosity J_i is calculated from the Equation (2-21), the heat transferred to the material (container or dough/bread) can be determined from Equation (2-12), and the temperature rise of the material can then be determined from the heat diffusion equation. This will be discussed in the analytical conduction theoretical formulation section (Section 2.2.1).

2.1.2 Radiation theoretical formulation in COMSOL

COMSOL uses equations very similar to those described earlier in the analytical theoretical formulation section. In order to model radiation exchange between surfaces it is necessary to use COMSOL's Heat Transfer Module, which is an add-on to the

COMSOL Multiphysics software. This theoretical formulation is outlined in COMSOL (2010 c).

COMSOL's Surface-to-Surface boundary condition feature handles surface to surface radiation with view factor calculation. The heat flux q on the Surface-to-Surface boundary is:

$$q = \varepsilon(G - \sigma T^4) \qquad (2-22)$$

where ε is the surface emissivity, G is the incoming heat flux, or irradiation, σ is the Stefan-Boltmann constant, and T is the temperature of the boundary. G is calculated according to the following equation:

$$G = G_{\mathrm{m}} + F_{\mathrm{amb}}\sigma T_{\mathrm{amb}}^4 \qquad (2-23)$$

where G_{m} is the mutual irradiation arriving from other boundaries in the model, F_{amb} is the ambient view factor whose value is equal to fraction of the field of view that is not covered by other boundaries, and T_{amb} (ambient temperature) is the assumed far-away temperature in the directions included in T_{amb}.

The Surface-to-Surface Radiation implementation requires evaluation of G_{m}. The incident radiation at one point in the boundary is a function of the exiting radiation, or radiosity, J, at every other point in view. The radiosity, in turn, is a function of G_{m}, which results in an implicit radiation balance:

$$J = (1-\varepsilon)\{G_{\mathrm{m}}(J) + F_{\mathrm{amb}}\sigma T_{\mathrm{amb}}^4 + \varepsilon\sigma T^4\} \qquad (2-24)$$

The view factor calculation in COMSOL for this research uses the Hemicube (see Figure 2.5) method, which can be thought of as rendering digital images of the model geometry in five different directions (in 3-D; in 2-D, only three directions are needed) and counting the pixels in each mesh element to determine its view factor.

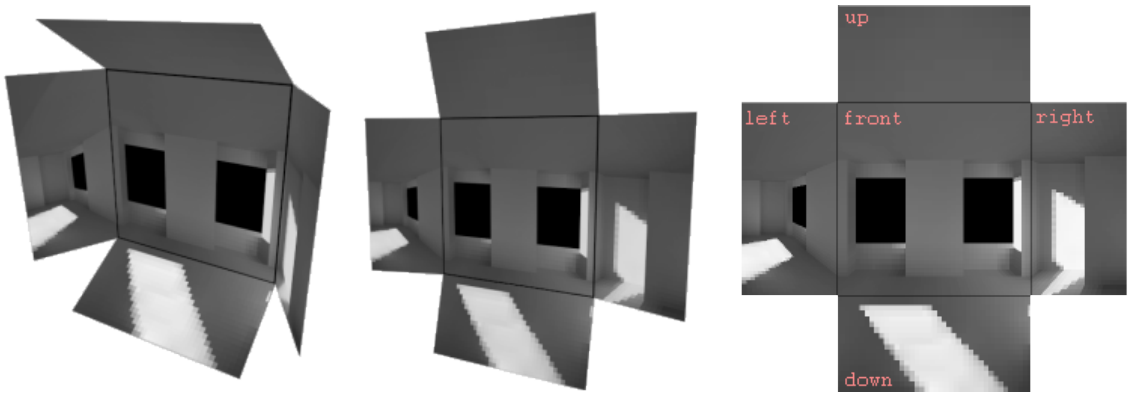

Figure 2.5: A hemicube unfolded (from Hemicube (computer graphics), 2007)

The boundaries in the COMSOL model are assigned as follows: the faces of the heating elements facing the dough/bread are specified as having a constant temperature

$$T = T_0 \qquad (2-25)$$

and the surfaces of the material and heating elements are each specified as having an appropriate emissivity ε.

The faces of the heating elements not facing the dough/bread may be specified as having a constant temperature, or as being insulated according to Equation (2-26):

$$\boldsymbol{n} \cdot (k\nabla T) = 0 \qquad (2-26)$$

2.2 Conduction theoretical formulation

The analytical and COMSOL theoretical formulations are discussed in this section.

2.2.1 Analytical conduction theoretical formulation

In order to find out how much the material (in this research, the container or dough/bread) rises in temperature, the heat diffusion equation (Incropera & DeWitt, 1990) is employed:

$$\frac{\partial}{\partial x}\left(k\frac{\partial T}{\partial x}\right)+\frac{\partial}{\partial y}\left(k\frac{\partial T}{\partial y}\right)+\frac{\partial}{\partial z}\left(k\frac{\partial T}{\partial z}\right)+\dot{q}=\rho C_p\frac{\partial T}{\partial t} \qquad (2-27)$$

where *x*, *y* , and *z* are the horizontal, vertical, and depth space coordinates in the Cartesian system, respectively, *T* is the variable temperature, *k* is the thermal conductivity of the material, $\dot{q}$ is the volume heat source, ρ is the density of the material, C_p is the specific heat (at constant pressure) of the material, and *t* is the variable time. In order to solve this equation a number of assumptions are to be made (the validity of these assumptions will be shown in Tables 11.1 and 11.2). First, it is assumed that there is no variation in temperature in the *x*, *y* , and *z* directions; this causes the first three terms on the left side of Equation (2-27) to be equal to zero. This results in the following equation:

$$\dot{q}=\rho C_p\frac{\partial T}{\partial t} \qquad (2-28)$$

Since T is now only a function of *t*, the ∂ operator can be changed to d.

$$\dot{q}=\rho C_p\frac{dT}{dt} \qquad (2-29)$$

Multiplying both sides of Equation 2-29 by dt:

$$\dot{q}dt=\rho C_p dT \qquad (2-30)$$

Rearranging:

$$\rho C_p dT = \dot{q}dt \qquad (2-31)$$

Multiplying both sides of Equation (2-31) by ρC_p:

$$dT = \frac{\dot{q}}{\rho C_p} dt \qquad (2-32)$$

Integrating, assuming $\frac{\dot{q}}{\rho C_p}$ is constant (to simplify the calculation):

$$\int dT = \frac{\dot{q}}{\rho C_p} \int dt \qquad (2-33)$$

$$T = \frac{\dot{q}}{\rho C_p} t + C \qquad (2-34)$$

where C is the constant of integration. Noting that at $t = t_0$, $T = T_0$

$$T_0 = \frac{\dot{q}}{\rho C_p} t_0 + C \qquad (2-35)$$

Rearranging:

$$T_0 - \frac{\dot{q}}{\rho C_p} t_0 = C \qquad (2-36)$$

$$T = \frac{\dot{q}}{\rho C_p} t + T_0 - \frac{\dot{q}}{\rho C_p} t_0 \qquad (2-37)$$

$$T - T_0 = \frac{\dot{q}}{\rho C_p} t - \frac{\dot{q}}{\rho C_p} t_0 \qquad (2-38)$$

$$T - T_0 = \frac{\dot{q}}{\rho C_p} (t - t_0) \qquad (2-39)$$

Since $\Delta T = T - T_0$ and $\Delta t = t - t_0$:

$$\Delta T = \frac{\dot{q}}{\rho C_p} \Delta t \qquad (2-40)$$

Multiplying both sides of Equation (2-40) by ρC_p , and rearranging, results in the following equation:

$$\dot{q}\,\Delta t = \rho C_p\,\Delta T \qquad (2-41)$$

where ΔT is the temperature change of the container.

In order to apply Equation (2-41) to the material being heated by the oven heating elements in this research, the heat flux of the heating elements upon the material is originally assumed to be equivalent to the heat source term $\dot{q}$.

2.2.2 Conduction theoretical formulation in COMSOL

COMSOL uses Equation (2-27) to calculate the temperature distribution in the material (container or dough/bread).

2.2.3 Conduction theoretical formulation for MATLAB

This formulation (including equations and figures) is outlined in Holman (1990). At the boundary of a solid, a convection resistance to heat flow is usually involved. In general, each convective boundary condition must be handled separately, depending on the geometric shape under consideration. The case of a flat wall will be considered as an example. For the one-dimensional system shown in Figure 2.6 one can make an energy balance at the convection boundary such that

$$-kA\frac{\partial T}{\partial x}\Big]_{\text{wall}} = hA(T_w - T_\infty) \qquad (2-42)$$

where *k* is the thermal conductivity of the material, *A* is the area of the wall, *T* is temperature, *x* is the horizontal space coordinate, *h* is the convective heat transfer

coefficient, T_w is the temperature at the wall, and T_∞ is the temperature of the surroundings.

The finite-difference approximation is given by

$$-k\frac{\Delta y}{\Delta x}(T_{m+1} - T_m) = h\Delta y(T_{m+1} - T_\infty) \qquad (2-43)$$

where y is the vertical space coordinate (which cancels out here due to the 1-D assumption),

or

$$T_{m+1} = \frac{T_m + (h\Delta x/k)T_\infty}{1 + h\Delta x/k} \qquad (2-44)$$

To apply this condition, one should calculate the surface temperature T_{m+1} at each time increment and then use this temperature in the nodal equations for the interior points of the solid. This is only an approximation because the heat capacity of the element of the wall at the boundary has been neglected. This approximation will work fairly well when a large number of increments in x are used because the portion of the heat capacity that is neglected is then small compared with the total. One may take the heat capacity into account in a general way by considering the two-dimensional wall of Figure 2-7 (where q is the heat transfer) exposed to a convective boundary condition. A transient energy balance is made on the node (m, n) by setting the sum of the energy conducted and convected into the node equal to the increase in the internal energy of the node. This is shown as

$$k\Delta y\left(\frac{T_{m-1,n}^{p}-T_{m,n}^{p}}{\Delta x}\right)+\ k\frac{\Delta x}{2}\left(\frac{T_{m,n+1}^{p}-T_{m,n}^{p}}{\Delta y}\right)+$$

$$k\frac{\Delta x}{2}\left(\frac{T_{m,n-1}^{p}-T_{m,n}^{p}}{\Delta x}\right)+h\Delta y\left(T_{\infty}-T_{m,n}^{p}\right)=\rho c\frac{\Delta x}{2}\Delta y\left(\frac{T_{m,n}^{p+1}-T_{m,n}^{p}}{\Delta\tau}\right) \qquad (2-45)$$

where p is the current time step, ρ is the density of the material, c is the specific heat of the material, and τ is the time increment.

If $\Delta x = \Delta y$, the relation for $T_{m,n}^{p+1}$ becomes

$$T_{m,n}^{p+1}=\frac{\alpha\Delta\tau}{(\Delta x)^2}\left\{2\frac{h\Delta x}{k}T_{\infty}+2T_{m-1,n}^{p}+T_{m,n+1}^{p}+T_{m,n-1}^{p}\right.$$

$$\left.+\left[\frac{(\Delta x)^2}{\alpha\Delta\tau}-2\frac{h\Delta x}{k}-4\right]T_{m,n}^{p}\right\} \qquad (2-46)$$

where α is the thermal diffusivity of the material.

The corresponding one-dimensional relation is

$$T_{m}^{p+1}=\frac{\alpha\Delta\tau}{(\Delta x)^2}\left\{2\frac{h\Delta x}{k}T_{\infty}+2T_{m-1}^{p}+\left[\frac{(\Delta x)^2}{\alpha\Delta\tau}-2\frac{h\Delta x}{k}-2\right]T_{m}^{p}\right\} \qquad (2-47)$$

The selection of the stabilization parameter $(\Delta x)^2/\alpha\ \Delta\tau$ is not as simple as it is for the interior node points because the heat-transfer coefficient influences the choice. It is still possible to choose the value of this parameter so that the coefficient of T_m^p or $T_{m,n}^p$ will be zero. The value for the one-dimensional case would be

$$\frac{(\Delta x)^2}{\alpha\Delta\tau}=2\left(\frac{h\Delta x}{k}+1\right) \qquad (2-48)$$

To ensure convergence of the one-dimensional numerical solution, all selections of the parameter $(\Delta x)^2/\alpha\ \Delta\tau$ must be restricted according to

$$\frac{(\Delta x)^2}{\alpha \Delta \tau} \geq 2\left(\frac{h\Delta x}{k} + 1\right) \qquad (2-49)$$

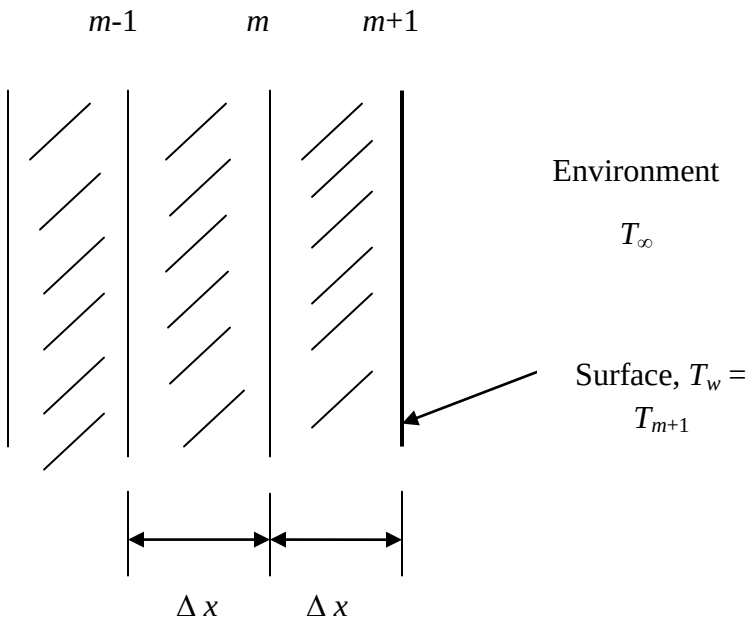

Figure 2.6: Nomenclature for numerical solution of unsteady-state conduction problem with convection boundary condition

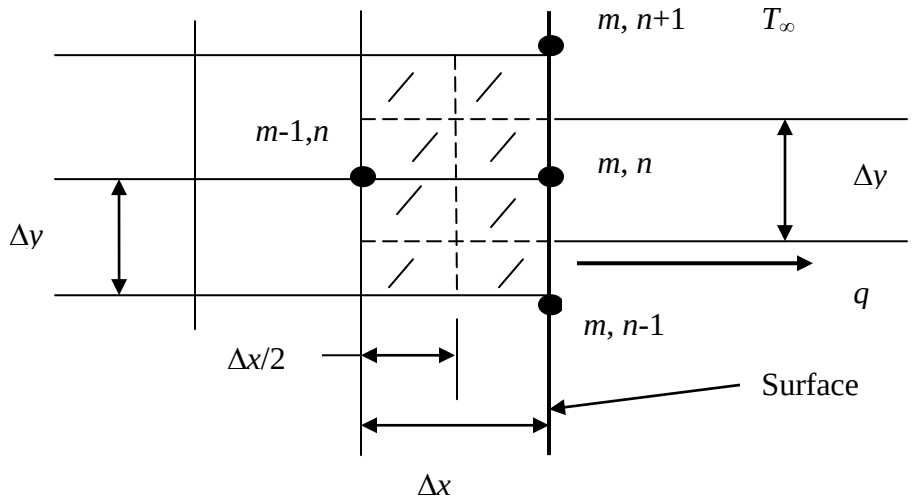

Figure 2.7: Nomenclature for nodal equation with convective boundary condition

2.3 Free (natural) convection theoretical formulation

The dimensional and nondimensional free (natural) convection theoretical formulation in COMSOL, and analytical formulation of the free convection flow regime will now be described.

2.3.1 Dimensional free (natural) convection theoretical formulation in COMSOL

This formulation is outlined in COMSOL (2010 b, e). The steady state Navier-Stokes equations (including the continuity equation) shown below govern the fluid flow within the room and oven enclosure:

$$\rho(\boldsymbol{u}\cdot\nabla)\boldsymbol{u} = -\nabla p + \nabla\cdot\mu(\nabla\boldsymbol{u}+(\nabla\boldsymbol{u})^{\mathrm{T}}) + F \qquad (2-50)$$

$$\nabla\cdot\boldsymbol{u} = 0 \qquad (2-51)$$

where ρ is the density of the fluid, $\boldsymbol{u}$ is the velocity vector, p is the pressure, μ is the dynamic viscosity of the fluid, and F is the source term. The superscript "T" is the transpose of the vector.

The volume force F is set to:

$$F = (\rho_\infty - \rho) * g \qquad (2-52)$$

where ρ_∞ is the density of the unheated fluid and g is the acceleration due to gravity. ρ is calculated according to the Boussinesq approximation:

$$\rho = \rho_\infty \left(1 - \frac{T - T_\infty}{T_\infty}\right) \qquad (2-53)$$

where T is the variable temperature of the fluid and T_∞ is the temperature of the unheated fluid. The Boussinesq approximation is desirable because it allows one to solve for the compressibility of air as a function of temperature (as opposed to pressure) only.

The fluid flow boundary conditions are as follows: the walls of the heating elements and the oven are specified as no-slip meaning the fluid velocity vector is 0, or

$$\boldsymbol{u} = 0 \qquad (2-54)$$

The boundaries of the room are specified as open, and the equation for this condition is:

$$\left(-p\boldsymbol{I} + \mu(\nabla \boldsymbol{u} + (\nabla \boldsymbol{u})^{\mathrm{T}})\right)\boldsymbol{n} = -f_0 \boldsymbol{n} \qquad (2-55)$$

where $\boldsymbol{I}$ is the identity matrix, $\boldsymbol{n}$ is the normal vector, and f_0 is the normal stress. For this research, f_0= 0, which means that there is nothing stopping the fluid from entering or exiting the boundary.

The heat balance within the room and oven enclosure is obtained via the conduction-convection equation:

$$\rho C_p \boldsymbol{u} \cdot \nabla T - \nabla \cdot (k \nabla T) = 0 \qquad (2-56)$$

where C_p is the specific heat of the fluid at constant pressure, k is the thermal conductivity of the fluid, and T is the temperature of the fluid.

The boundary conditions for the heat transfer of the natural convection formulation will now be presented. For the heating elements, the boundaries are specified as having a constant temperature of $T = T_0$. The boundaries of the oven walls are specified as insulated, meaning that there is no heat flux across the boundaries as shown in Equation (2-57):

$$\boldsymbol{n} \cdot (k \nabla T) = 0 \qquad (2-57)$$

2.3.2 Nondimensional free (natural) convection theoretical formulation in COMSOL

This formulation is outlined in COMSOL (2010 e). The incompressible Navier-Stokes equations (including the continuity equation) shown below govern the fluid flow within the room and oven enclosure:

$$\rho(\boldsymbol{u} \cdot \nabla)\boldsymbol{u} = -\nabla p + \nabla \cdot \mu(\nabla \boldsymbol{u} + (\nabla \boldsymbol{u})^{\mathrm{T}}) + \rho_0 \boldsymbol{g} \beta (T - T_0) \qquad (2-58)$$

$$\nabla \cdot \boldsymbol{u} = 0 \qquad (2-59)$$

where ρ is the density of the fluid, $\boldsymbol{u}$ is the velocity vector, p is the pressure, μ is the dynamic viscosity of the fluid, ρ_0 is the reference density, $\boldsymbol{g}$ is gravity acceleration, β is

the coefficient of volumetric thermal expansion, T is temperature, and T_0 is the reference temperature. In this model the Rayleigh number (*Ra*) is employed, and is defined as:

$$Ra = \frac{\left(C_p \rho^2 g \beta T L^3\right)}{(\mu k)} \qquad (2-60)$$

where C_p is the specific heat of the fluid, L is the length of a heating element, and k is the thermal conductivity. The Prandtl number (*Pr*) is also used in this model, and is defined as:

$$Pr = \frac{\mu C_p}{k} \qquad (2-61)$$

Specifying the body force in the *y*-direction for the momentum equation to F_y :

$$F_y = \left(\frac{Ra}{Pr}\right)(T - T_c) \qquad (2-62)$$

and the fluid properties to C_p=*Pr*, and ρ=μ=k=1 produces a set of equations with nondimensional variables p, $\boldsymbol{u}$, and T. T_c is the low (cold) temperature.

As in Section 2.3.1, the fluid flow boundary conditions are that the walls of the heating elements and the oven are specified as no-slip; this means the fluid velocity vector is 0, or

$$\boldsymbol{u} = 0 \qquad (2-63)$$

The boundaries of the room are also specified as no-slip (dissimilar to Section 2.3.1).

The heat balance within the room and oven enclosure is shown by the following equation:

$$\rho_0 C_P \boldsymbol{u} \cdot \nabla T - \nabla \cdot (k \nabla T) = 0 \qquad (2-64)$$

The boundary conditions for the heat transfer of the nondimensional natural convection formulation will now be presented. For the heating elements and oven walls, the boundaries are specified as each having a constant temperature of $T = T_0$. The boundaries of the room are specified as insulated, meaning that there is no heat flux across the boundaries as shown in Equation (2-65):

$$\boldsymbol{n} \cdot (k \nabla T) = 0 \qquad (2-65)$$

2.3.3 Analytical formulation of free convection flow regime

This formulation is outlined in Incropera and Dewitt (1990). In order to calculate whether the flow is laminar or turbulent, the Rayleigh number must be calculated. Here, we can use the same Rayleigh number calculation whether the top surface or bottom surface of a heating element is being considered. The sides of the heating elements are 0.01 m and are not considered to have a significant impact on the analysis at this point in the research. For a horizontal plate, the Rayleigh number is calculated as follows:

$$Ra_L = \frac{g\beta(T_s - T_\infty)L^3}{\nu\alpha} \qquad (2-66)$$

where T_s is the temperature of the heating element surface, T_∞ is the temperature of the unheated fluid, and L is the characteristic length of the heating element surface. The variable g is the acceleration due to gravity, and the variables β, ν, and α are the volumetric thermal expansion coefficient, kinematic viscosity, and thermal diffusivity of the fluid respectively. Here, all of the fluid properties are evaluated at the film temperature, given by:

$$T_f = \frac{T_s + T_\infty}{2} \qquad (2-67)$$

The variable β for ideal gases is defined as follows:

$$\beta = \frac{1}{T_f} \qquad (2-68)$$

For this geometry (horizontal flat plate), L is defined as:

$$L = \frac{A_s}{P} \qquad (2-69)$$

where A_s is the surface area of the plate, and P is the perimeter of the plate. At this point it must be stated that since this is a two-dimensional simulation, the depth of the plate must be specified: this (the third dimension) is 1 meter.

2.4 Forced convection theoretical formulation

The theoretical formulation for forced convection in COMSOL, and the analytical formulation of the forced convection flow regime will now be discussed.

2.4.1 Forced convection theoretical formulation in COMSOL

Forced convection is induced upon the food in the oven due to the suction of air through the exhaust chimneys. Forced convection is important to include in the research because it affects both heat transfer to the food, and moisture loss from the food.

This formulation is outlined in COMSOL (2010 b). The steady state Navier-Stokes equations (including the continuity equation) shown below govern the fluid flow within the oven:

$$\rho(\boldsymbol{u} \cdot \nabla)\boldsymbol{u} = -\nabla p + \nabla \cdot \mu(\nabla \boldsymbol{u} + (\nabla \boldsymbol{u})^{\mathrm{T}}) \qquad (2-70)$$

$$\nabla \cdot \boldsymbol{u} = 0 \qquad (2-71)$$

The boundary condition for the walls are specified as no slip, as shown in Equation (2-72):

$$\boldsymbol{u} = 0 \qquad (2-72)$$

The exhaust stack is specified with a normal inflow velocity of $-U_0$ as shown in Equation (2-73), meaning that fluid flow is exiting the oven:

$$U = -U_0 \qquad (2-73)$$

The outlet boundaries are specified as having a pressure of p_0, and no viscous stress:

$$p = p_0 \qquad (2-74)$$

$$\mu(\nabla \boldsymbol{u} + (\nabla \boldsymbol{u})^{\mathrm{T}})\boldsymbol{n} = 0 \qquad (2-75)$$

where p_0 is the specified pressure. In this model when the outlet boundaries are as specified above, this is equivalent to flow being drawn (suction) from a large container.

2.4.2 Analytical formulation of forced convection flow regime

This formulation is based on White (1986). In order to determine if the flow is laminar or turbulent, the Reynolds number *Re* is calculated:

$$Re = \frac{\rho U L}{\mu} \qquad (2-76)$$

where ρ is the density of the fluid, U is the velocity of the fluid, L is the characteristic length, and μ is the dynamic viscosity of the fluid. If *Re* is less than 2300, the flow is considered laminar; if *Re* is greater than 2300, flow is considered turbulent. However, the Reynolds number at which flow becomes turbulent can be delayed to much higher values for rounded entrances, smooth walls, and steady inlet streams. U is calculated by employing the conservation of mass equation:

$$\dot{m}_{top} = \dot{m}_{side} + \dot{m}_{side} \qquad (2-77)$$

where $\dot{m}_{top}$ and $\dot{m}_{side}$ are the mass flow rates through the top and sides of the oven, (see Figure 6.15) respectively. This equation can be expanded as:

$$(\rho UA)_{top} = (\rho UA)_{side} + (\rho UA)_{side} \qquad (2-78)$$

where ρ is the density of the fluid and A is the area of the cross section of the duct. Since air is considered to be incompressible and the openings of the duct are of equal area, Equation (2-78) reduces to:

$$(U)_{top} = 2(U)_{side} \qquad (2-79)$$

Solving for U_{side} :

$$U_{side} = 0.5\, U_{top} \qquad (2-80)$$

which means that the free stream air velocity through the sides of the oven are half of the free stream air velocity through the top of the oven.

In this research L is calculated as follows:

$$L = D_h = \frac{4A}{P} \qquad (2-81)$$

where D_h is the hydraulic diameter of the non-circular duct, A is the cross-sectional area, and P is the perimeter.

2.5 Moisture theoretical formulation

The analytical and COMSOL theoretical formulations are described in this section.

2.5.1 Analytical moisture theoretical formulation

The moisture theoretical formulation (including all equations and figures, except where noted) is derived from Geankoplis (2003). In this research, it is feasible to calculate the loss of moisture from the bread using a constant drying rate analysis. This means that the rate at which the bread loses moisture to the oven air does not change with time. According to Baik et al (2000 b), for cookie baking in a continuous oven the constant rate drying period occupies about 40 % of the baking time. Figure 2.8 shows a typical drying rate curve for constant drying conditions (R_C is shown in Equation (2-109)), and more specifically, the rate of drying curve as rate versus free moisture content. The free moisture is the moisture that can be removed by drying under the given percent relative humidity. In this figure the initial free moisture content is shown as Point *A*. When the bread at room temperature enters the hot oven there is an initial drying period when the drying rate is increasing (from Point *A* to *B*); this period is often small and can be neglected in most circumstances. From Point *B* to *C* is known as the constant rate drying period, and from Point *C* to *D*, the linear falling rate drying period. The falling rate drying period signifies the time when the drying rate is decreasing with time. From Point *D* to *E* is the nonlinear drying rate period; the falling rate periods will not be covered in this research, due to the fact they must be determined from data that has been produced experimentally.

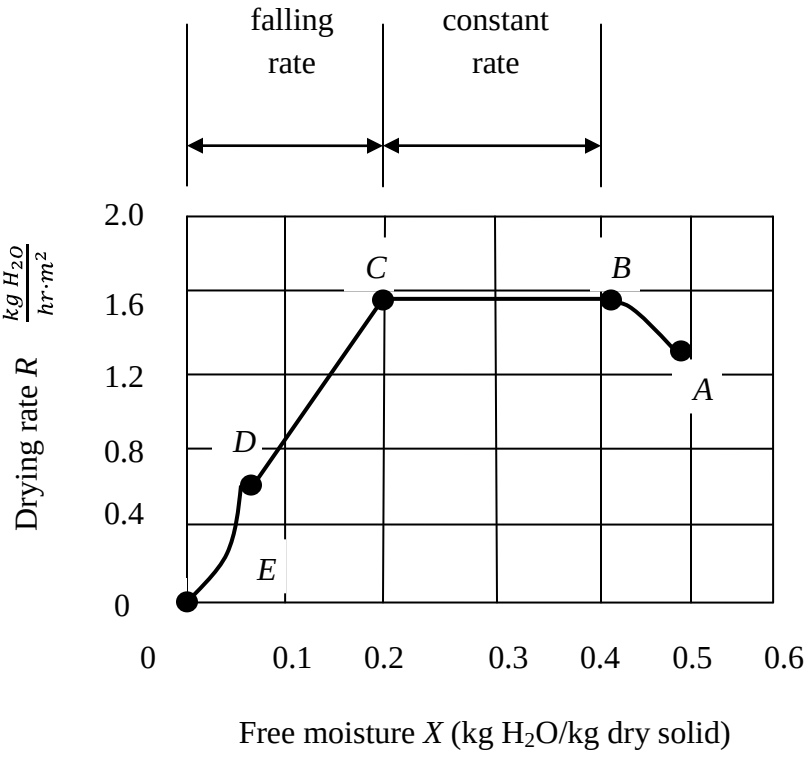

Figure 2.8: Typical drying rate curve for constant drying conditions: rate of drying curve as rate versus free moisture content

In Figure 2-9 a solid material (in this research, bread) is being dried by a stream of air as shown:

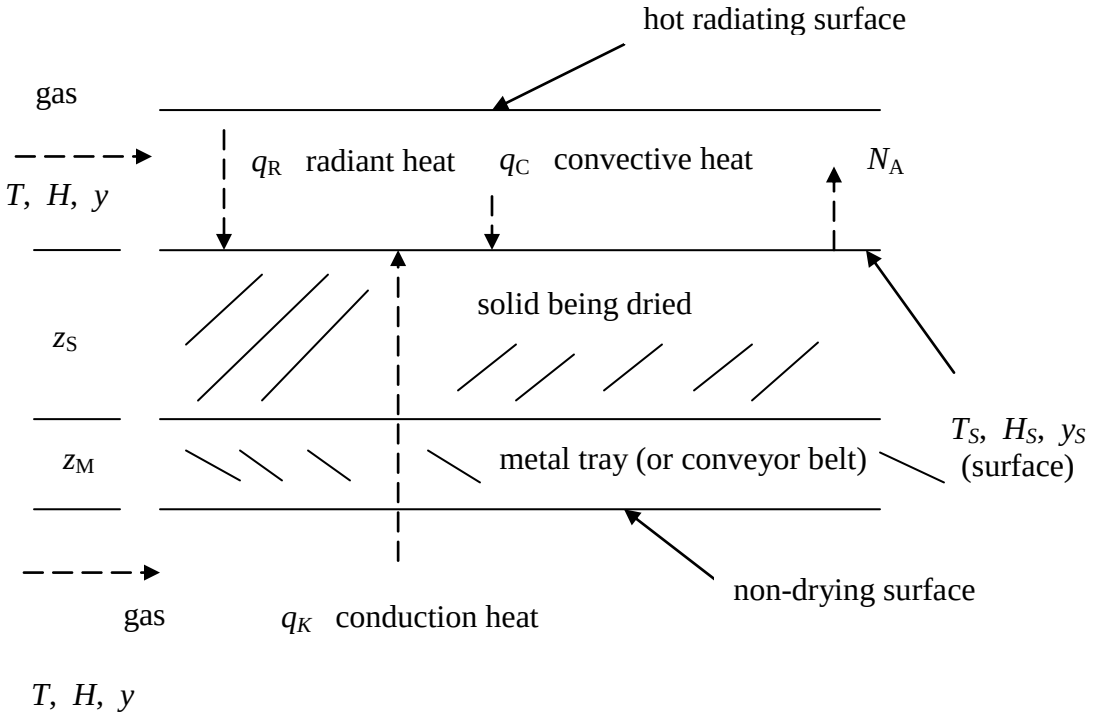

Figure 2.9: Heat and mass transfer in drying a solid from the top surface

The total rate of heat transfer to the drying surface is:

$$q = q_C + q_R + q_K \qquad (2-82)$$

where q_C is the convective heat transfer from the gas at temperature T to the solid surface at T_S, q_R is the radiant heat transfer from the radiating surface at T_R to the solid surface, and q_K is the rate of heat conduction from the bottom. The rate of convective heat transfer is as follows:

$$q_C = h_C(T - T_S)A \qquad (2-83)$$

where A is the exposed surface area and h_C is the convective heat transfer coefficient. For air flowing parallel to the drying surface, the leading edge of the surface can cause turbulence. The following equation can be used to calculate h_C when the air temperature range is 45-150°C and the air velocity range is 0.61-7.6 m/s:

$$h_c = 0.0204G^{0.8} \qquad (2-84)$$

where G is the air mass velocity, and is calculated as:

$$G = v\rho \text{ kg/hr·m}^2 \qquad (2-85)$$

where

$$\rho = \frac{1.0 + H}{v_H} \qquad (2-86)$$

where H is the specific humidity (also known as the humidity ratio) of the gas stream, and v_H is:

$$v_H = (2.83 \times 10^{-3} + 4.56 \times 10^{-3}H)T \text{ K} \qquad (2-87)$$

where T is the temperature of the gas stream. The coefficients in Equation (2-87) are derived from the ideal gas equation at standard temperature and pressure, using the molecular weights of air and water.

The radiant heat transfer is calculated as:

$$q_R = h_R(T - T_R)A \qquad (2-88)$$

where

$$h_R = \varepsilon(5.676)\frac{\left(\frac{T_R}{100}\right)^4 - \left(\frac{T_S}{100}\right)^4}{T_R - T_S} \qquad (2-89)$$

The derivation of Equation (2-89) will now be shown. For a small object (in this research, bread) in a large enclosure (in this research, the oven), the radiation to the small object is:

$$q = A_1\varepsilon\sigma(T_1^4 - T_2^4) \qquad (2-90)$$

where A_1 is the area of the small object, ε is the emissivity of the object, σ is the Stefan-Boltzman constant, T_1 is the temperature of the object, and T_2 is the temperature of the enclosure. A radiation heat transfer coefficient h_R can be defined as:

$$q_{\text{rad}} = h_R A_1(T_1^4 - T_2^4) \qquad (2-91)$$

where q_{rad} is the heat transfer rate by radiation.

Equating Equations (2-90) and (2-91), and solving for h_R results in Equation (2-92):

$$h_R = \varepsilon\sigma\frac{(T_1)^4 - (T_2)^4}{T_1 - T_2} \qquad (2-92)$$

Substituting the Stefan-Boltzman constant into Equation (2-92) yields Equation (2-93):

$$h_R = \varepsilon(5.676)\frac{\left(\frac{T_1}{100}\right)^4 - \left(\frac{T_2}{100}\right)^4}{T_1 - T_2} \qquad (2-93)$$

For the heat transfer by conduction from the bottom, the heat transfer is first by convection from the gas to the metal (in this research, the bread container and/or

conveyor belt), then by conduction though the metal, and finally conduction through the solid. The heat transfer by conduction is:

$$q_K = U_K(T - T_S)A \qquad (2-94)$$

where U_K is the overall heat transfer coefficient and is calculated as:

$$U_K = \frac{1}{\frac{1}{h_C} + \frac{z_M}{k_M} + \frac{z_S}{k_S}} \qquad (2-95)$$

where h_C is the convective heat transfer coefficient, z_M is the thickness of the metal, k_M is the thermal conductivity of the metal, z_S is the thickness of the solid, and k_S is the thermal conductivity of the solid.

The equation for the rate of mass transfer is:

$$N_A = k_y \frac{M_A}{M_B}(H_S - H) \qquad (2-96)$$

where N_A is the flux of chemical *A* (water, in this research), k_y is the mass transfer coefficient, M_A is the molecular weight of chemical *A*, M_B is the molecular weight of chemical *B* (air, in this case), H_S is the saturation humidity, and *H* is the humidity. k_y is defined as:

$$k_y = \frac{k'_y}{x_{BM}} \qquad (2-97)$$

where k'_y is the mass transfer coefficient with respect to mole fraction, and x_{BM} is the log mean inert mole fraction of chemical *B*. For a dilute mixture of chemical *A* in chemical *B*, $x_{BM} \cong 1.0$, and then $k_y \cong k'_y$.

Equation $(2-96)$ is derived by looking at the concept of wet bulb temperature. The method used to measure wet bulb temperature is illustrated in Figure 2.10, where a

thermometer is covered by a wick. The wick is kept wet with water and immersed in a flowing stream of air-water vapor having a temperature T (dry bulb temperature) and humidity H. At steady-state, water is evaporating from the wick to the gas stream.

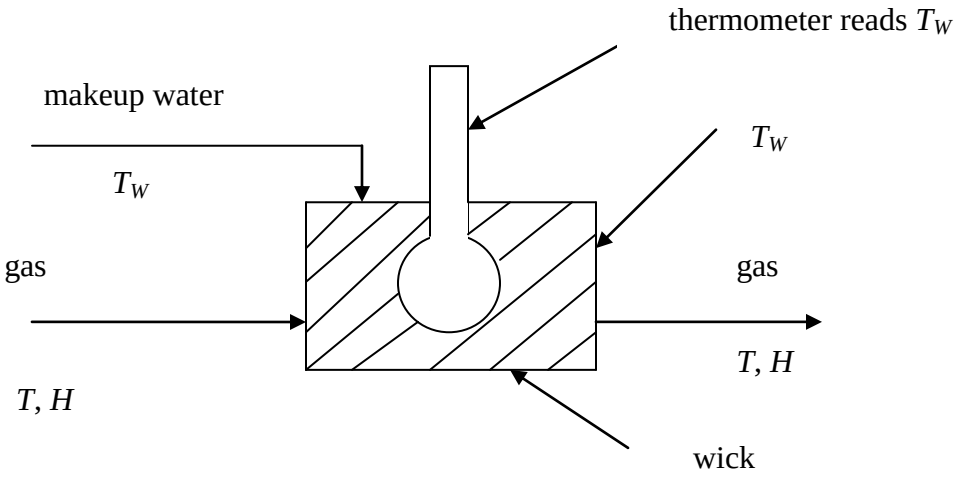

Figure 2.10: Measurement of wet bulb temperature

A heat balance on the wick can be made. The amount of heat lost by vaporization is:

$$q = M_A N_A \lambda_W A \qquad (2-98)$$

where M_A is the molecular weight of the water, N_A is the flux of water evaporating, A is the surface area, and λ_W is the latent heat of vaporization at T_W. The flux N_A is:

$$N_A = \frac{k'_y}{x_{BM}} (y_W - y) = k_y (y_W - y) \qquad (2-99)$$

where k'_y and x_{BM} are defined as before, y_W is the mole fraction of water vapor in the gas at the surface, and y is the mole fraction in the gas. As stated before, for dilute mixtures, $x_{BM} \cong 1.0$, and then $k_y \cong k'_y$. The relation between H and y is:

$$y = \frac{\frac{H}{M_A}}{\frac{1}{M_B} + \frac{1}{M_A}} \qquad (2-100)$$

where M_B is the molecular weight of air and M_A is the molecular weight of water. Since H is small, as an approximation:

$$y \cong \frac{HM_B}{M_A} \qquad (2-101)$$

Substituting Equation (2-101) into Equation (2-99):

$$N_A = \frac{k'_y}{x_{BM}}(y_W - y) = k_y(y_W - y) = k_y\left(\frac{H_W M_B}{M_A} - \frac{HM_B}{M_A}\right) \qquad (2-102)$$

$$N_A = k_y \frac{M_B}{M_A}(H_W - H) \qquad (2-103)$$

Substituting Equation (2-103) into (2-98):

$$q = M_B k_y \lambda_W (H_W - H) \qquad (2-104)$$

The rate of convective heat transfer from the gas stream at T to the wick at T_W is:

$$q = h(T - T_W)A \qquad (2-105)$$

where h is the heat transfer coefficient.

Equating Equation (2-104) to Equation (2-105) and rearranging:

$$\frac{H - H_W}{T - T_W} = -\frac{h/M_B k_y}{\lambda_W} \qquad (2-106)$$

The ratio $h/M_B k_y$ is known as the psychrometric ratio, and has been experimentally determined for water vapor-air mixtures to be approximately 0.96 to 1.005. The value of $h/M_B k_y$ can then be approximated to be equal to c_S , which is the humid heat of an air-water vapor mixture, and is the amount of heat required to raise the temperature of 1 kg dry air plus the water vapor present by 1K or 1°C . Essentially, this means that the adiabatic saturation lines on a humidity chart (see Figure 3.5) can also be used for wet bulb lines with reasonable accuracy. c_S is assumed constant over the temperature ranges encountered at 1.005 kJ/kg dry air · K and 1.88 kJ/kg water vapor. Therefore c_S is defined as follows:

$$c_S = (1.005 + 1.88H)10^3 \text{J/kg·K} \qquad (2-107)$$

Referring back to Figure 2.9, and rewriting Equation (2-98) in terms of the surface:

$$q = M_A N_A \lambda_S A \qquad (2-108)$$

Combining Equations (2-82), (2-83), (2-88), (2-94), (2-96), and (2-108):

$$R_C = \frac{q}{A\lambda_S} = \frac{(h_C + U_K)(T - T_S) + h_R(T_R - T_S)}{\lambda_S} = k_y M_B (H_S - H) \qquad (2-109)$$

where R_C is the rate of drying in the constant drying period. This period occurs when there is a sufficient amount of water on the surface of the solid. Equation (2-109) gives the surface temperature T_S greater than the wet bulb temperature T_W. The above equation can be rearranged to facilitate trial and error solution as follows:

$$\frac{(H_S - H)\lambda_S}{h_C/k_y M_B} = \left(1 + \frac{U_K}{h_C}\right)(T - T_S) + \frac{h_R}{h_C}(T_R - T_S) \qquad (2-110)$$

2.5.2 Moisture theoretical formulation in COMSOL

This theoretical formulation is outlined in COMSOL (2008). Moisture loss with heat transfer and convection from the dough/bread in this research is governed by Equation (2-111), which is Fick's law of diffusion, and Equation (2-112), which is the heat equation. These two equations are shown below:

$$\frac{\partial c}{\partial t} + \nabla \cdot (-D\nabla c) = 0 \qquad (2-111)$$

where c is the concentration of the species, t is time in seconds, and D is the diffusion coefficient.

$$\rho C_p \frac{\partial T}{\partial t} - \nabla \cdot (k\nabla T) = 0 \qquad (2-112)$$

where ρ is the density of the solid, C_p is the heat capacity of the solid, k is the thermal conductivity of the solid, and T is the temperature of the solid.

The boundary conditions for the diffusion are shown as Equations (2-113) and (2-114):

$$\boldsymbol{n} \cdot (-D\nabla c) = 0 \qquad (2-113)$$

where $\boldsymbol{n}$ is the vector normal to the boundary surface. This equation specifies that there is no mass transfer across the boundary.

$$\boldsymbol{n} \cdot (D\nabla c) = k_c(c_b - c) \qquad (2-114)$$

where k_c is the mass transfer coefficient, and c_b is the outside air (bulk) moisture concentration. This boundary condition describes the fact that there is mass (water) being transferred across the boundary.

The boundary conditions for the heat equation are Equations (2-115) and (2-116):

$$\boldsymbol{n} \cdot (-k\nabla T) = 0 \qquad (2-115)$$

The above equation specifies that there is no heat transfer across the boundary; that is, the boundary is adiabatic.

$$\boldsymbol{n} \cdot (k\nabla T) = h_T\left(T_{inf} - T\right) + \boldsymbol{n} \cdot (D_m \lambda \nabla c) \qquad (2-116)$$

where h_T is the heat transfer coefficient, T_{inf} is the oven air temperature, D_m is the moisture diffusion coefficient, and λ is the latent heat of vaporization of the water. The above equation describes the fact that there is a heat flux out of the dough/bread due to a vaporization of water from the surface.

The diffusion coefficient D and the mass transfer coefficient k_c are calculated according to Equations (2-117) and (2-118):

$$D = \frac{k_m}{\rho C_m} \qquad (2-117)$$

where k_m is the moisture conductivity, ρ is the density of the dough/bread, and C_m is the specific moisture capacity.

$$k_c = \frac{h_m}{\rho C_m} \qquad (2-118)$$

where h_m is the mass transfer coefficient in mass units.

The moisture loss without heat transfer and convection in the dough/bread is governed by Equation (2-111) only. The boundaries of everything but the dough bread are specified as having no flux, which is Equation (2-113).

CHAPTER III

ANALYTICAL CALCULATIONS

In this chapter numerical values will be substituted into the equations of the theoretical formulations from Chapter II, yielding analytical results. First, the radiation calculations are performed, followed by the conduction calculations. The natural (free) and forced convection regimes relevant to this research are then calculated, followed by the analytical calculations of moisture loss from the dough/bread.

3.1 Radiation analytical calculations

In this section, numerical values will be used in the governing equations from Section 2.1.1, yielding numerical results.

3.1.1 Distantly-spaced heating elements with container

An analytical solution was completed that corresponds to the COMSOL model shown in Section 6.1.1. In order to effect an analytical solution that corresponds to the COMSOL solution, a geometry appropriate to the COMSOL solution had to be found; this geometry is shown in Figure 2.4. This geometry is used in the analytical solution below.

For this analysis it is assumed that the container surface (which will be called Surface 2) is opaque, diffuse, and gray, and that the heater surface (which will be called Surface 1) and surroundings (which will be called Surface 3) are blackbody surfaces.

First, the values to calculate the view factor between the two surfaces can be substituted into Equation (2-13). The surfaces can be related to the COMSOL model (Section 6.1.1) as follows (see Figure 3.1): Surface *i* corresponds to Surface 2, which is the container surface; Surface *j* corresponds to Surface 1, which is the heating element surface.

$$W_i = W_2 = \frac{0.1\ \text{m}}{0.5\ \text{m} - 0.05\ \text{m} - 0.005\ \text{m}} = 0.2247 \qquad (3-1)$$

The values in Equation (3-1) can be explained as follows (see Figure 6.1: Radiation effect on surface of container: COMSOL geometry): the numerator is w_2 = 0.1 m, which is the width of the container; the denominator is L, which is the perpendicular distance between the surface of the container and the surface of the heating element. L is equal

to the vertical distance between the centers of the heating element and container, minus the vertical distance between the center and surface of the container, minus the vertical distance between the center and surface of the heating element.

$$W_j = W_1 = \frac{1\text{ m}}{0.5\text{ m} - 0.05\text{ m} - 0.005\text{ m}} = 2.247 \qquad (3-2)$$

The values in Equation (3-2) are determined similarly to Equation (3-1); only the numerator is different: the numerator is w_1 = 1 m, which is the width of the heating element.

Substituting the values W_1 and W_2 into Equation (2-13):

$$F_{21} = \frac{[(0.2247 + 2.247)^2 + 4]^{1/2} - [(2.247 - 0.2247)^2 + 4]^{1/2}}{2(0.2247)} = 0.7461 \qquad (3-3)$$

The above view factor F_{21} is necessary to calculate the radiation reaching Surface 2 (the container surface) from Surface 1 (the heating element surface). Later in this analytical section we will need the view factor F_{23}, which is the fraction of radiation leaving surface 2 (the container surface) that is intercepted by surface 3 (the surroundings). In order to calculate F_{23}, we use the view factor summation rule for surfaces exchanging radiation in an *N*-sided enclosure (Equation 2-14):

$$\sum_{j=1}^{N} F_{ij} = 1 \qquad (2-14)$$

For the current enclosure problem:

$$F_{21} + F_{22} + F_{23} = 1 \qquad (3-4)$$

In Equation (3-4), F_{21} and F_{23} have been previously explained; F_{22} is the fraction of radiation leaving surface 2 (the container surface) that is intercepted by surface 2 (the container surface). Since surface 2 is not convex, F_{22} = 0. Substituting the known view factors into Equation (3-4):

$$0.7461 + 0 + F_{23} = 1 \qquad (3-5)$$

$$F_{23} = 0.2539 \qquad (3-6)$$

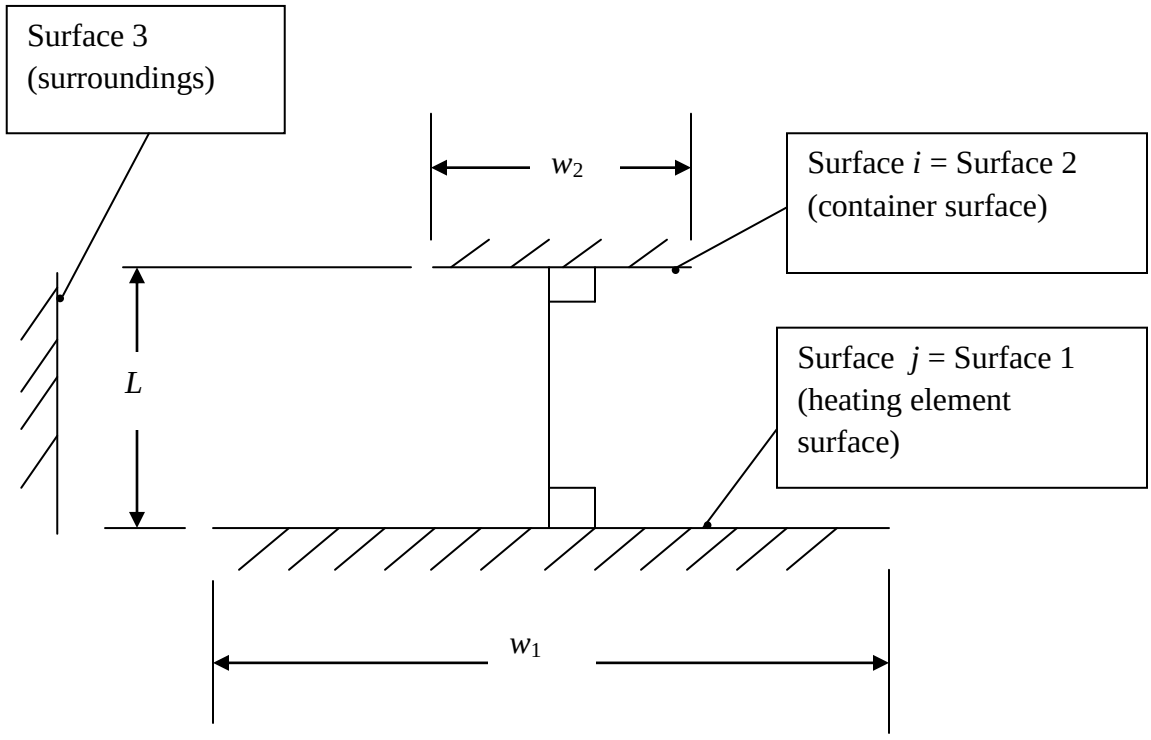

Figure 3.1: Surfaces 1 (heating element), 2 (container), 3 (surroundings)

Now we are ready to apply the foregoing analysis to find the amount of radiation that surface 2 (the container surface) intercepts. This will allow us to calculate the amount of energy the container material absorbs, which will then enable us to determine the temperature rise in the container material. The amount of energy the container material absorbs is given by applying Equation (2-12) to Surface 2 (the container surface):

$$q_2 = \frac{E_{b2} - J_2}{(1 - \varepsilon_2)/\varepsilon_2 A_2} \qquad (3-7)$$

In order to find J_2, we must apply equation (2-21) to Surface 2:

$$\frac{E_{b2} - J_2}{(1 - \varepsilon_2)/\varepsilon_2 A_2} = \frac{J_2 - J_1}{1/A_2 F_{21}} + \frac{J_2 - J_3}{1/A_2 F_{23}} \qquad (3-8)$$

The temperatures of Surface 1 (the heating element surface), Surface 2 (the container surface) and Surface 3 (the surroundings) are obtained from the COMSOL simulation specifications in Section 6.1.1. These temperatures are specified for Surfaces 1, 2, and 3 as 533.15 K, 293.15 K (an initial value of room temperature, 20 °C), and 293.15 K (room temperature, 20 °C), respectively. The value of 533.15 K corresponds to value of 260 °C, which is equivalent to 500 °F (the temperature of a food baking oven in a retail establishment, from the author's observation). Similarly, the area of Surface 2 (the only area needed at this point in the calculation) is obtained from Section 6.1.1: the *x* dimension of the container surface is 0.1 m, and a depth for the area of the surface had to be specified (chosen to be 1 meter).

Applying Equation (2-9) to Surfaces 3 (the surroundings) and 1 (the heating element), assuming that each surface is a blackbody:

$$J_3 = E_{b3} = \sigma T_3^4 = \left(5.670 \times 10^{-8} \frac{\text{W}}{\text{m}^2\text{K}^4}\right)(293.15\ \text{K})^4 = 418.7 \frac{\text{W}}{\text{m}^2} \qquad (3-9)$$

$$J_1 = E_{b1} = \sigma T_1^4 = \left(5.670 \times 10^{-8} \frac{\text{W}}{\text{m}^2\text{K}^4}\right)(533.15\ \text{K})^4 = 4581.2\ \frac{\text{W}}{\text{m}^2} \qquad (3-10)$$

Applying Equation (2-9) to Surface 2 (the container):

$$E_{b2} = \sigma T_2^4 = \left(5.670 \times 10^{-8} \frac{\text{W}}{\text{m}^2\text{K}^4}\right)(293.15\ \text{K})^4 = 418.7\ \frac{\text{W}}{\text{m}^2} \qquad (3-11)$$

Substituting values (here the emissivity is 0.1 from Section 6.1.1, and the dimensions are from Figure 6-1) into Equation (3-8):

$$\frac{418.7 \frac{\text{W}}{\text{m}^2} - J_2}{(1-0.1)/[(0.1)(0.1\ \text{m})(1\ \text{m})]} = \frac{J_2 - 4581.2 \frac{\text{W}}{\text{m}^2}}{1/[(0.1\ \text{m})(1\ \text{m})(0.7461)]} + \frac{J_2 - 418.7 \frac{\text{W}}{\text{m}^2}}{1/[(0.1\ \text{m})(1\ \text{m})(0.2539)]} \qquad (3-12)$$

$$J_2 = 3213.7\ \frac{\text{W}}{\text{m}^2} \qquad (3-13)$$

Substituting values into Equation (3-7):

$$q_2 = \frac{418.7\ \frac{\text{W}}{\text{m}^2} - 3213.7\ \frac{\text{W}}{\text{m}^2}}{(1-0.1)/[(0.1)(0.1\ \text{m})(1\ \text{m})]} = -31.1\ \text{W} \qquad (3-14)$$

In Equation (3-14), since the equation originally assumed the energy to be leaving as positive, the negative sign indicates that the energy (31.1 W) is being absorbed by the container surface.

3.1.2 Closely-spaced heating elements with dough/bread

As a result of performing a COMSOL simulation that had the heating elements closer to the dough/bread (see Section 6.1.3), it is seen from the results that the sides of the dough/bread are being heated more. This created the belief that the view factor had significantly changed, therefore a new view factor had to be found. Ultimately, the goal is to find the heat transferred to the dough/bread from the heating elements; this analysis starts with Equation (2-21):

$$\frac{E_{bi} - J_i}{(1-\varepsilon_i)/\varepsilon_i A_i} = \sum_{j=1}^{N} \frac{(J_i - J_j)}{(A_i F_{ij})^{-1}} \qquad (2-21)$$

An appropriate enclosure must be applied to the geometry shown in Figure 6.4 in order to find the necessary view factors. This problem is divided into two enclosure problems: the first enclosure problem (see Figure 3.2) is used to find the radiation heat transfer between the sides of the food and the other surfaces, and the second enclosure problem (see Figure 3.3) is used to find the radiation heat transfer between the top and bottom of the food and the other surfaces. For the first enclosure problem, Equation (2-21) is as follows:

$$\frac{E_{b2} - J_2}{(1-\varepsilon_2)/\varepsilon_2 A_2} = \frac{J_2 - J_1}{1/A_2 F_{21}} + \frac{J_2 - J_3}{1/A_2 F_{23}} + \frac{J_2 - J_4}{1/A_2 F_{24}} \qquad (3-15)$$

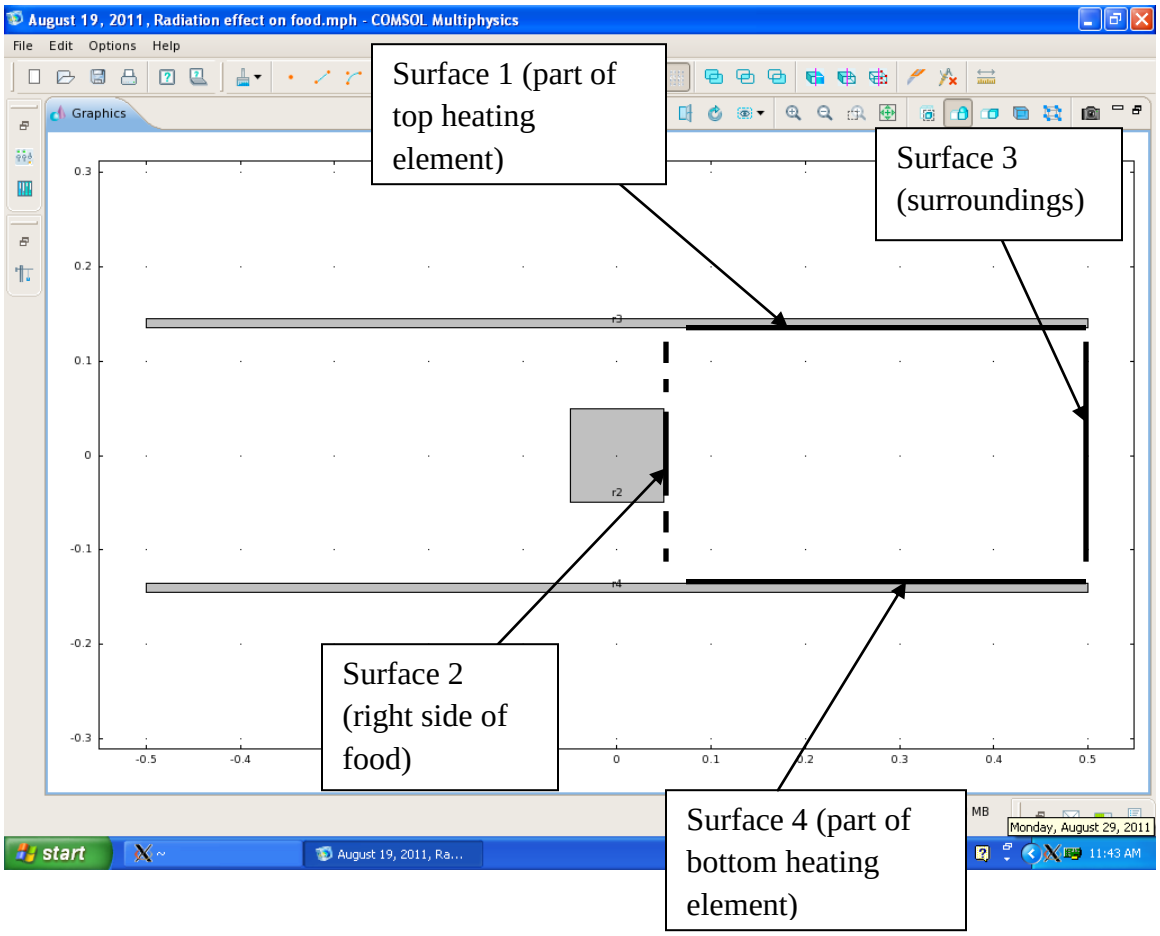

Figure 3.2: First enclosure problem of closely-spaced heating element simulation

The view factors that need to be found are F_{21}, F_{23} and F_{24} (F_{22} =0 because Surface 2 is not concave). The view factor F_{23} can be found using Equation (2-13):

$$F_{ij} = \frac{\left[\left(W_i + W_j\right)^2 + 4\right]^{1/2} - \left[\left(W_j - W_i\right)^2 + 4\right]^{1/2}}{2W_i} \qquad (2-13)$$

Specifying Equation (2-13) for F_{23}:

$$F_{23} = \frac{[(W_2 + W_3)^2 + 4]^{1/2} - [(W_3 - W_2)^2 + 4]^{1/2}}{2W_2} \qquad (3-16)$$

L is the distance between Surface 2 and Surface 3, which is the distance from the end of the heating elements to the surface of the food, minus half the horizontal thickness of the food:

$$L = 0.5\text{ m} - \left(\frac{1}{2}\right)(0.10\text{ m}) = 0.45\text{ m} \qquad (3-17)$$

Following the same method of solution as Section 3.1.1:

$$W_2 = \frac{w_2}{L} = \frac{0.10\text{ m}}{0.45\text{ m}} = 0.2222 \qquad (3-18)$$

$$W_3 = \frac{w_3}{L} = \frac{0.27\text{ m}}{0.45\text{ m}} = 0.60 \qquad (3-19)$$

$$F_{23} = \frac{[(0.2222 + 0.6)^2 + 4]^{1/2} - [(0.6 - 0.2222)^2 + 4]^{1/2}}{2(0.2222)} \qquad (3-20)$$

$$F_{23} = 0.2859 \qquad (3-21)$$

F_{21} and F_{24} can be found from the following application of the summation rule:

$$F_{21} + F_{22} + F_{23} + F_{24} = 1 \qquad (3-22)$$

This equation can be simplified by noticing that $F_{21} = F_{24}$ (because the fraction of radiation from Surface 2 to Surface1 is the same as that from Surface 2 to Surface 4):

$$F_{21} + F_{23} + F_{21} = 1 \qquad (3-23)$$

$$2F_{21} + F_{23} = 1 \qquad (3-24)$$

$$2F_{21} + 0.2859 = 1 \qquad (3-25)$$

$$F_{21} = F_{24} = 0.3571 \qquad (3-26)$$

$$J_3 = E_{b3} = \sigma T_3^4 = \left(5.670 \times 10^{-8} \frac{\mathrm{W}}{\mathrm{m^2 K^4}}\right)(293.15\ \mathrm{K})^4 = 418.7 \frac{\mathrm{W}}{\mathrm{m^2}} \qquad (3-27)$$

$$J_1 = E_{b1} = \sigma T_1^4 = \left(5.670 \times 10^{-8} \frac{\mathrm{W}}{\mathrm{m^2 K^4}}\right)(533.15\ \mathrm{K})^4 = 4581.2\ \frac{\mathrm{W}}{\mathrm{m^2}} \qquad (3-28)$$

$$J_4 = E_{b4} = \sigma T_4^4 = \left(5.670 \times 10^{-8} \frac{\mathrm{W}}{\mathrm{m^2 K^4}}\right)(533.15\ \mathrm{K})^4 = 4581.2\ \frac{\mathrm{W}}{\mathrm{m^2}} \qquad (3-29)$$

Applying Equation (2-9) to Surface 2 (the food):

$$E_{b2} = \sigma T_2^4 = \left(5.670 \times 10^{-8} \frac{\mathrm{W}}{\mathrm{m^2 K^4}}\right)(293.15\ \mathrm{K})^4 = 418.7\ \frac{\mathrm{W}}{\mathrm{m^2}} \qquad (3-30)$$

In order to find J_2, we must apply equation (2-21) to Surface 2 (using inputs from Section 6.1.3):

$$\frac{418.7\,\frac{\mathrm{W}}{\mathrm{m}^2} - J_2}{\frac{(1-0.9)}{[(0.9)(0.1\ \mathrm{m})(1\ \mathrm{m})]}} = \frac{J_2 - 4581.2\,\frac{\mathrm{W}}{\mathrm{m}^2}}{\frac{1}{[(0.1\ \mathrm{m})(1\ \mathrm{m})(0.3571)]}} + \frac{J_2 - 418.7\,\frac{\mathrm{W}}{\mathrm{m}^2}}{\frac{1}{[(0.1\ \mathrm{m})(1\ \mathrm{m})(0.2859)]}} + \frac{J_2 - 4581.2\,\frac{\mathrm{W}}{\mathrm{m}^2}}{\frac{1}{[(0.1\ \mathrm{m})(1\ \mathrm{m})(0.3571)]}} \qquad (3-31)$$

$$J_2 = 716.0\ \ \frac{\mathrm{W}}{\mathrm{m}^2} \qquad (3-32)$$

Substituting values (the emissivity is from Geankoplis, 2003) into Equation (2-12), with respect to Surface 2:

$$q_2 = \frac{E_{b2} - J_2}{(1-\varepsilon_2)/\varepsilon_2 A_2} \qquad (3-33)$$

$$q_2 = \frac{418.7\ \ \frac{\mathrm{W}}{\mathrm{m}^2} - 716.0\ \frac{\mathrm{W}}{\mathrm{m}^2}}{(1-0.9)/[(0.9)(0.1\ \mathrm{m})(1\ \mathrm{m})]} = -267.6\ \mathrm{W} \qquad (3-34)$$

The minus sign in front of the 267.6 W signifies that the energy is being absorbed by the dough/bread. Since there are two such first enclosures, the total amount of energy being absorbed by the dough/bread (at all times) is:

$$2(-267.6\ \mathrm{W}) = -535.1\ \mathrm{W} \qquad (3-35)$$

Now the second enclosure problem must be analyzed to find the energy the dough/bread receives from that enclosure.

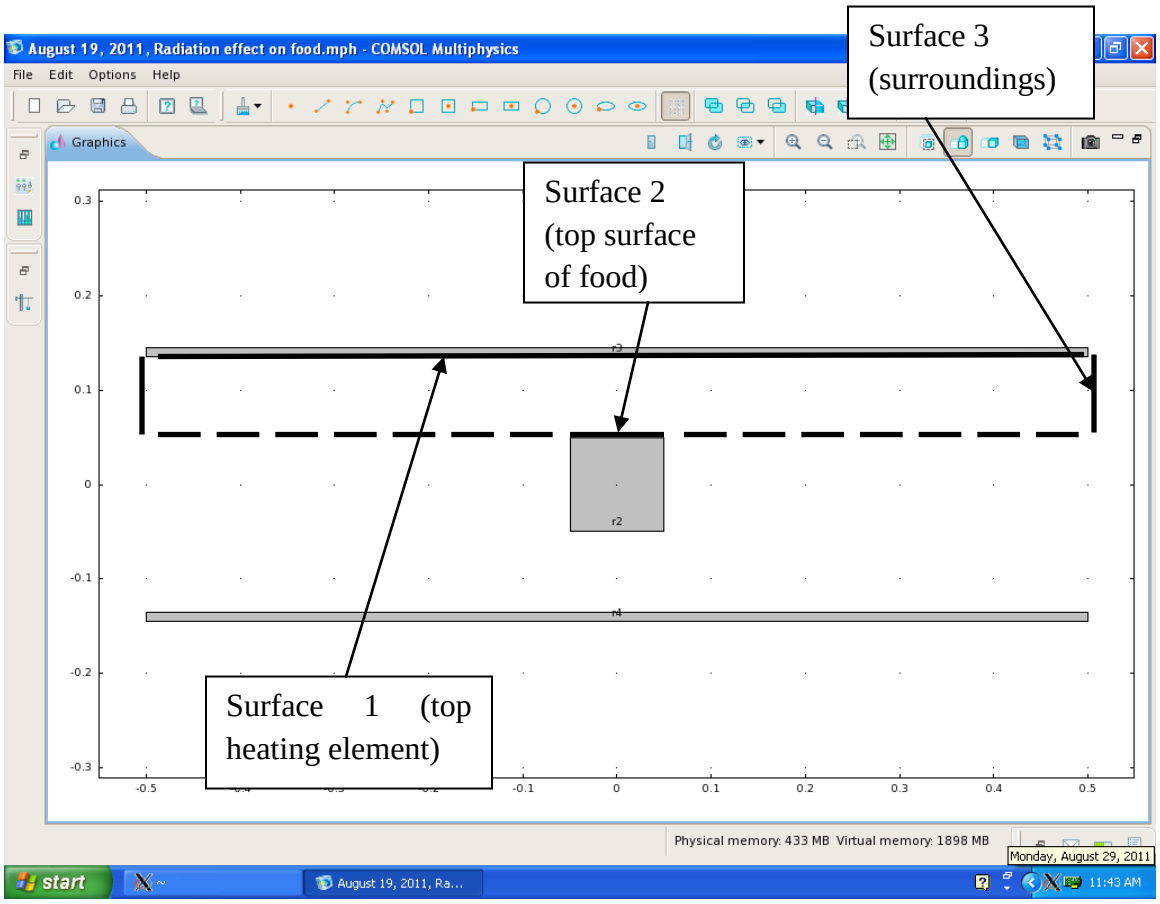

Figure 3.3: Second enclosure problem of closely-spaced heating element simulation

For the second enclosure problem, Equation (2-21) is as follows:

$$\frac{E_{b2} - J_2}{(1-\varepsilon_2)/\varepsilon_2 A_2} = \frac{J_2 - J_1}{1/A_2 F_{21}} + \frac{J_2 - J_3}{1/A_2 F_{23}} \qquad (3-36)$$

The view factors that need to be found are F_{21}, F_{23}. The view factor F_{21} can be found using Equation (2-13):

$$F_{ij} = \frac{\left[\left(W_i + W_j\right)^2 + 4\right]^{1/2} - \left[\left(W_j - W_i\right)^2 + 4\right]^{1/2}}{2W_i} \qquad (2-13)$$

$$F_{21} = \frac{[(W_2 + W_1)^2 + 4]^{1/2} - [(W_1 - W_2)^2 + 4]^{1/2}}{2W_2} \qquad (3-37)$$

L is the distance from Surface 1 to Surface 2, which is the vertical distance between the centers of the heating element and dough/bread, minus the vertical distance between the center and surface of the dough/bread, minus the vertical distance between the center and surface of the heating element.

$$L = 0.14\ \text{m} - \left(\frac{1}{2}\right)(0.10\ \text{m}) - \left(\frac{1}{2}\right)(0.01\ \text{m}) = 0.085\ \text{m} \qquad (3-38)$$

$$W_2 = \frac{w_2}{L} = \frac{0.10\ \text{m}}{0.085\ \text{m}} = 1.1765 \qquad (3-39)$$

$$W_1 = \frac{w_1}{L} = \frac{1\ \text{m}}{0.085\ \text{m}} = 11.7647 \qquad (3-40)$$

$$F_{21} = \frac{[(1.1765 + 11.7647)^2 + 4]^{1/2} - [(11.7647 - 1.1765)^2 + 4]^{1/2}}{2(1.1765)} \qquad (3-41)$$

$$F_{21} = 0.9857 \qquad (3-42)$$

F_{23} can be found from the following summation rule:

$$F_{21} + F_{22} + F_{23} = 1 \qquad (3-43)$$

$$0.9857 + 0 + F_{23} = 1 \qquad (3-44)$$

$$F_{23} = \ 0.01428 \qquad (3-45)$$

$$\frac{E_{b2} - J_2}{(1-\varepsilon_2)/\varepsilon_2 A_2} = \frac{J_2 - J_1}{1/A_2 F_{21}} + \frac{J_2 - J_3}{1/A_2 F_{23}} \qquad (3-46)$$

$$\frac{418.7\,\frac{\mathrm{W}}{\mathrm{m}^2} - J_2}{\frac{(1-0.9)}{[(0.9)(0.1\ \mathrm{m})(1\ \mathrm{m})]}} = \frac{J_2 - 4581.2\,\frac{\mathrm{W}}{\mathrm{m}^2}}{\frac{1}{[(0.1\ \mathrm{m})(1\ \mathrm{m})(0.98572)]}} + \frac{J_2 - 418.7\,\frac{\mathrm{W}}{\mathrm{m}^2}}{\frac{1}{[(0.1\ \mathrm{m})(1\ \mathrm{m})(0.01428)]}} \qquad (3-47)$$

$$J_2 = \ 829.0 \ \ \frac{\mathrm{W}}{\mathrm{m}^2} \qquad (3-48)$$

$$q_2 = \frac{418.7\ \frac{\mathrm{W}}{\mathrm{m}^2} - 829.0\ \frac{\mathrm{W}}{\mathrm{m}^2}}{(1-0.9)/[(0.9)(0.1\ \mathrm{m})(1\ \mathrm{m})]} = -369.3\ \mathrm{W} \qquad (3-49)$$

The minus sign in front of the 369.3 W signifies that the energy is being absorbed by the food. Since there are two such second enclosures, the total amount of energy being absorbed by the food is:

$$2(-369.3\ \mathrm{W}) = -738.5\ \mathrm{W} \qquad (3-50)$$

3.2 Conduction analytical calculations

The conduction analytical calculations will be performed in this section.

3.2.1 Distantly-spaced heating elements with container

Table 3.1: Properties of material, radiation effect on surface of container, analytical solution

Thermal conductivity (W/(m·C))	Density (kg/m^3)	Heat Capacity at constant pressure (J/(kg·C))
52	7800	465

Table 3.1 shows the properties of the material (steel) used in the analytical solution of the radiation effect on the surface of container. These properties are obtained from Incropera and Dewitt (1990).

On the left side of Equation (2-41), the energy is enumerated by realizing that for 3600 seconds (see Table 8.1) in the transient simulation, there are two heating elements (see Figure 6.1: Radiation effect on surface of container: COMSOL geometry) that are

heating the container material at the rate of 31.1 J/s per heating element. The container material has a volume (see Figure 6.1) of (0.1 m height)(0.1 m width)(1m depth). The 1 m depth is arbitrarily chosen because the COMSOL geometry is two dimensional, and it is assumed that whatever happens in those two dimensions, happens at any depth. The right side of Equation (2-41) is enumerated by multiplying the density of the container with the specific heat and temperature difference. Substituting the appropriate values into Equation (2-41):

$$\left[\frac{\left(31.1\ \frac{\mathrm{J}}{\mathrm{s}}\ \text{per heating elements}\right)(2\ \text{heating elements})}{(0.1\ \mathrm{m})(0.1\ \mathrm{m})(1\ \mathrm{m})}\right](3600\ \mathrm{s}) = \left(7800\,\frac{\mathrm{kg}}{\mathrm{m}^3}\right)\left(465\,\frac{\mathrm{J}}{\mathrm{kg}\cdot\mathrm{K}}\right)(\Delta T) \qquad (3-51)$$

$$\Delta T = 6.2\ \mathrm{K} \qquad (3-52)$$

Equation (3-52) will be compared with the results of the corresponding COMSOL simulation in Section 8.1.1.

3.2.2 Closely-spaced heating elements with dough/bread

Substituting values of energy from Section 3.1.2, geometric dimensions from Figure 6.4, time from Section 8.1.3, and thermal properties from Table 6.3 into Equation (2-41):

$$\left[\frac{\left(535.1\ \frac{\mathrm{J}}{\mathrm{s}} + 738.5\ \frac{\mathrm{J}}{\mathrm{s}}\right)}{(0.1\ \mathrm{m})(0.1\ \mathrm{m})(1\ \mathrm{m})}\right](240\ \mathrm{s}) = \left(380\,\frac{\mathrm{kg}}{\mathrm{m}^3}\right)\left(1941\,\frac{\mathrm{J}}{\mathrm{kg}\cdot\mathrm{K}}\right)(\Delta T) \qquad (3-53)$$

$$\Delta T = 41.4\ \mathrm{K} \qquad (3-54)$$

Equation (3-54) will be compared with the results of the two-dimensional COMSOL simulation in Section 8.1.3, the results of the three-dimensional COMSOL simulations in Sections 9.1 and 9.2, and the MATLAB simulation in Section 10.3.1.

3.2.3 Calculations for MATLAB

The equations in this section are based upon the equations in Section 2.2.3, with the exception that radiation replaces convection. These calculations are outlined in Holman (1990).

The dough/bread is divided into five nodes as shown in Figure 3.4. The width of the dough/bread is 0.10 m (from Figure 6.4), and a heating element (radiation source) is at 533.15 K (as in Section 3.1.2). The oven temperature is calculated from the average of heating element temperature and room temperature.

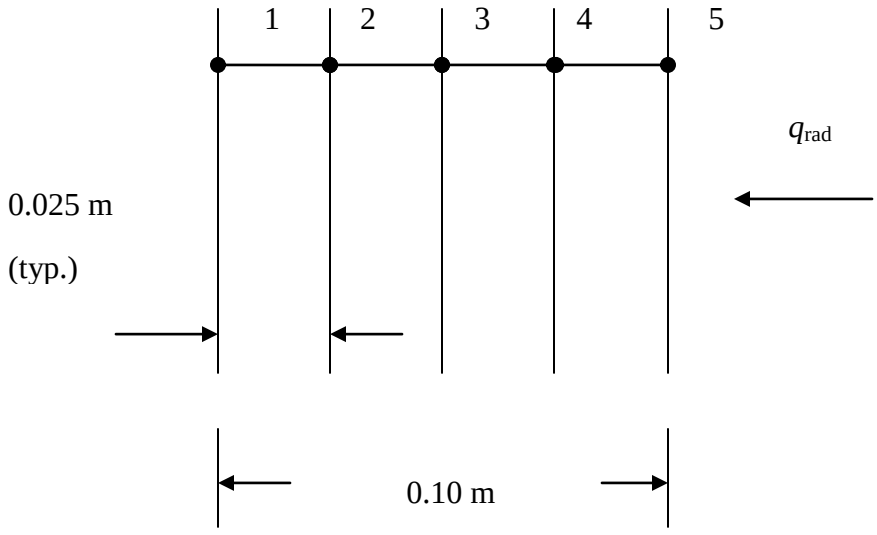

Figure 3.4: Nodal system

For node 1 the transient energy equation is

$$\sigma\epsilon\left(T_\infty^4 - T_1^{p\,4}\right) + \frac{k}{\Delta x}\left(T_2^p - T_1^p\right) = \rho c\frac{\Delta x}{2}\left(\frac{T_1^{p+1} - T_1^p}{\Delta\tau}\right) \qquad (3-55)$$

Similarly, for node 5

$$\sigma\epsilon\left((533.15\ K)^4 - T_5^{p\,4}\right) + \frac{k}{\Delta x}\left(T_4^p - T_5^p\right) = \rho c\frac{\Delta x}{2}\left(\frac{T_5^{p+1} - T_5^p}{\Delta\tau}\right) \qquad (3-56)$$

Equations (3-55) and (3-56) may be written as

$$T_1^{p+1} = \frac{\Delta\tau}{C_1}\left[\sigma\epsilon\left(413.15^2 + T_1^{p\,2}\right)\left(413.15 + T_1^p\right)(413.15) + \frac{k}{\Delta x}T_2^p\right]$$

$$+\left\{1 - \frac{\Delta\tau}{C_1}\left[\sigma\epsilon\left(413.15^2 + T_1^{p\,2}\right)\left(413.15 + T_1^p\right) + \frac{k}{\Delta x}\right]\right\}T_1^p \qquad (3-57)$$

$$T_5^{p+1} = \frac{\Delta\tau}{C_5}\left[\sigma\epsilon\left(533.15^2 + T_5^{p\,2}\right)\left(533.15 + T_5^p\right)(533.15) + \frac{k}{\Delta x}T_4^p\right]$$

$$+\left\{1 - \frac{\Delta\tau}{C_5}\left[\sigma\epsilon\left(533.15^2 + T_5^{p\,2}\right)\left(533.15 + T_5^p\right) + \frac{k}{\Delta x}\right]\right\}T_5^p \qquad (3-58)$$

where $C_1 = C_5 = \rho c\Delta x/2$. C_1 and C_5 are found as follows (using dough/bread property values from Table 6.3):

$$C_1 = C_5 = \frac{\left(380\,\frac{\text{kg}}{\text{m}^3}\right)\left(1941\,\frac{\text{J}}{\text{kg}\cdot\text{K}}\right)(0.025\ \text{m})}{2} = 9219.75\ \frac{\text{kg}}{\text{s}^2\cdot\text{K}} \qquad (3-59)$$

For the other three nodes the expressions are:

$$T_2^{p+1} = \frac{\Delta\tau}{C_2}\frac{k}{\Delta x}\left(T_1^p + T_3^p\right) + \left(1 - \frac{2k}{C_2}\frac{\Delta\tau}{\Delta x}\right)T_2^p \qquad (3-60)$$

$$T_3^{p+1} = \frac{\Delta\tau}{C_3}\frac{k}{\Delta x}\left(T_2^p + T_4^p\right) + \left(1 - \frac{2k}{C_3}\frac{\Delta\tau}{\Delta x}\right)T_3^p \qquad (3-61)$$

$$T_4^{p+1} = \frac{\Delta\tau}{C_4}\frac{k}{\Delta x}\left(T_3^p + T_5^p\right) + \left(1 - \frac{2k}{C_4}\frac{\Delta\tau}{\Delta x}\right)T_4^p \qquad (3-62)$$

where $C_2 = C_3 = C_4 = 2C_1 = 2C_5 = \rho c \Delta x$ (due to the fact that each interior node has a heat capacity twice that of each exterior node (Holman, 1990)) . C_2 , C_3 and C_4 are found as follows:

$$C_2 = C_3 = C_4 = \left(380\,\frac{\text{kg}}{\text{m}^3}\right)\left(1941\,\frac{\text{J}}{\text{kg}\cdot\text{K}}\right)(0.025\text{ m}) = 18439.5\,\frac{\text{kg}}{\text{s}^2\cdot\text{K}} \qquad (3-63)$$

To determine the transient response, a suitable value of $\Delta\tau$ is chosen, and one "marches" through the calculations. The stability criterion is chosen so that the last term in each equation is not negative. For (3-60), (3-61), and (3-62), the maximum allowable time increment is (using dough/bread properties from Table 6.3):

$$\Delta\tau_{\max} = \frac{C_3\Delta x}{2k} = \frac{\left(18439.5\,\frac{\text{kg}}{\text{s}^2\cdot\text{K}}\right)(0.025\text{ m})}{2\left(0.1133\,\frac{\text{W}}{\text{m}\cdot\text{K}}\right)} = 2034.37\text{ s} \qquad (3-64)$$

For Equation (3-58) the worst (most restrictive) case is at the start when $T_5^p = 293.15$ K . Therefore:

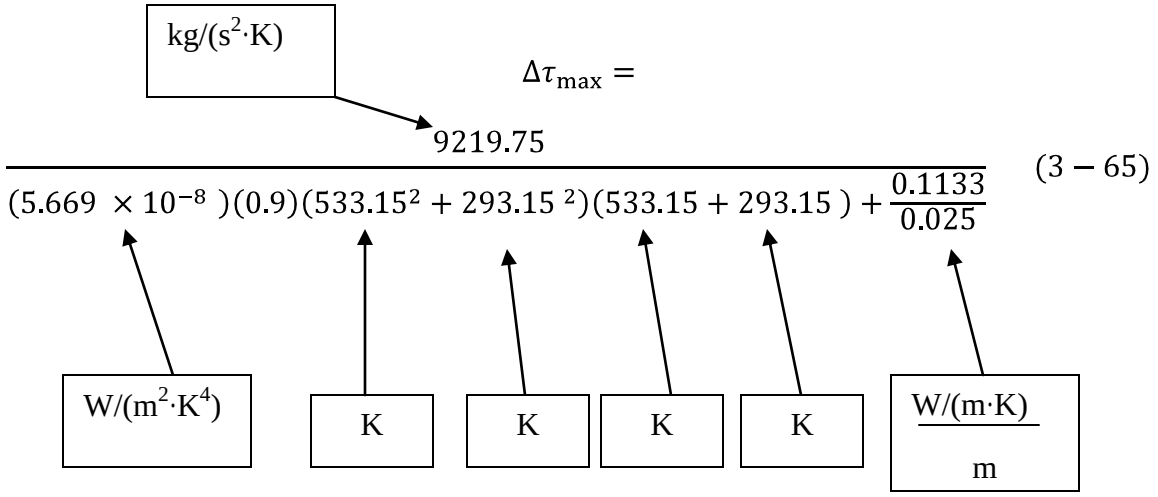

$$\Delta\tau_{\max} = 457.82 \text{ s} \qquad (3-66)$$

For node 1 (Equation (3-57)) the most restrictive condition occurs when $T_1^p = 293.15$ K ;

therefore:

$$\Delta\tau_{\max} = \frac{9219.75}{(5.669 \times 10^{-8})(0.9)(293.15^2 + 293.15^2)(293.15 + 293.15) + \frac{0.1133}{0.025}} \qquad (3-67)$$

$$\Delta\tau_{\max} = 953.11 \text{ s} \qquad (3-68)$$

Node 5 is therefore the most restrictive and $\Delta\tau$ must be chosen so that $\Delta\tau < 457.82$ s. $\Delta\tau$ is chosen to be 10 s.

The equations and input values in this section were directly coded into a MATLAB program, which is shown in Appendix D.

3.3 Convection analytical calculations

The natural and forced convection analytical calculations will be performed in this section.

3.3.1 Natural convection analytical calculations

Substituting the appropriate values from Table 6.9, Figure 6.11, and Figure 6.12 into Equations (2-67), (2-68), and (2-69):

$$T_f = \frac{533.15\ \text{K} + 293.15\ \text{K}}{2} = 413.15\ \text{K} \qquad (3-69)$$

$$\beta = \frac{1}{413.15\ \text{K}} = 0.002420\ \text{K}^{-1} \qquad (3-70)$$

$$L = \frac{(1\text{m})(0.8\text{m})}{(1\text{m}+0.8\text{m}+1\text{m}+0.8\text{m})} = 0.2222\ \text{m} \qquad (3-71)$$

From Table A.4 of Incropera and Dewitt (1990), $\nu = 27.98 \times 10^{-6}\ \frac{\text{m}^2}{\text{s}}$, $\alpha = 40.64 \times 10^{-6}\ \frac{\text{m}^2}{\text{s}}$.

Substituting the above values into Equation (2-66):

$$Ra_L = \frac{\left(9.81\frac{\text{m}}{\text{s}^2}\right)(0.002420\ \text{K}^{-1})(533.15\ \text{K} - 293.15\ \text{K})(0.2222\ \text{m})^3}{\left(27.98 \times 10^{-6}\ \frac{\text{m}^2}{\text{s}}\right)\left(40.64 \times 10^{-6}\ \frac{\text{m}^2}{\text{s}}\right)} \qquad (3-72)$$

$$Ra_L = 5.5 \times 10^7 \qquad (3-73)$$

This flow is considered laminar (Incropera & DeWitt, 1990). It is then appropriate to use the laminar flow application in the corresponding natural convection COMSOL simulations.

3.3.2 Forced convection analytical calculations

Using values from Figures 6.14 and 6.15:

$$D_h = \frac{4\ (1\ \text{m})(0.1\ \text{m})}{(1\ \text{m} + 0.1\ \text{m} + 1\text{m} + 0.1\ \text{m})} = \frac{0.4\ \text{m}^2}{2.2\ \text{m}} = 0.1818\ \text{m} \qquad (3-74)$$

$$U_{side} = 0.5\ \left(1\frac{\text{m}}{\text{s}}\right) = 0.5\frac{\text{m}}{\text{s}} \qquad (3-75)$$

Substituting the values from Section 6.2.3 into Equation (2-76) yields:

$$Re = \frac{\left(1\frac{\text{kg}}{\text{m}^3}\right)\left(0.5\ \frac{\text{m}}{\text{s}}\right)(0.1818\ \text{m})}{(1\times 10^{-5}\ \text{Pa}\cdot\text{s})} = \ 9091 \qquad (3-76)$$

This Reynolds number is greater than 2300, but the forced convection COMSOL model was created using the laminar flow application. The results show laminar flow, so the assumption of non-turbulent flow is valid.

3.4 Moisture analytical calculations

The values relevant to this research will be substituted into the equations of the corresponding theoretical formulation (Section 2.5.1). The goal here is to find the drying rate R_C, which is the amount of water in kg that has evaporated from the dough/bread per m^2 per unit time (chosen to be one hour). The starting point is Equation (2-109), and this equation can be solved by using Equation (2-110). At this point the values for Equation (2-110) will be found.

$$\frac{(H_s - H)\lambda_S}{h_C/k_y M_b} = \left(1 + \frac{U_K}{h_C}\right)(T - T_S) + \frac{h_R}{h_C}(T_R - T_S) \qquad (2-110)$$

H is the humidity, and H = 0.050 kg H_2O / kg dry air (from Baik et al, 2000 a). T = 120 °C because the range of the available data on the psychrometric chart used restricted T to no higher than this value.

H_S is the saturation humidity and involves knowing or guessing T_S , which is the surface temperature. Since T_S is not known at this time, it must be guessed. At this time, a value for the surface temperature of the solid will be estimated (the actual psychrometric chart, not shown, is used from Geankoplis, 2003). T_S will be above the wet bulb temperature T_W. T_W is determined as follows (see Figure 3.4 for a corresponding, but not the current, analysis): first, from the temperature of the air-water vapor stream, which is assumed to be 120°C, the humidity chart is followed vertically until one reaches the H = 0.05 kg water vapor/kg dry air. Then, one follows the diagonal line until hitting the 100% percentage humidity curve. Then one follows the vertical line down until hitting the temperature horizontal line again. This is the dew point temperature T_W, which is about 49 degrees Celsius. Since T_S will be above wet bulb temperature according to Equation (2-105), estimate T_S to be 55°C.

To find H_S, use the humidity chart (the actual psychrometric chart, not shown, is used from Geankoplis, 2003) , follow (see Figure 3.5 for a corresponding, but not the current, analysis) the T_S temperature of 55 °C vertically to 100 % humidity, then follow horizontally until hit humidity on vertical axis. this is H_S, = 0.115 kg water vapor/kg dry air.

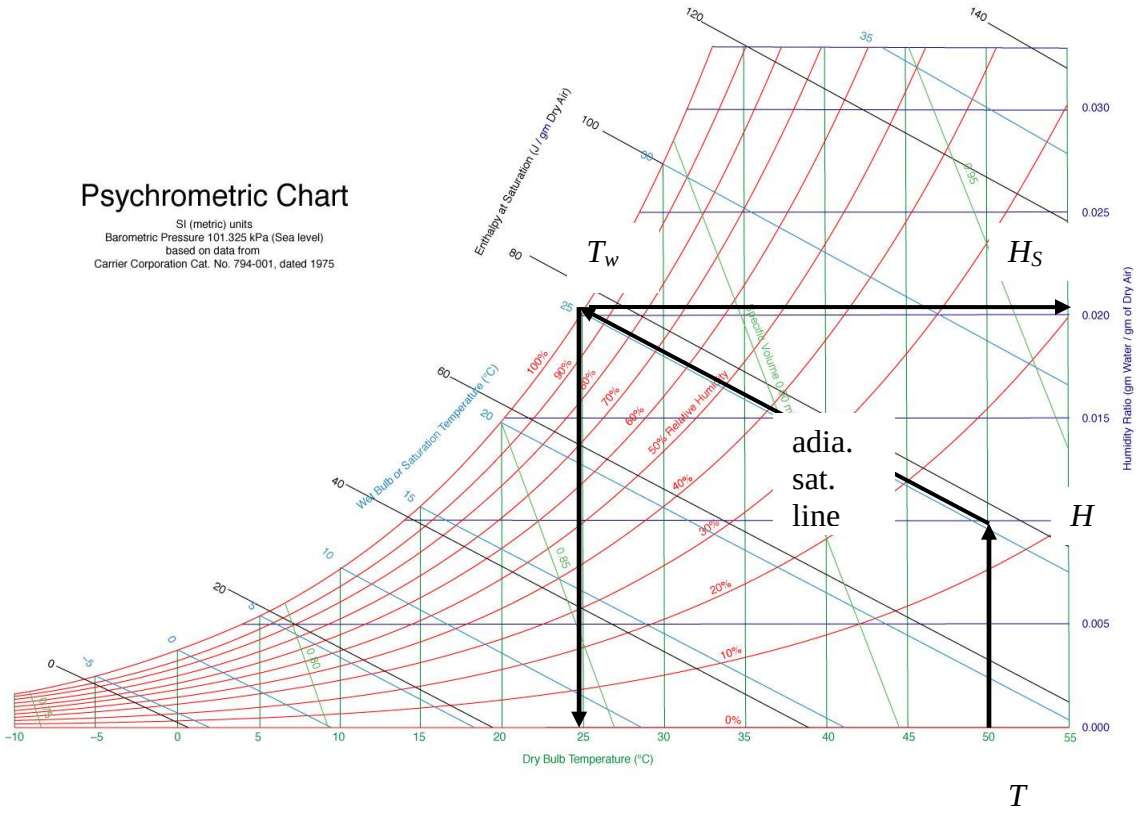

Figure 3.5 Psychrometric chart (from Ogawa, 2007)

λ_S is the latent heat corresponding to the surface temperature T_S . From the guessed T_S of 55° C, find λ_S from the steam tables of Geankoplis (2003). The λ_S is calculated as 2600.9 kJ/kg - 230.20 kJ/kg= 2370.7 kJ/kg.

Table 3.2: Excerpt of steam table (from Geankoplis, 2003)

Temperature (°C)	Vapor Pressure (kPa)	Enthalpy (kJ/kg)	
55	15.758	Liquid	Sat'd Vapor
		230.23	2600.9

The ratio $h_C/k_y M_b$ is approximately:

$$c_S = (1.005 + 1.88H)10^3 \text{J/kg·K} \qquad (2-107)$$

$$c_S = \big(1.005 + 1.88(0.050)\big)10^3 \text{J/kg·K} = 1099 \text{ J/kg·K} \qquad (3-77)$$

U_K is found by the following equation:

$$U_K = \frac{1}{\frac{1}{h_C} + \frac{z_M}{k_M} + \frac{z_S}{k_S}} \qquad (2-95)$$

h_C is the convective heat transfer coefficient and is determined from the following equation:

$$h_C = 0.0204 G^{0.8} \qquad (2-84)$$

where:

$$G = v\rho \text{ kg/hr·m}^2 \qquad (2-85)$$

where v is the velocity of the air flow and is 0.61 m/s. This value is obtained from the observation that air velocities in similar tunnel ovens are less than 0.61 m/s (Baik et al, 2000 a), but the equations in Geankoplis (2003) are not valid below 0.61 m/s.

$$\rho = \frac{1.0 + 0.050}{v_H} \qquad (3-78)$$

where

$$v_H = (2.83 \times 10^{-3} + 4.56 \times 10^{-3} H)T \ K \qquad (2-87)$$

$$v_H = \big(2.83 \times 10^{-3} + 4.56 \times 10^{-3}(0.05)\big)(393.15 \ K) = 1.202 \ \frac{\text{m}^3}{\text{kg dry air}} \qquad (3-79)$$

$$\rho = \frac{1.0 + 0.050}{1.202} = 1.041 \ \frac{\text{kg}}{\text{m}^3} \qquad (3-80)$$

$$G = v\rho \ \text{kg/hr·m}^2 = \left(0.5 \ \frac{\text{m}}{\text{s}}\right)\left(1.041 \ \frac{\text{kg}}{\text{m}^3}\right)\left(\frac{3600 \ \text{s}}{\text{hr}}\right) = 2287.33 \ \ \text{kg/hr·m}^2 \qquad (3-81)$$

$$h_C = 0.0204(2287.33 \ \ \text{kg/hr·m}^2)^{0.8} = 9.933 \ \frac{\text{W}}{\text{m}^2\text{·K}} \qquad (3-82)$$

The remaining values for Equation (2-95) are found (if possible) from corresponding models or simulations. Use k_M = 52 (W/m C) for steel, as in Table 3.1; use z_M as 2 mm, which corresponds to an appropriate thickness of a container (Geankoplis, 2003), use z_S = 0.10 m, from Figure 6.4; and use k_S =$0.1133 \frac{\text{W}}{\text{m·K}}$ from Table 6.3.

$$U_K = \frac{1}{\frac{1}{h_C} + \frac{z_M}{k_M} + \frac{z_S}{k_S}} = \frac{1}{\frac{1}{9.933 \ \frac{\text{W}}{\text{m}^2\text{·K}}} + \frac{0.002 \ \text{m}}{52 \frac{\text{W}}{\text{m·K}}} + \frac{0.10 \ \text{m}}{0.1133 \frac{\text{W}}{\text{m·K}}}} \qquad (3-83)$$

$$U_K = \frac{1}{0.101 \frac{\text{m}^2\text{·K}}{\text{W}} + 3.8 \times 10^{-5} \frac{\text{m}^2\text{·K}}{\text{W}} + .88 \frac{\text{m}^2\text{·K}}{\text{W}}} = \frac{1}{0.98 \frac{\text{m}^2\text{·K}}{\text{W}}}$$

$$= 1.02 \frac{\text{W}}{\text{m}^2\text{·K}} \qquad (3-84)$$

In order to find h_R, a value for T_R is specified as 260 °C+273.15 K = 533.15 K (as in Section 3.1.2), the emissivity of the dough bread is 0.9 (also from Section 3.1.2), and the

guessed temperature of the surface is translated into Kelvin; substituting in Equation (2-93):

$$h_R = (0.9)(5.676)\frac{\left(\frac{533.15\ \text{K}}{100}\right)^4 - \left(\frac{328.15\ \text{K}}{100}\right)^4}{533.15\ \text{K} - 328.15\ \text{K}} \qquad (3-85)$$

$$h_R = (0.9)(5.676)\frac{807.97 - 115.96}{533.15\ \text{K} - 328.15\ \text{K}} \qquad (3-86)$$

$$h_R = (0.9)\left(5.676\frac{\text{W}}{\text{m}^2\cdot\text{K}^4}\right)\frac{692.01\ \text{K}^4}{205\ \text{K}} = 17.24\ \frac{\text{W}}{\text{m}^2\cdot\text{K}} \qquad (3-87)$$

Substituting the acquired values into Equation (2-105):

$$\frac{\left(0.115\ \left(\frac{\text{kg H}_2\text{O}}{\text{kg dry air}}\right) - 0.05\left(\frac{\text{kg H}_2\text{O}}{\text{kg dry air}}\right)\right)\left(2370.7\times10^3\frac{\text{J}}{\text{kg}}\right)}{1099\left(\frac{\text{J}}{\text{kg}\cdot\ ^\circ\text{C}}\right)}$$

$$= \left(1 + \frac{1.02\frac{\text{W}}{\text{m}^2\cdot\text{C}}}{9.93\ \frac{\text{W}}{\text{m}^2\cdot\text{C}}}\right)(120\ ^\circ\text{C} - T_S) + \left(\frac{17.2\ \frac{\text{W}}{\text{m}^2\cdot\text{C}}}{9.93\ \frac{\text{W}}{\text{m}^2\cdot\text{C}}}\right)(260\ ^\circ\text{C} - T_S) \qquad (3-88)$$

This gives a T_S =156.2 °C; substituting into Equation (2-109) to obtain the drying rate R_C:

$$R_C = \frac{\left(9.933\ \frac{\mathrm{W}}{\mathrm{m^2 \cdot K}} + 1.02\frac{\mathrm{W}}{\mathrm{m^2 \cdot K}}\right)(120\ ^\circ\mathrm{C} - 156.2\ ^\circ\mathrm{C}) + 17.24\ \frac{\mathrm{W}}{\mathrm{m^2 \cdot K}}(260\ ^\circ\mathrm{C} - 156.2\ ^\circ\mathrm{C})}{2370.7 \times 10^3\ \frac{\mathrm{J}}{\mathrm{kg}}} \qquad (3-89)$$

$$R_C = 0.000588\frac{\mathrm{kg}}{\mathrm{m^2 \cdot s}} \qquad (3-90)$$

$$R_C = 0.000588\frac{\mathrm{kg}}{\mathrm{m^2 \cdot s}}\left(\frac{3600\ \mathrm{s}}{\mathrm{hr}}\right) = 2.115\ \frac{\mathrm{kg}}{\mathrm{hr \cdot m^2}} \qquad (3-91)$$

Given the calculated T_S = 156.2 °C, then the initial guess for T_S = 55°C was too low an estimate; say new guess for T_S = 90 °C, use this new T_S to find the new H_S. Use the new T_S to find the new λ_S from steam tables as 2660.1 kJ/kg – 376.92 kJ/kg = 2283.18 kJ/kg ; continue as shown in the previous analysis. Then substitute the new acquired values back into Equation (2-105) to get a new value for T_S, then into Equation (2-104) to get a new R_C. This process is continued until the desired accuracy is obtained.

In order to compare the calculated R_C = 2.115 kg/(hr·m^2) with literature values, the compared values must be dimensionally consistent; the values will be chosen to have the units of (kg water lost)/hour, which will mean the kilograms of water lost by a loaf of dough/bread per hour. First converting the calculated value to (kg water lost)/hour requires knowing the surface area of the top of the dough/bread, which is determined to

be (0.1 m)(0.2 m). The 0.1 m is obtained from Figure 6.1; the 0.2 m is obtained from an approximation of the length of an ordinary small loaf of store-bought bread.

$$\left(2.115\,\frac{\text{kg}}{\text{hr}\cdot\,\text{m}^2}\right)\,(0.1\text{ m})(0.2\text{ m}) = 0.0423\,\frac{\text{kg water lost}}{\text{hour}} \qquad (3-92)$$

From Baik et al (2000 b), for bread baking in an electric batch oven at 200 degrees C, the drying rate ranged from 2.78×10^{-5} kg water /(kg dry solid · second) to 2.36×10^{-4} kg water / (kg dry solid · second). Converting these literature values to kg water lost/hour requires the following steps, shown below.

$$\left(2.78 \times 10^{-5}\,\frac{\text{kg water}}{\text{kg dry solid}\ \cdot\ \text{second}}\right)\left(\frac{3600\text{ seconds}}{\text{hour}}\right)$$

$$= 0.1001\ \left(\frac{\text{kg water}}{\text{kg dry solid}\ \cdot\ \text{hour}}\right) \qquad (3-93)$$

$$\left(2.36 \times 10^{-4}\,\frac{\text{kg water}}{\text{kg dry solid}\ \cdot\ \text{second}}\right)\left(\frac{3600\text{ seconds}}{\text{hour}}\right)$$

$$= 0.8496\ \left(\frac{\text{kg water}}{\text{kg dry solid}\ \cdot\ \text{hour}}\right) \qquad (3-94)$$

To convert the results of Equations (3-93) and (3-94) to kg water lost/hour, it is necessary to know how many kilograms of dry solid are in a loaf of bread. The water content in dough/bread is approximately 40 % by weight (Czuchajowska et al, 1988, Thorvaldsson & Janestad, 1999). This means that for 1 kg of dough/bread, 0.4 kg of it

will be water; therefore 0.6 kg is dry solid. Using a value of 0.5 kg for an ordinary loaf of bread: 0.2 kg is water, and 0.3 kg is dry solid.

$$0.1001\ \left(\frac{\text{kg water}}{\text{kg dry solid}\ \cdot\ \text{hour}}\right)(0.3\ \text{kg dry solid}) = 0.03\ \frac{\text{kg water lost}}{\text{hour}} \qquad (3-95)$$

$$0.8496\ \left(\frac{\text{kg water}}{\text{kg dry solid}\ \cdot\ \text{hour}}\right)(0.3\ \text{kg dry solid}) = 0.2549\ \frac{\text{kg water lost}}{\text{hour}} \qquad (3-96)$$

These analytical and literature values will be compared with the results of the COMSOL and MATLAB simulations of Sections 8.3 and 10.3.3, respectively.

CHAPTER IV

DESCRIPTION OF CLEVELAND STATE UNIVERSITY AND OHIO SUPERCOMPUTER CENTER COMPUTING RESOURCES

This work was effectively performed at Cleveland State University, using a Dell Vostro 410 Central Processing Unit, and a ViewSonic Profession Series P810 Monitor. The Dell Vostro 410 has an Intel ® Core ™ 2 Quad CPU Q 6600 @ 2.40 GHz, with 3.00 GB of RAM.

The Ohio Supercomputer Center (OSC) provides supercomputing resources to a diverse state and national community, including education, academic research, industry, and state government (Ohio Supercomputer Center, 2011).

4.1 Preparation of computer for communication with OSC server

The software COMSOL is accessed via an internet-enabled personal computer; if the personal computer is Windows-based, then certain software must be downloaded in order to communicate with the OSC computer, which is Linux-based (Ohio Supercomputer Center, 2010 a).

4.2 Parallel processing

Figure 4.2 shows a batch script that is required to run a simulation in parallel on the OSC computer. This batch script is created by typing "emacs December_15_2011_3D_radiation_on_dough_bread_close_heating_elements_defined_side_boundaries.job " at the "$" prompt. "emacs" is a text editor; an explanation of the information contained in Figure 4.2 can be found in Larson (2010).

Figure 4.3 shows the text of a submission of a batch job to the OSC computer. Information about this procedure can be found in Ohio Supercomputer Center (2012 a).

Figure 4.4 shows monitoring the status of the submitted job through the command "qstat". Information about this command can be found in Ohio Supercomputer Center (2012 b).

Figure 4.5 shows an email stating the job has completed. Information about this type of email can be found in Ohio Supercomputer Center (2010 b).

```
#PBS -N
December_15_2011_3D_radiation_on_dough_bread_close_heating_
elements_defined_side_boundaries

#PBS -l walltime=00:15:00

#PBS -l nodes=2:ppn=1

#PBS -j oe

#PBS -m b

#PBS -m e

# The following lines set up the COMSOL environment

module load comsol40a

# Move to the directory where the job was submitted

cd $PBS_WORKDIR

cp
December_15_2011_3D_radiation_on_dough_bread_close_heating_
elements_defined_side_boundaries.mph $TMPDIR

cd $TMPDIR

# Run COMSOL

comsol batch -inputfile

December_15_2011_3D_radiation_on_dough_bread_close_heating_
elements_defined_side_boundaries.mph

-outputfile

December_15_2011_3D_radiation_on_dough_bread_close_heating_
elements_defined_side_boundaries_results.mph

#

#Now, copy data back once the simulation has completed

pbsdcp * $PBS_O_WORKDIR
```

Figure 4.1: Batch script for parallel processing

```
 -bash-3.2$ cd /nfs/05/cls0140/Fall_2011_COMSOL_files


 -bash-3.2$ qsub
December_15_2011_3D_radiation_on_dough_bread_close_heating_elements_def
ined_side_boundaries.job

6752562.opt-batch.osc.edu
```

Figure 4.2: Submit of batch job to OSC computer

```
 -bash-3.2$

-bash-3.2$: qstat:

.

.

6752562.opt-batch        … de_boundaries cls0140              0 R parallel
```

Figure 4.3: Status of batch job

```
PBS Job Id: 6752562.opt-batch.osc.edu
Job Name:
December_15_2011_3D_radiation_on_dough_bread_close_heating_elements_def
ined_side_boundaries
Exec host:  opt2342/0+opt2041/0
Execution terminated
Exit_status=271
resources_used.cput=01:15:27
resources_used.mem=5345240kb
resources_used.vmem=6942740kb
resources_used.walltime=00:15:09
```

Figure 4.4: Email sent to user upon completion of simulation

4.3 Transfer of files between local computer and OSC computer

In this research work, a software called WinSCP is employed to transfer files between the personal local computer and the OSC computer. Information about this software can be found in Tatum (2011).

CHAPTER V

DESCRIPTION OF COMSOL CODE

In this chapter, the COMSOL code relevant to this research will be briefly described. The description is from COMSOL (2010 b,c). The purpose of this chapter is to familiarize the reader with the COMSOL software, so that the COMSOL models and simulations in later chapters will be more readily understandable.

5.1 Geometry

Usually the space dimension (0-D, 1-D, 2-D, or 3-D) is specified first in the building of a COMSOL model, and the geometry is specified after the physics and study type (stationary, time dependent, etc) are chosen.

5.2 Stationary or transient analysis

In this research, the stationary and transient study types are used for the oven and container/dough/bread simulations, respectively.

5.3 Physics

The physics used in the COMSOL models and simulations will be discussed in this section.

5.3.1 Radiation

In order to model radiation exchange between surfaces it is necessary to use COMSOL's Heat Transfer Module, which is an add-on to the COMSOL Multiphysics software.

5.3.2 Heat Transfer in Solids

The Heat Transfer in Solids node is a subnode of the Heat Transfer interface, and this models the conduction of heat within the container and dough/bread in this research.

5.3.3 Heat Transfer in Fluids

The Heat Transfer in Fluids node is a subnode of the Heat Transfer interface, and this models the heat transfer in the nondimensional natural convection model in this research.

5.3.4 Non-Isothermal Flow

The Non-Isothermal Flow Interface automatically couples the heat transfer and laminar flow in the dimensional natural convection model in this research.

5.3.5 Laminar Flow

The Laminar Flow interface calculates the fluid flow in the forced convection simulation in this research.

5.3.6 Mass transfer

The models in this research that involve mass transfer require the Transport of Diluted Species interface (a Chemical Species Transport interface) in COMSOL's base license.

5.4 Solving

COMSOL uses the finite element method to solve the models created by the user. This method is discussed next.

5.4.1 Finite element method

This section describes how the finite element method approximates a partial differential equation problem with a problem that has a finite number of unknowns, which is a discretization of the original problem.

The starting point in the finite element method is the partition of the geometry into mesh elements, which are small units of a simple shape. Once the mesh has been created, approximations to the dependent variables can be introduced. For this discussion, one can start with the case of a single dependent variable u. The idea is to approximate u with a function that one can describe with a finite number of parameters called degrees of freedom. Inserting this approximation into the weak form of the equation generates a system of equations for the degrees of freedom.

One can start with a simple example: linear elements in one dimension (1-D). Assume that the mesh consists of only two mesh intervals: $0 < x < 1$ and $1 < x < 2$. Linear elements means that on each mesh interval the continuous function is linear (affine); therefore, the

only fact one needs to know in order to characterize u uniquely is its values at the node points $x_1 = 0$, $x_2 = 1$, $x_3 = 2$. Identify these as $U_1 = u(0)$, $U_2 = u(1)$, $U_3 = u(2)$; these are the degrees of freedom.

One can then write

$$U(x) = U_1\varphi_1(x) + U_2\varphi_2(x) + U_1\varphi_3(x) \qquad (5-1)$$

where $\varphi_i(x)$ are certain piecewise linear functions. Specifically, $\varphi_i(x)$ is the function that is linear on each mesh interval, and equals 1 at the i^{th} node point, and equals 0 at the other node points. For example:

$$\varphi_1(x) = \begin{cases} 1-x & \text{if } 0 \le x \le 1 \\ 0 & \text{if } 1 \le x \le 2 \end{cases} \qquad (5-2)$$

The $\varphi_i(x)$ are called the basis functions. The set of functions $u(x)$ is a linear function space called the finite element space.

The preceding examples are special cases of the Lagrange element. Consider a positive integer k, the order of the Lagrange element. The functions u in this finite element space are piecewise polynomials of degree k ; in other words, on each mesh element u is a polynomial of degree k. To describe such a function it is sufficient to give its values in the Lagrange points of order k. These are the points whose local (element) coordinates are integer multiples of $1/k$. For a triangular mesh in 2-D with $k = 2$, this means that there are node points at the corners and side midpoints of all mesh triangles. For each of these node points p_i, there exists a degree of freedom $Ui = u(p_i)$ and a basis

function φ_i . The restriction of the basis function φ_i to a mesh element is a polynomial of degree (at most) *k* in the local coordinates such that $\varphi_i = 1$ at node *i*, and $\varphi_i = 0$ at all other nodes. Therefore the basis functions are continuous and:

$$u = \sum_i U_i \varphi_i \qquad (5-3)$$

The next step in the finite element method is the discretization of the partial differential equation that describes the physics of the COMSOL simulation; a 2-D stationary problem will be considered for simplicity. The starting point is the weak formulation of the problem. First is the discretization of the constraints:

$$0 = R^{(2)} \text{on } \Omega \qquad (5-4)$$

$$0 = R^{(1)} \text{on B} \qquad (5-5)$$

$$0 = R^{(0)} \text{on P} \qquad (5-6)$$

where $R^{(n)}$ is the Euclidean *n*-space, and Ω, B, and P are the are domain, boundary, and point. The weak equation is then discretized. The weak equation is the differential equation (such as the Navier-Stokes equation) that is rewritten without derivatives of the unknown function, usually by multiplying by an arbitrary "test function" (here the basis function), and then integrating (Amit, 2012). A discretization of the stationary problem is then:

$$0 = L(U) - N_F(U)\Lambda \qquad (5-7)$$

$$0 = M(U) \qquad (5-8)$$

where L is the residual vector, U is the solution vector, Λ is the Lagrange multiplier vector, N_F is the constraint force Jacobian matrix, and M is the constraint residual; Λ and U are then solved for.

5.5 Postprocessing

After the solver has arrived at solution to the problem, the results are then visualized through Surface plots (showing temperature distributions, for example) and Arrow Surface plots (showing velocity distributions, for example).

5.5.1 Line Integration, Surface integration, Volume Integration

The different types of Integrations are used in this research to find an average value over 1-D (Line), 2-D (Surface) and 3-D (Volume) domains. In this research, the Integrations are used to find average temperatures, concentrations, and velocity magnitudes.

5.5.2 Cut Point 2D

The Cut Point 2D is a subnode that is added under the Data Sets node when information is needed at a point in the geometry; in this research, the temperature at the center of the dough/bread as a function of time is required.

5.5.3 Cut Line 2D

The Cut Line 2D is a subnode that is added under the Data Sets node when information is needed along an arbitrary line in the geometry; in this research, the temperatures along a central vertical line through the container material and dough/bread are needed.

CHAPTER VI

COMSOL MODELS, TWO-DIMENSIONAL

This chapter presents the two-dimensional COMSOL models created in this research.

6.1 Radiation COMSOL models

One of the first oven and food models was derived from a model that involved the effect of radiation on a block of steel. This block of steel is referred to as the container material. Researchers often use a model material (steel instead of dough/bread, in this research) to gain confidence in their use of CFD packages (Denys et al, 2007). Later, the idea of modeling the food within the container was abandoned, keeping only the modeling of the food.

6.1.1 Distantly-spaced heating elements, steel container

A COMSOL simulation was performed that corresponds to the analytical calculations in Section 3.1.1. Figure 6.1 shows the COMSOL geometry of this model.

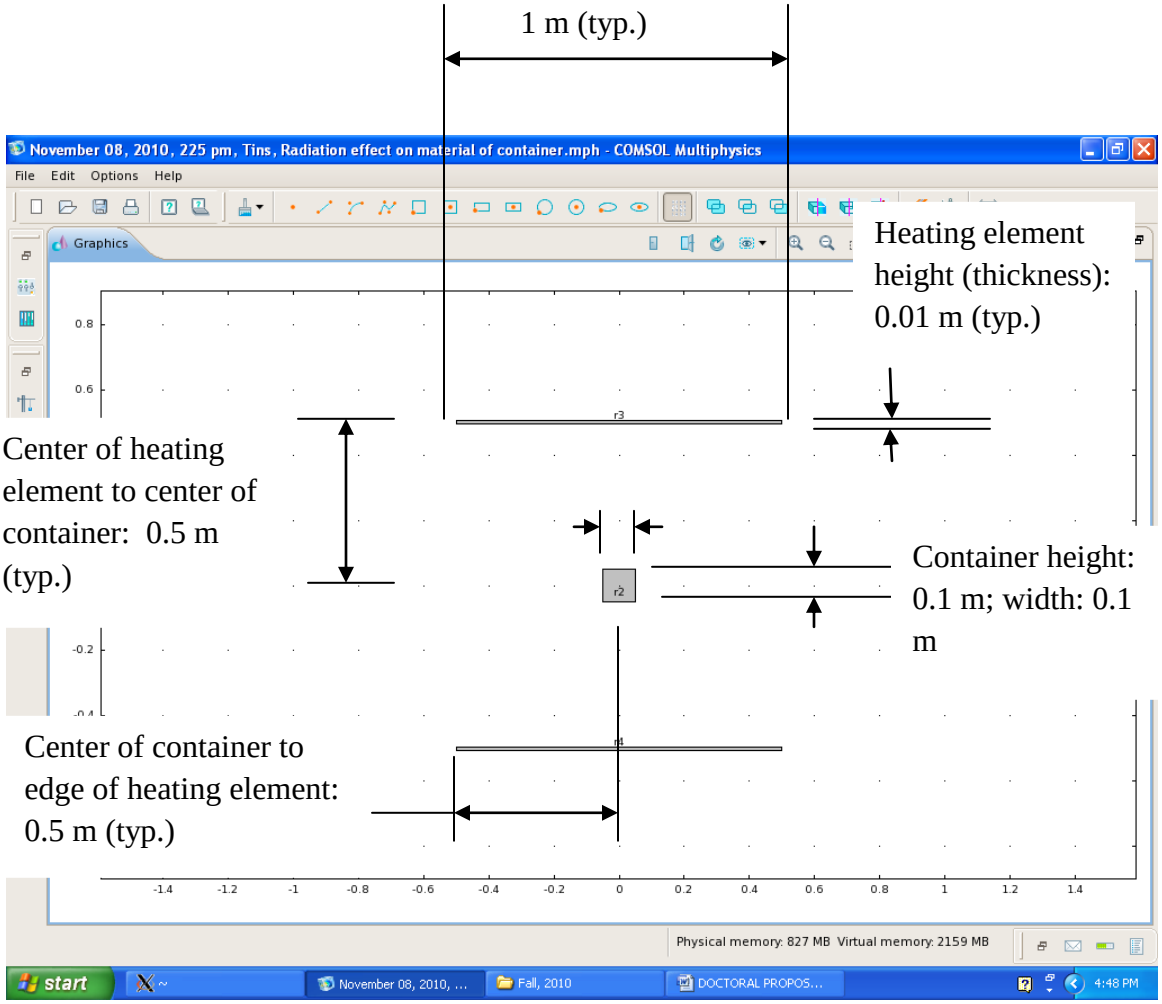

Figure 6.1: Radiation effect on surface of container material, COMSOL geometry

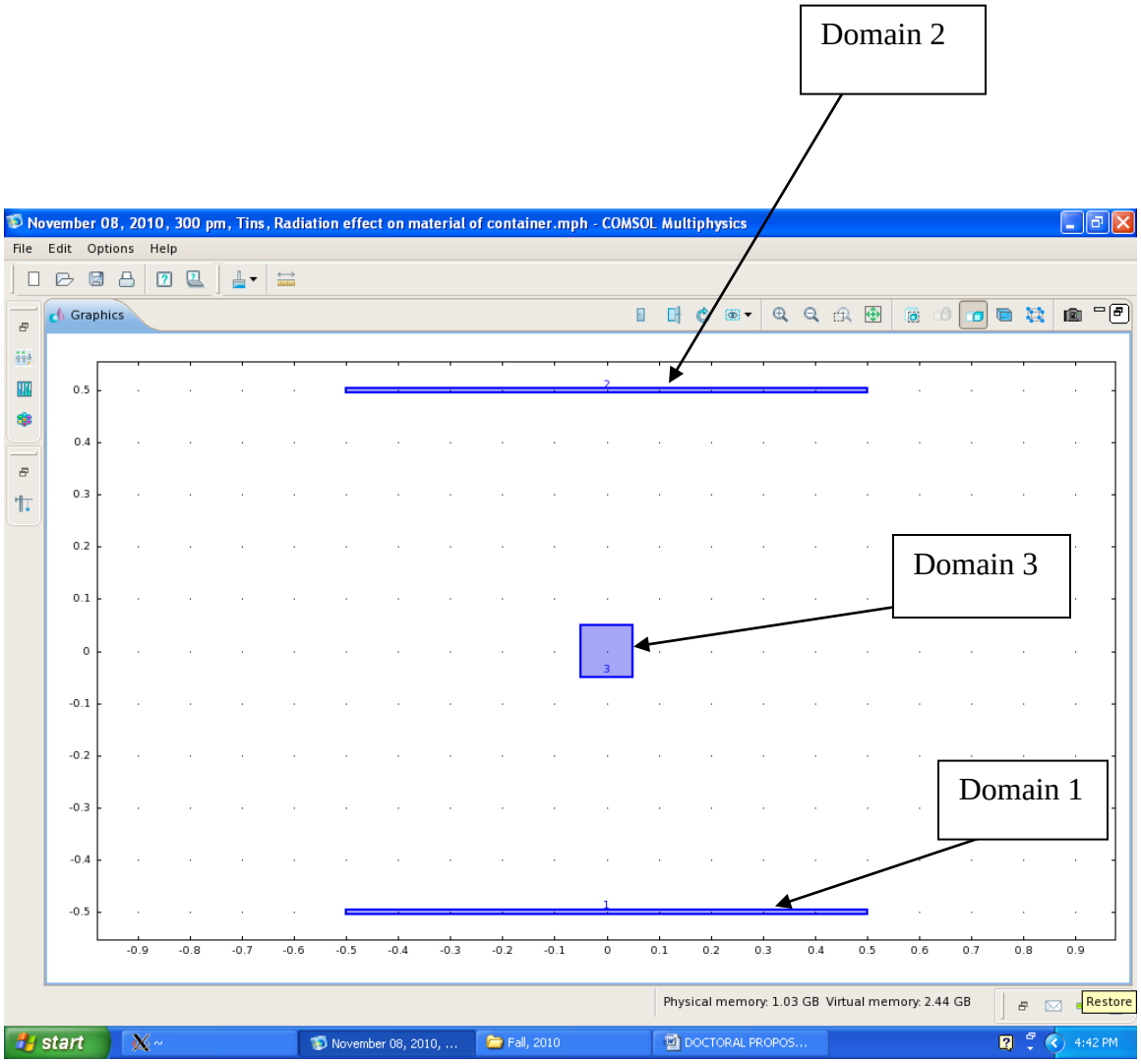

Figure 6.2: Radiation effect on surface of container, COMSOL domains

Figure 6.2 shows the COMSOL domains used in the model of the radiation effect on the surface of the container. The mesh used is COMSOL's initial mesh (not refined). The base COMSOL Multiphysics license and Heat Transfer Module are used in this model.

Table 6.1: Domain material properties and initial conditions, radiation effect on surface of container, COMSOL model

Thermal conductivity (W/(m·C))	Density (kg/m^3)	Heat Capacity at constant pressure (J/(kg·C))	Initial Temperature (K)	Initial Surface Radiosity (default) (W/m^2)
52	7800	465	293.15	0

Domains 1, 2, and 3 have the properties and initial conditions listed in the Table 6.1; the properties are from Table 3.1, and the initial temperature is room temperature.

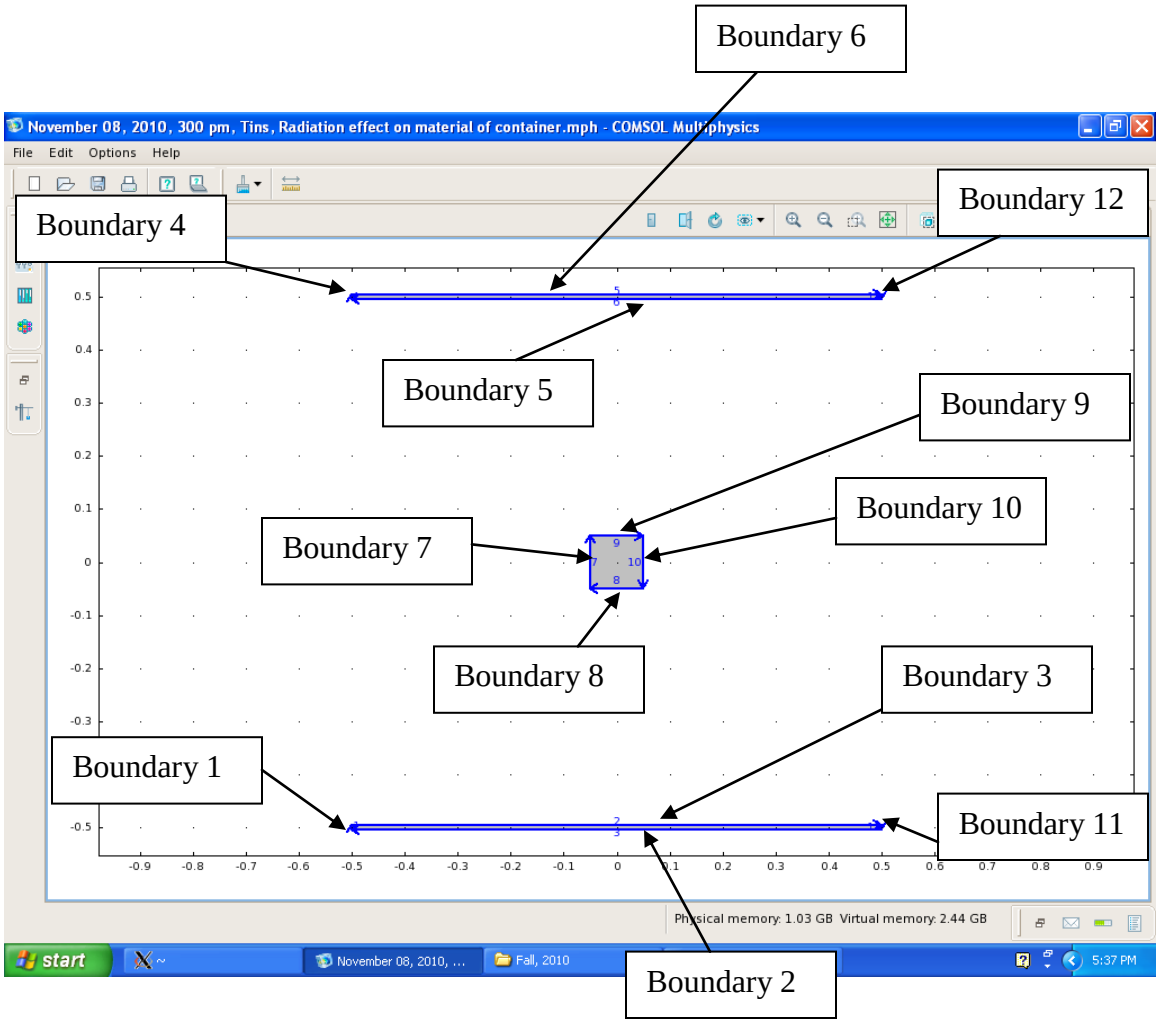

Figure 6.3: Radiation effect on surface of container, COMSOL boundary conditions

Figure 6.3 shows the boundary conditions used in the COMSOL model of the radiation effect on the surface of the container. The boundaries 1, 2, 3, 4, 5, 6, 11, and 12 are all fixed at a temperature of 533.15 K. The emissivity of steel can range from 0.1 (polished sheet) to 0.8 (sheet with rough oxide layer) (Siegel & Howell, 1981), and these two emissivities were individually modeled.

6.1.2 Distantly-spaced heating elements, food with constant properties

The first attempt at modeling food within an oven considered taking an average each of the following thermal properties: conductivity, specific heat, and density. Using the data in Table 1.1, these averages are as follows: average thermal conductivity is 0.1133 W m^{-1} °C^{-1}, average specific heat is 1941 (J kg^{-1} °C^{-1}), average density is 380 (kg/m^3). The COMSOL Multiphysics license and Heat Transfer Module are employed in this model.

Table 6.2: Domains 1 and 2 material properties and initial conditions, radiation effect on dough/bread, COMSOL model

Thermal conductivity (W/(m·C))	Density (kg/m^3)	Heat Capacity at constant pressure (J/(kg·C))	Initial Temperature (K)	Initial Surface Radiosity (default) (W/m^2)
52	7800	465	293.15	0

Domains 1 and 2 have the properties (from Table 3.1) and initial conditions listed in Table 6.2. These domains have the same geometry and location as shown in Figures 6.1 and 6.2. The default mesh is used for these domains.

Table 6.3: Domain 3 material properties and initial conditions, radiation effect on dough/bread, COMSOL model

Thermal conductivity (W/(m·C))	Density (kg/m^3)	Heat Capacity at constant pressure (J/(kg·C))	Initial Temperature (K)	Initial Surface Radiosity (default) (W/m^2)
0.1133	380	1941	293.15	0

Domain 3 has the properties and initial conditions listed in Table 6.4. This domain has the same geometry and location as shown in Figures 6.1 and 6.2. This domain mesh is refined twice (using COMSOL's default mesh refinement parameters).

Table 6.4 Boundary conditions, radiation effect on dough/bread, COMSOL model

Emissivity of Boundaries 1,2,3,4,5,11, 12	Emissivity of Boundaries 7,8,9,10	Temperature of Boundaries 1,2,3,4,5,11, 12
1	0.9	533.15 K

The boundary conditions for the Radiation Effect on Dough/Bread COMSOL model are shown in Table 6.4; the boundaries have the same locations as shown in Figure 6.3. The boundary parameters correspond to those given in Section 3.1.2. When the model was changed to that of 240 seconds (instead of 3600 seconds), only the heating element boundaries facing the dough/bread had an emissivity of 1; the rest of the heating element boundaries were insulated.

6.1.3 Closely-spaced heating elements, food with constant properties

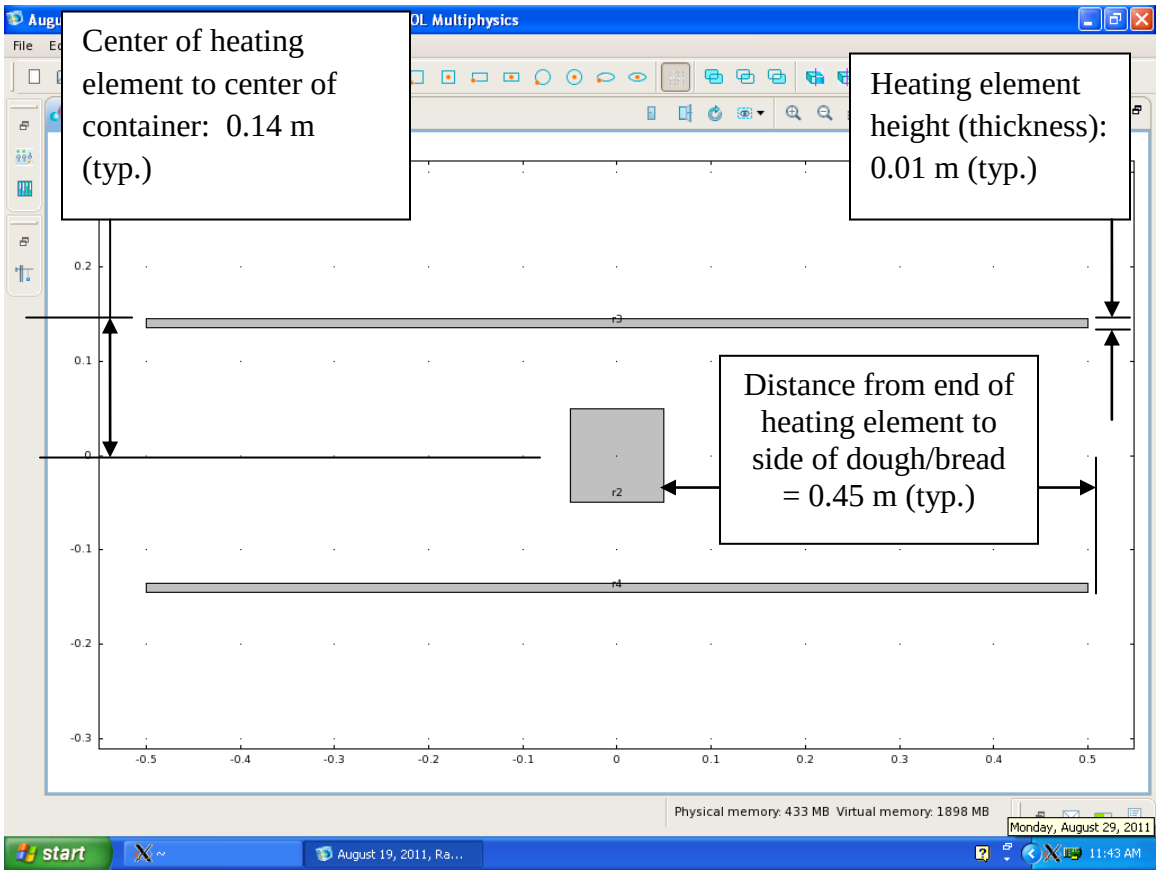

Figure 6.4: Radiation effect on dough/bread for closely-spaced heating elements, COMSOL geometry

Figure 6.4 shows the COMSOL geometry for the radiation effect on the dough/bread for the closely-spaced heating elements. All of the boundary conditions, domain

properties, initial conditions, and the rest of the geometry are the same as in Section 6.1.2. This model used the COMSOL Multiphysics license and Heat Transfer Module.

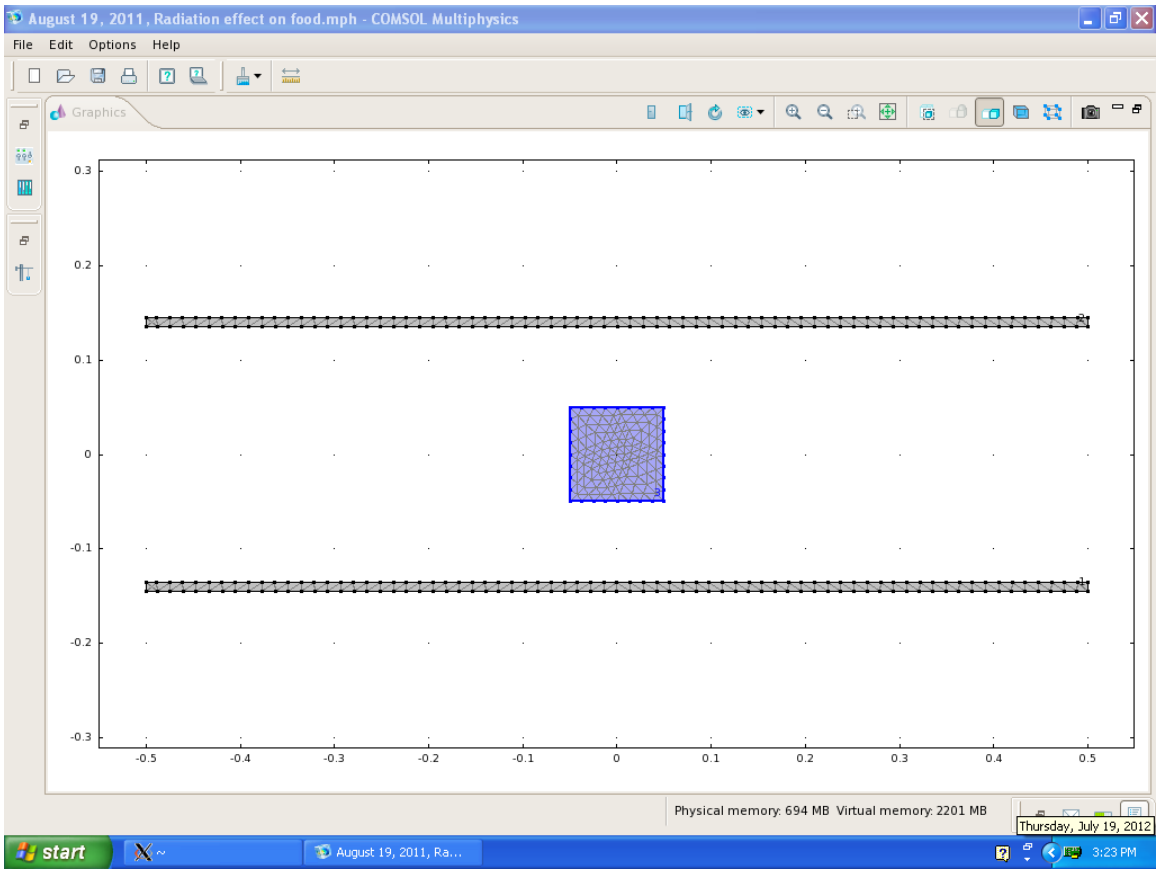

Figure 6.5: Radiation effect on dough/bread for closely-spaced heating elements, COMSOL mesh

Figure 6.5 shows the COMSOL mesh for the radiation effect on the dough/bread for the closely-spaced heating elements. The mesh for the dough/bread was refined twice.

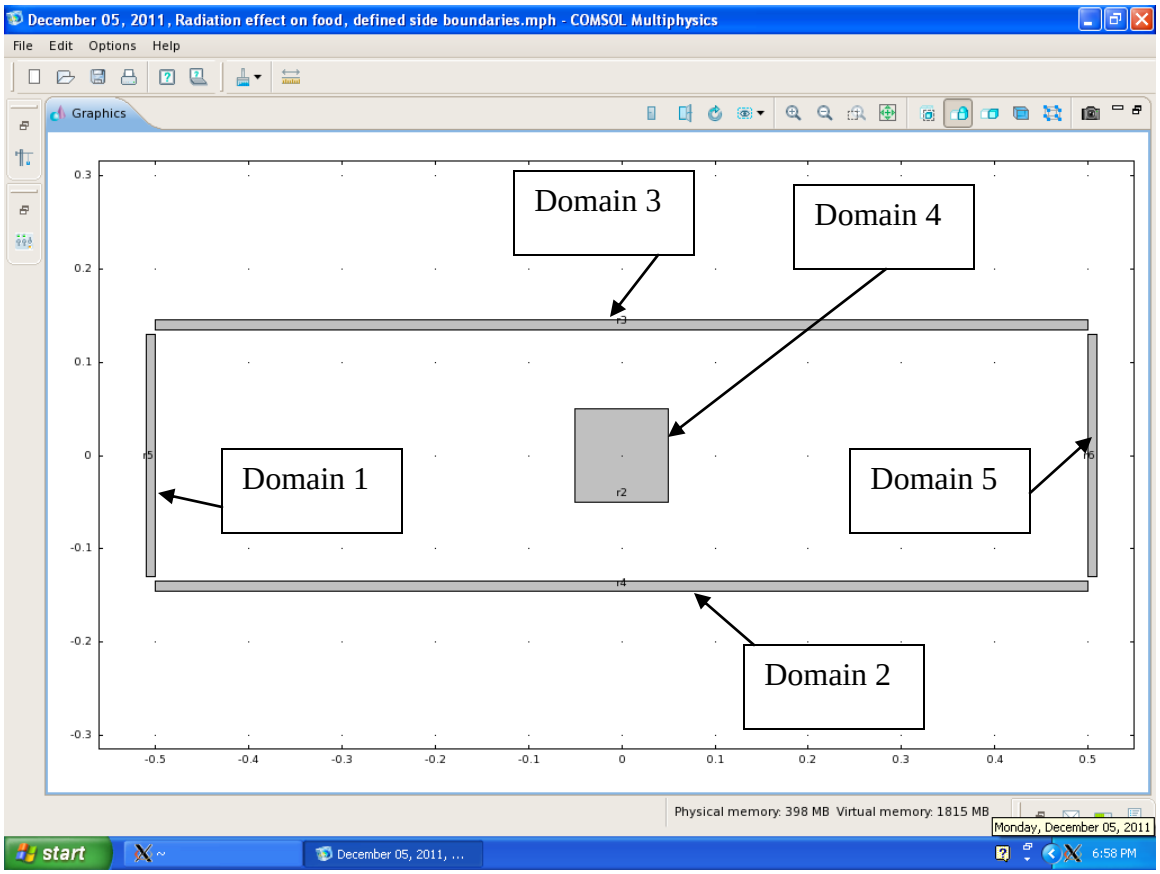

Figure 6.6 Radiation effect on dough/bread, with defined side boundaries geometry

Figure 6.6 shows the geometry for the radiation effect on dough/bread with defined side boundaries model. This geometry is the same as Figure 6.4 except for the addition of the rectangles associated with Domains 1 and 5; these two domains have widths and heights of 0.01m and 0.26 m, respectively, and each domain is horizontally positioned 0.505 m to the left and right, respectively, from (0,0). This model uses COMSOL's Multiphysics license and Heat Transfer Module. Domains 1, 2, 3, and 5 use the default mesh defined by COMSOL; Domain 4's mesh is refined twice. Domains 1, 2, 3, and 5 have the specifications of Table 6.2; Domain 4 has the specifications of Table 6.3. The boundaries of Domains 1 and 5 are specified as having a constant temperature of 293.15

K (room temperature); the boundaries of Domains 2 and 3 are 533.15 K. The emissivities of the boundaries of Domains 1, 2, 3, and 5 are 1.

Lastly, a model that involved the heating elements impinging radiation upon dough/bread of various heights was effected. This model is the same as in Section 6.1.2 (without defined side boundaries, and at 240 seconds), except the dough/bread height is specified as 2 inches, 4 inches, then 6 inches.

6.1.4 Distantly-spaced heating elements, food with varying properties

The next step is to model the food with properties that vary with temperature (but not moisture). This model is similar to Zhou and Therdai (2007), who modeled the dough/bread with only temperature-dependent properties; their justification is that the moisture content difference in dough versus crumb is not significant, and that bread is significantly more crumb than crust. They therefore did not model the dough/bread as having moisture-dependent properties. First, a curve is fitted to the density data in Table 1.1 via quadratic regression to yield the Equation (6-1):

$$\rho = -0.647\,T + 587 \qquad (6-1)$$

Figure 6.7 shows a graph of the dough/bread density versus temperature, along with a polynomial fitted to the data.

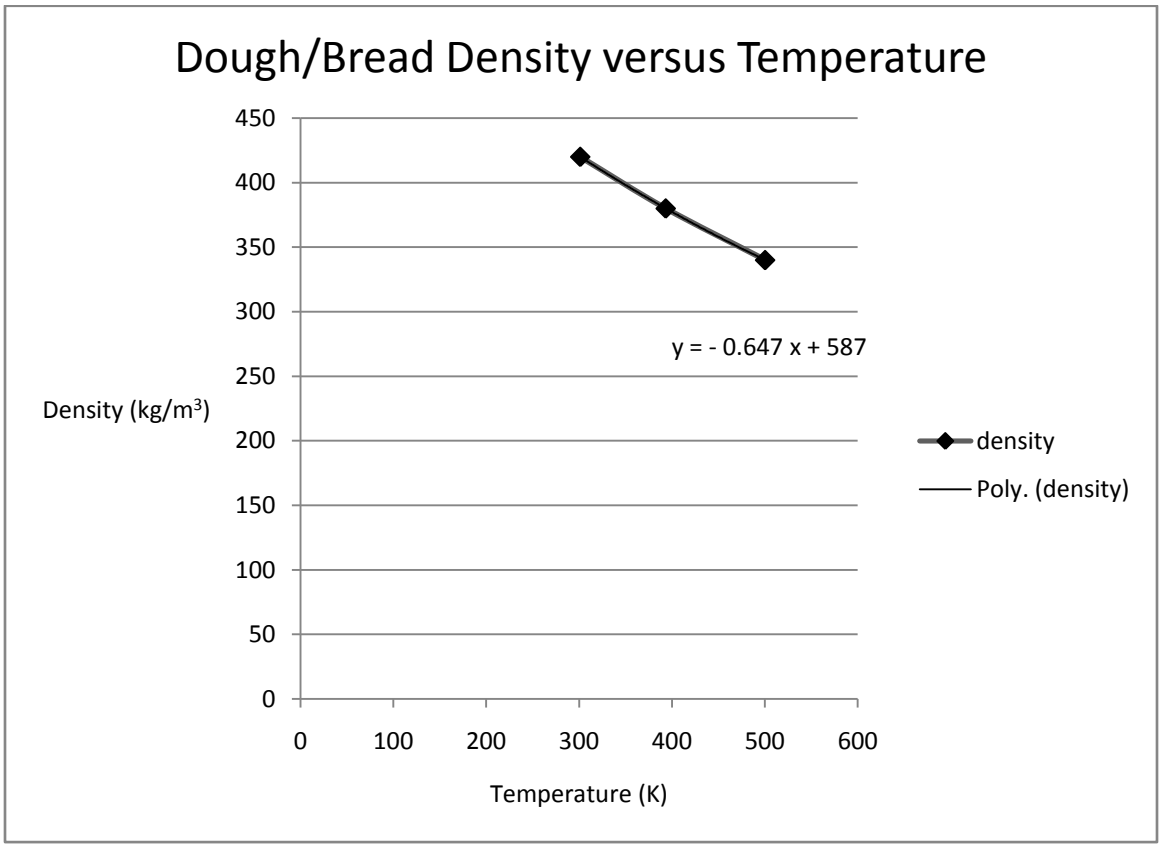

Figure 6.7: Dough/bread density versus temperature

This model (and the other models involving temperature-varying properties) uses the COMSOL Multiphysics License in conjunction with the Heat Transfer Module. All of the models involving temperature-varying properties use the default mesh for all domains. The geometry for the models are the same as in Figure 6.1, the boundaries have the same locations as shown in Figure 6.3, and the boundary specifications are the same as in Table 6.4. The domain numbering is the same as in Figure 6.2. Table 6.5 shows the Domains 1 and 2 (both domains of the heating elements) material properties (from Table

3.1) and initial conditions for all of the models having dough/bread temperature-varying properties. The initial conditions were chosen to match predicted final values in order to promote convergence; The initial temperature is from Section 3.1.1, and the initial surface radiosity is from Equation (3-10). Table 6.6 shows the Domain 3 (dough/bread domain) material properties (from Table 6.3, except density) and initial conditions for the temperature-varying density model. The initial temperature is room temperature, and the initial surface radiosity is chosen to match the predicted final value to promote convergence; this value is calculated from Appendix C.

Table 6.5: Domains 1 and 2 material properties and initial conditions, radiation effect on dough/bread with temperature-varying density, COMSOL model

Thermal conductivity (W/(m·C))	Density (kg/m^3)	Heat Capacity at constant pressure (J/(kg·C))	Initial Temperature (K)	Initial Surface Radiosity (W/m^2)
52	7800	465	533.15	4581.2

Table 6.6: Domain 3 material properties and initial conditions, radiation effect on dough/bread with temperature-varying density, COMSOL model

Thermal conductivity (W/(m·C))	Density (kg/m^3)	Heat Capacity at constant pressure (J/(kg·C))	Initial Temperature (K)	Initial Surface Radiosity (W/m^2)
0.1133	Equation (6-1)	1941	293.15	729.3

Next, a curve is fitted to the specific heat data in Table 1.1 via quadratic regression to yield Equation (6-2):

$$C_p = 0.077\,T^2 - 68.94\,T + 16646 \qquad (6-2)$$

Figure 6.8 shows a graph of the dough/bread specific heat versus temperature, along with a polynomial fitted to the data.

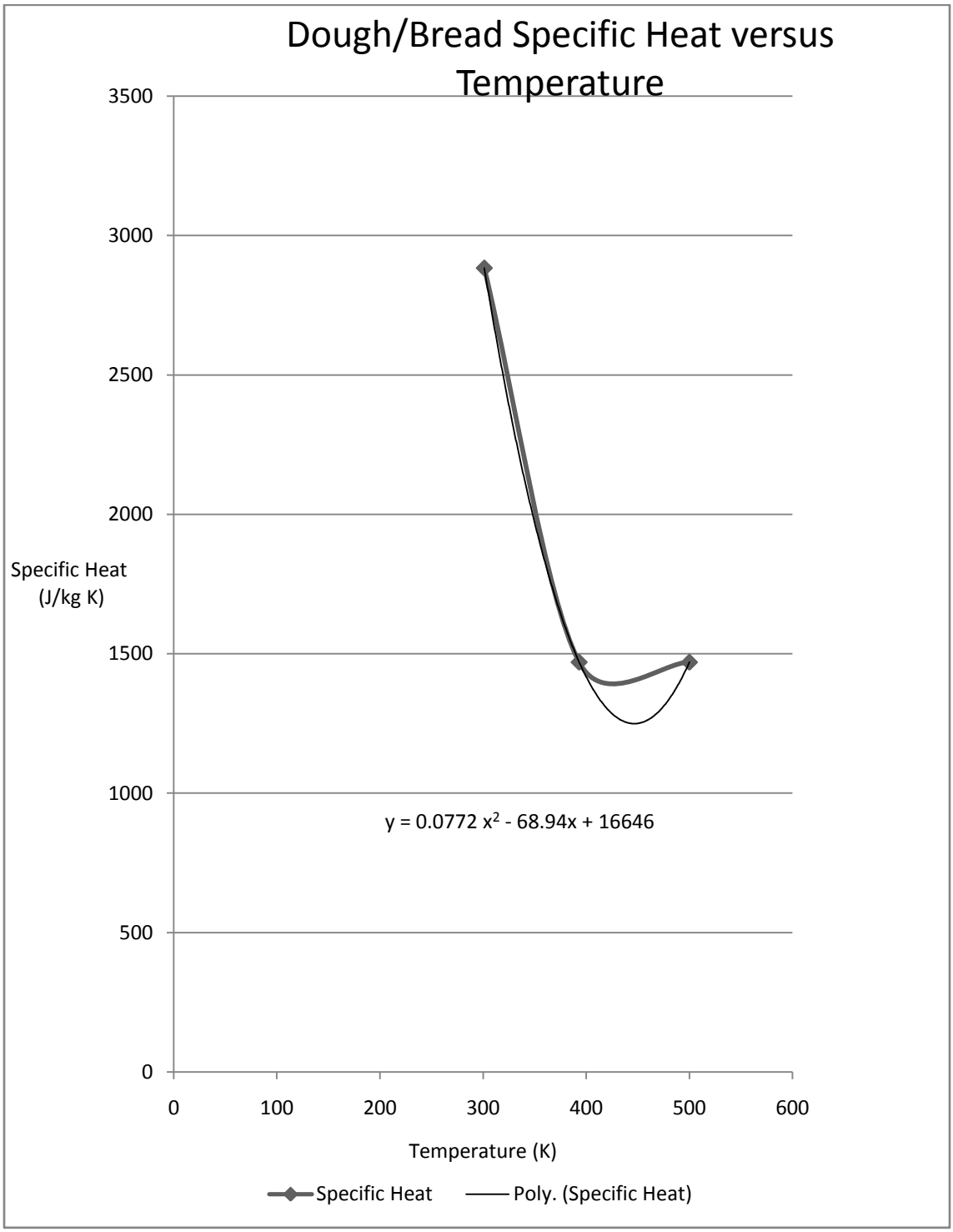

Figure 6.8: Dough/bread specific heat versus temperature

Table 6.7 displays the Domain 3 (dough/bread domain) material properties and initial conditions for the temperature-varying specific heat model. This table is filled similar to the Table 6.6.

Table 6.7: Domain 3 material properties and initial conditions, radiation effect on dough/bread with temperature-varying specific heat, COMSOL model

Thermal conductivity (W/(m·C))	Density (kg/m^3)	Heat Capacity at constant pressure (J/(kg·C))	Initial Temperature (K)	Initial Surface Radiosity (W/m^2)
0.1133	380	Equation (6-2)	293.15	729.3

The committee stated that it would be appropriate to model the dough/bread as having a thermal conductivity that varied with temperature. A member of the committee believed that thermal conductivity would decrease during the baking process, due to the fact that there is loss of water from the dough. This is believed to be at least partly the case.

A graph was made of the dough/bread thermal conductivity using Table 1.1; a curve was fitted to the graph, thereby giving an equation for thermal conductivity as a function of temperature. This equation was incorporated into the material properties of the dough/bread COMSOL model.

Fitting a curve to the data for conductivity yields the Equation (6-3):

$$k = 0.00001\,T^2 - 0.00634\,T + 1.47 \qquad (6-3)$$

Figure 6.9 shows a graph of dough/bread conductivity versus temperature, along with a polynomial fitted to the data.

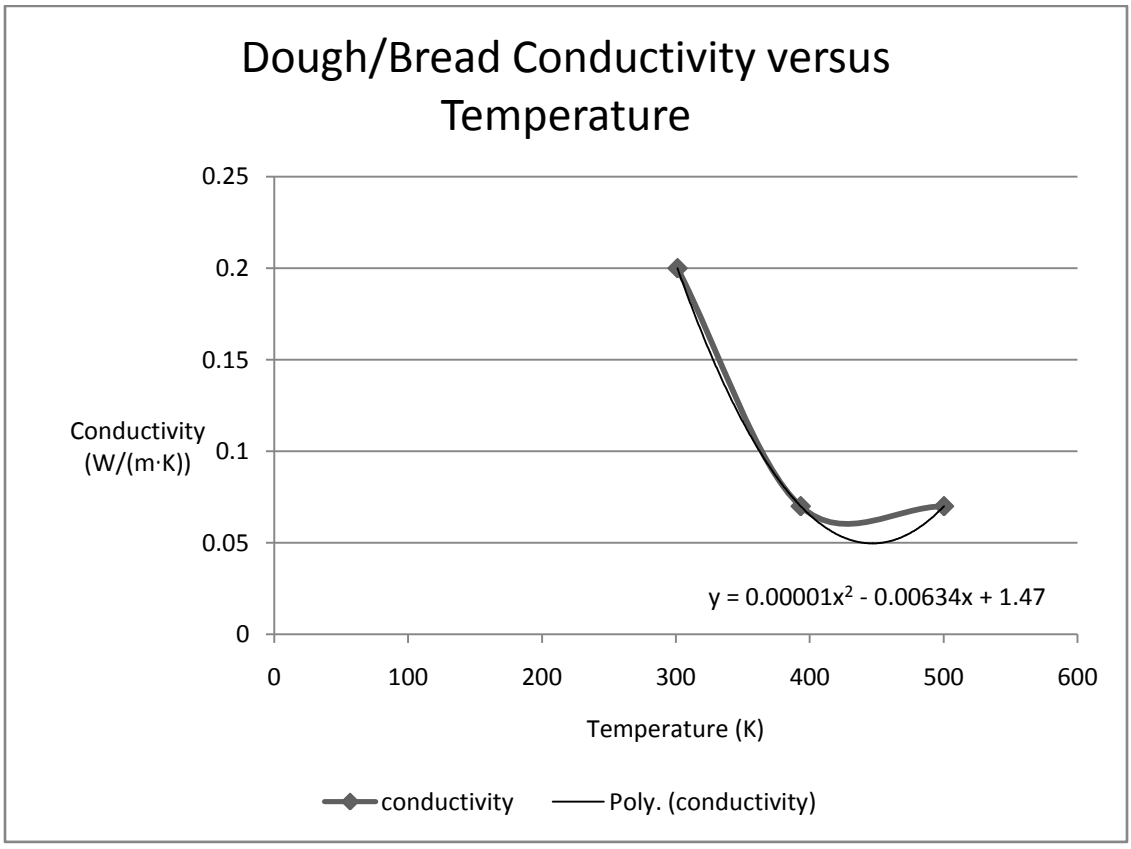

Figure 6.9: Dough/bread thermal conductivity versus temperature

At this point, a COMSOL model was completed in which dough/bread thermal conductivity varies with temperature. Domain 3 has the properties and initial conditions listed in Table 6.8; this table is created similar to Table 6.6.

Table 6.8: Domain 3 material properties and initial conditions, radiation effect on dough/bread with temperature-varying thermal conductivity, COMSOL model

Thermal conductivity (W/(m·C))	Density (kg/m^3)	Heat Capacity at constant pressure (J/(kg·C))	Initial Temperature (K)	Initial Surface Radiosity (W/m^2)
Equation (6-3)	380	1941	293.15	729.3

6.2 Convection COMSOL model

According to Mirade et al (2004), for biscuit baking in band ovens, the total heat transfer is 37 % by convection. Both free (natural) and forced convection are examined in the research.

6.2.1 Dimensional free (natural) convection

Figure 6.10 shows the COMSOL geometry of a room, and an oven with heating elements. This model used the COMSOL Multiphysics license, and the Heat Transfer Module; the initial COMSOL mesh (unrefined) was employed.

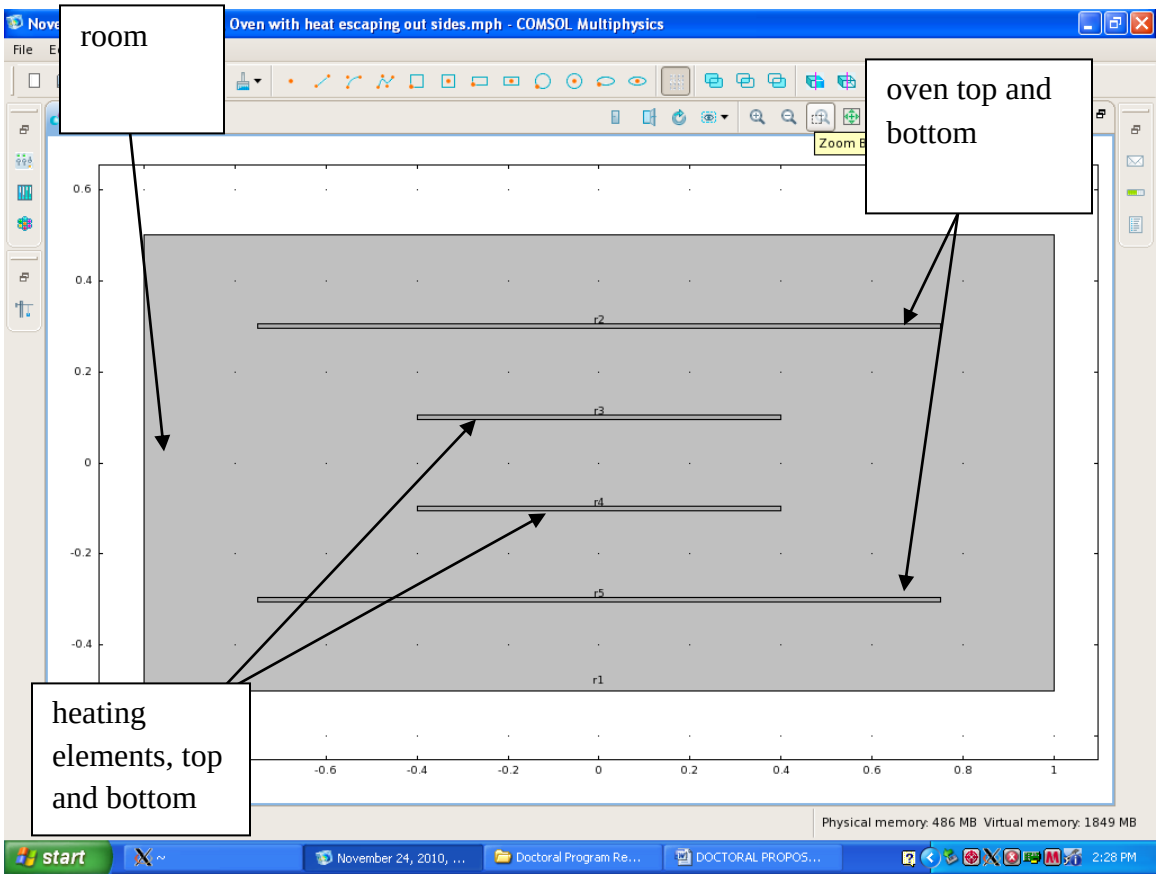

Figure 6.10: Oven with heating elements inside room, COMSOL model

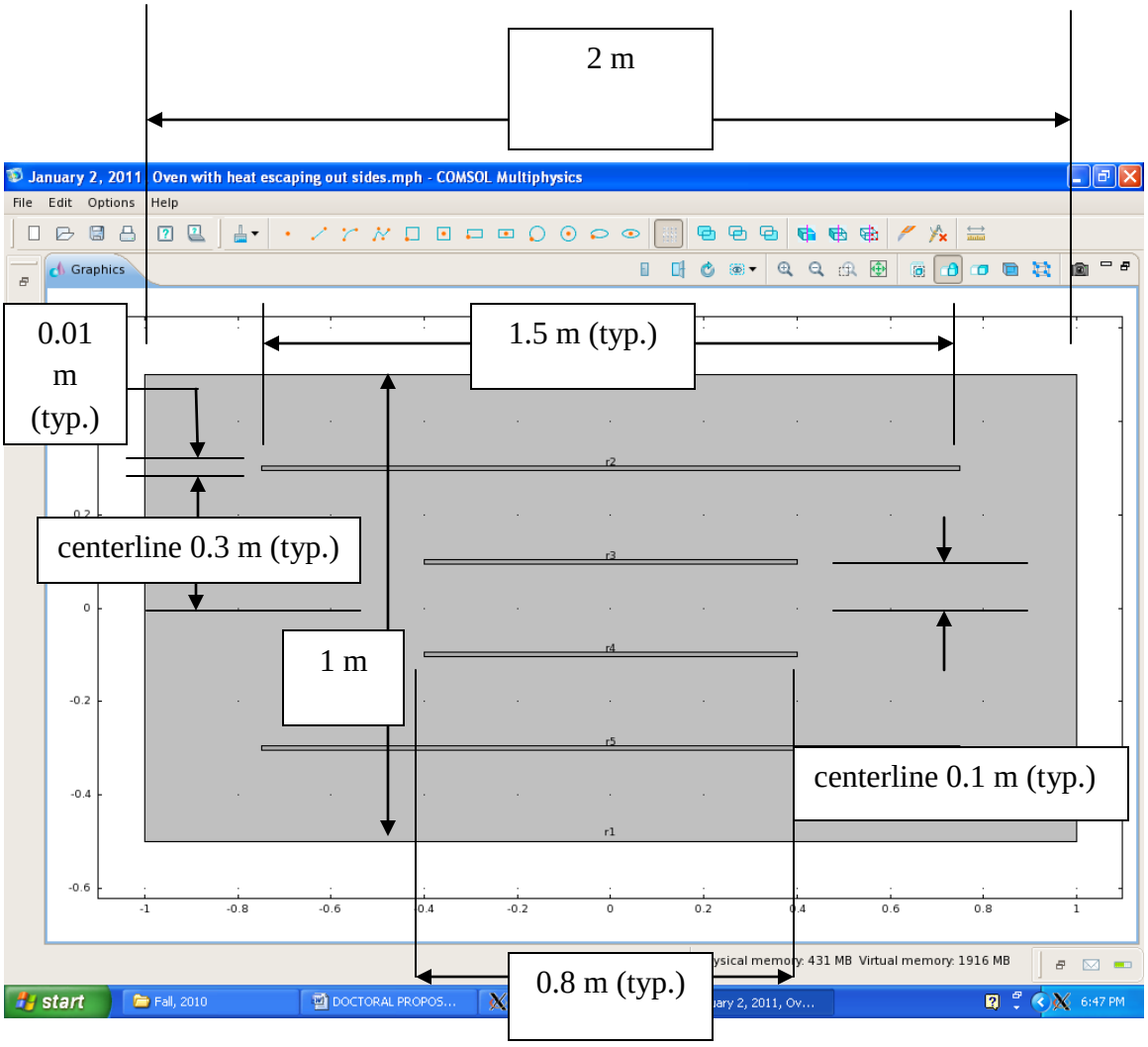

Figure 6.11: Oven with heating elements inside room, COMSOL geometry

Figure 6.11 shows the geometry of the room, oven, and heating elements. The horizontal center point of all the rectangles shown is at x= 0.

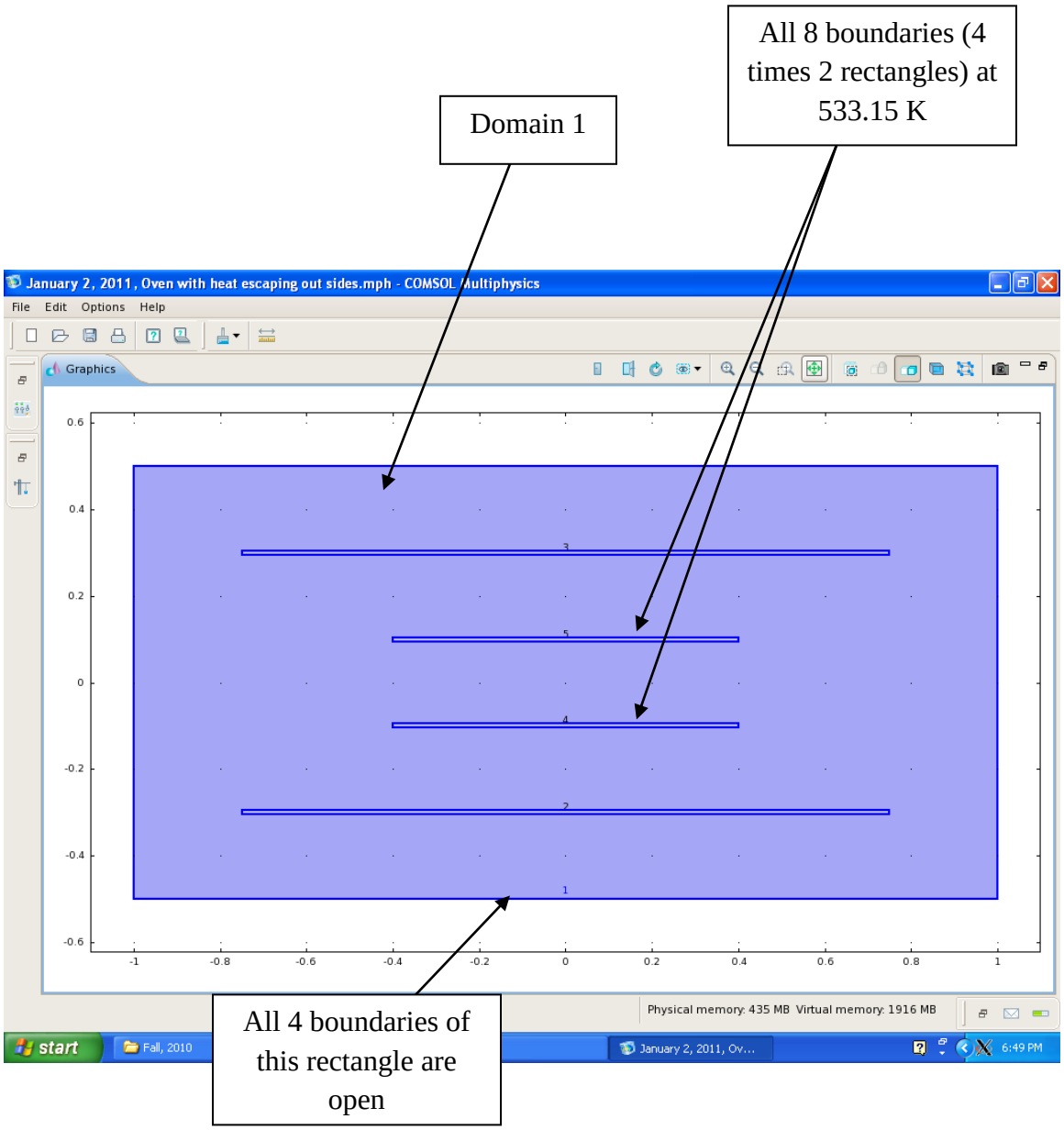

Figure 6.12: Oven with heating elements inside room, COMSOL boundary conditions and domain

Figure 6.12 shows the boundary conditions and domain of the room, and oven with heating elements.

Table 6.9: Domain 1 material properties and initial condition, room and oven with heating elements, COMSOL model

Thermal conductivity (W/(m·C))	Density (kg/m^3)	Heat Capacity at constant pressure (J/(kg·C))	Initial Temperature (K)	Ratio of Specific Heats	Dynamic Viscosity (Pa·s)
27e-03	Initially 1.21, then rho	1006	293.15	1.4	1.81E-05

Table 6.9 shows the properties and initial condition (room temperature) of the fluid used in the COMSOL simulation of room and oven with heating elements. The thermal and physical properties are from Incropera and Dewitt (1990), and the fluid property is from White (1986). The nonisothermal flow application is employed.

6.2.2 Nondimensional free (natural) convection

This model's oven and room definitions are as shown in Figure 6.10. The geometry of the nondimensional model are also the same as the dimensional model, and are shown in Figure 6.11. This model uses COMSOL's Multiphysics license, with a default mesh.

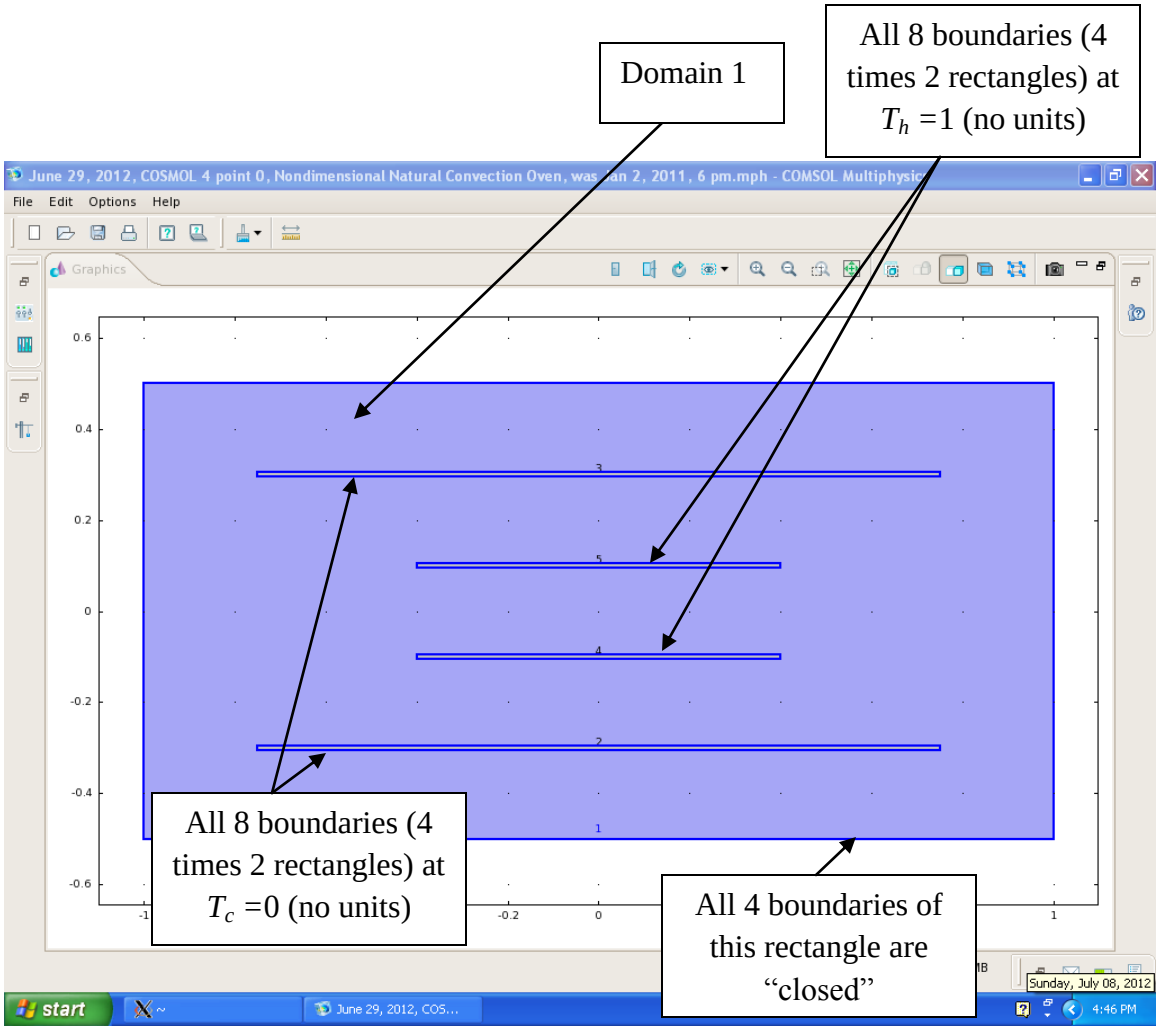

Figure 6.13: Nondimensional, oven with heating elements inside room, COMSOL boundary conditions and domain

Table 6.10: Domain 1 laminar flow material properties and initial condition, room and oven with heating elements, nondimensional COMSOL model

Density (kg/m^3)	Dynamic Viscosity (Pa·s)	Initial Velocity field	Initial Pressure (no units)	Rayleigh number
1	1	0	0	1, 1E1, 1E2, 1E3, 1E4,1E5

Table 6.10 shows the domain 1 laminar flow material properties and initial condition for the room and oven with heating elements for the nondimensional COMSOL model. Table 6.11 shows the domain 1 heat transfer material properties and initial condition for the room and oven with heating elements for the nondimensional COMSOL model. The values for both of these tables are obtained from COMSOL (2010 e).

Table 6.11 Domain 1 heat transfer material properties and initial conditions, room and oven with heating elements, nondimensional COMSOL model

Absolute pressure (no units)	Thermal conductivity (W/(m·C))	Heat Capacity at constant pressure (J/(kg·K))	Ratio of Specific Heats	Initial Temperature (no units)
0	1	$Pr = 0.71$	1	0

6.2.3 Forced convection

A COMSOL geometry of an oven with exhaust stack is shown in Figure 6.14. This model uses COMSOL's Multiphysics license, with a default mesh.

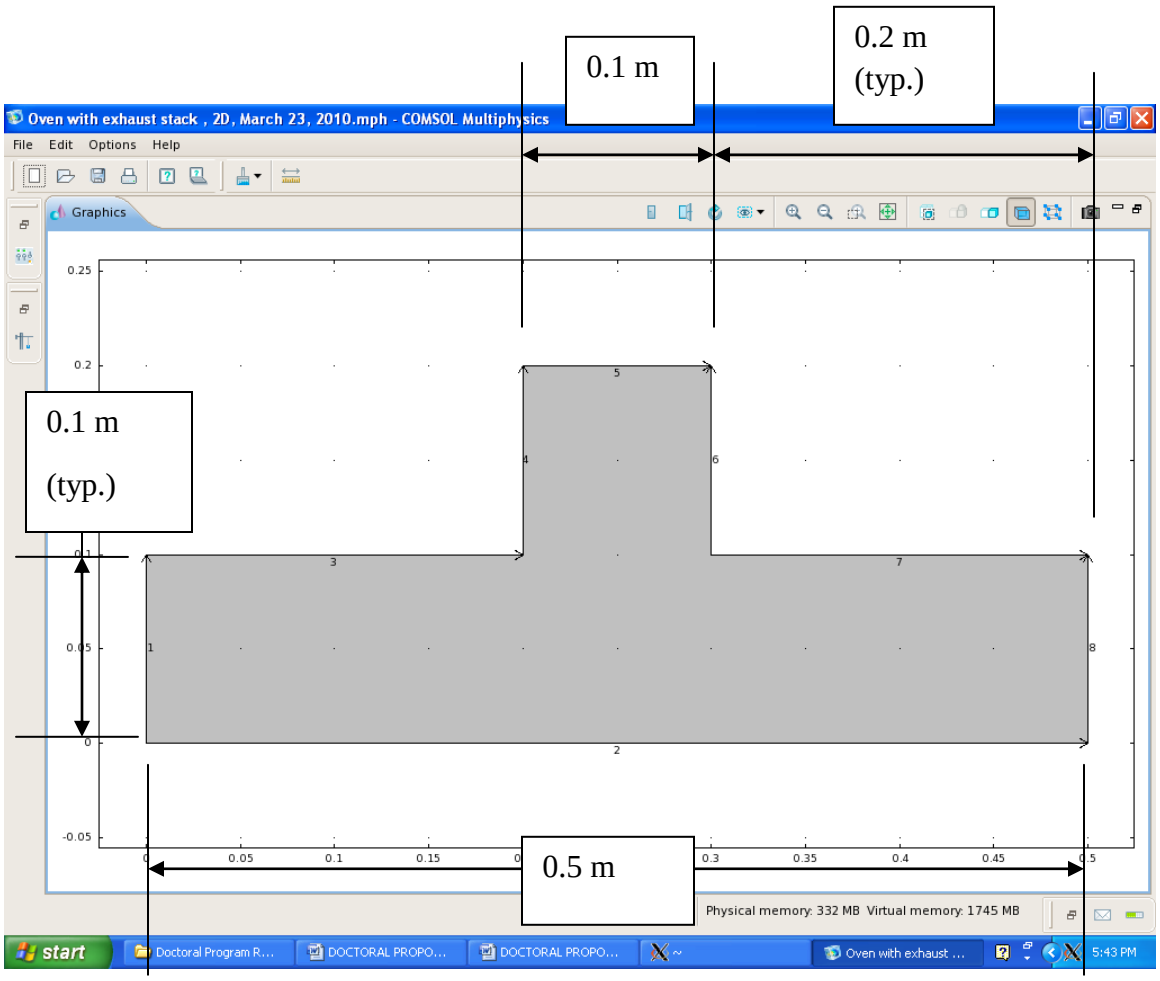

Figure 6.14: Oven with exhaust stack, COMSOL geometry

Figure 6.15 shows the boundary conditions and domain of the COMSOL model of an oven with exhaust stack; the boundary conditions are obtained from Baik et al (2000 a).

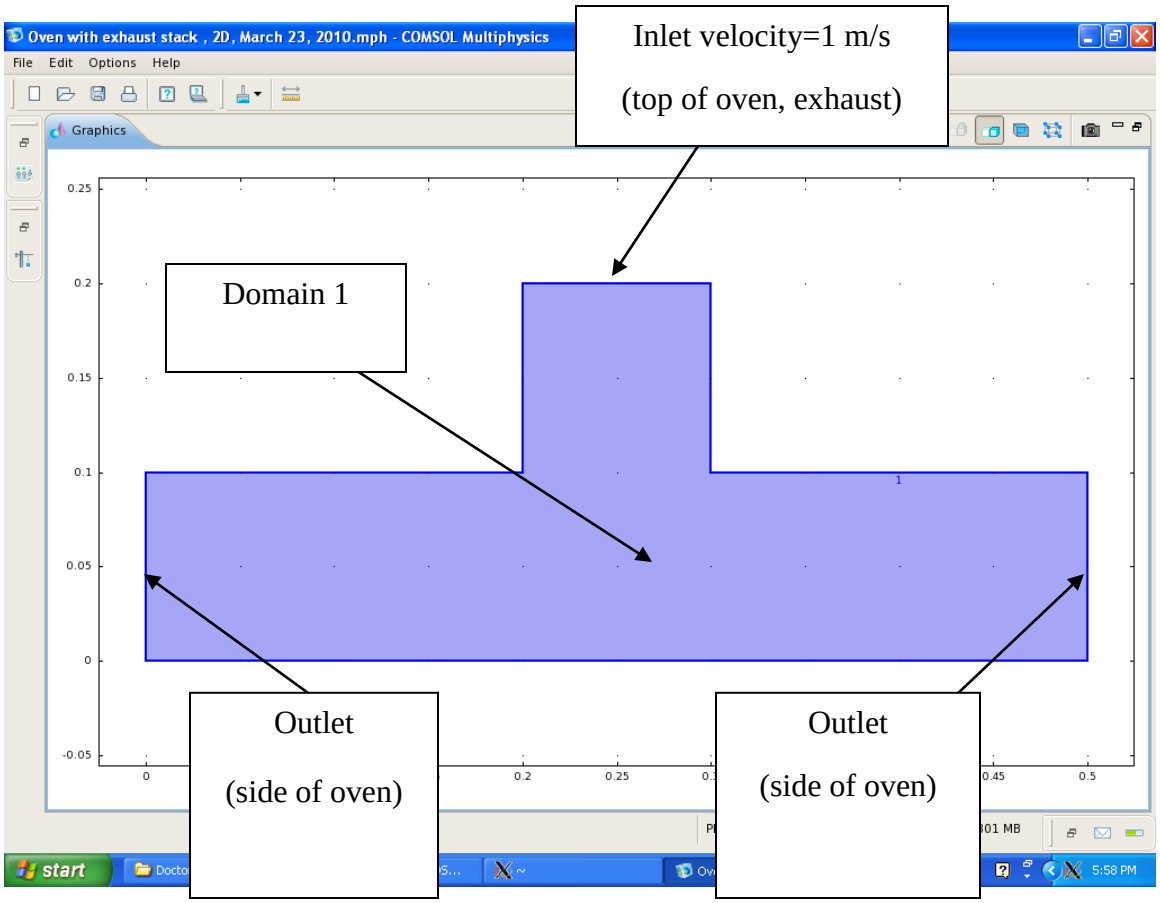

Figure 6.15: Oven with exhaust stack, COMSOL boundary conditions and domain

Table 6.12: Domain 1 material properties, oven with exhaust stack, COMSOL model

Density (kg/m^3)	Dynamic viscosity (Pa·s)
1	1E-05

Table 6.12 shows the properties of the fluid used in the COMSOL model of an oven with an exhaust stack. These properties are similar to, but not exactly the same as that of air from White (1986). The initial pressure is set to 0 Pa, which is the default value in COMSOL.

6.3 Moisture COMSOL models

The moisture COMSOL models (with, and without heat transfer and convection) are presented in this section.

6.3.1 Moisture loss without heat transfer and convection

The committee suggested doing as moisture analysis on the dough/bread; Figure 6.16 shows a COMSOL model (including the domains) started to that effect. The geometry of the oven, heating elements, and room are the same as in Figure 6.11. The geometry of the dough is the same as the container geometry in Figure 6.1. The base COMSOL Multiphysics license is employed; the Transport of Dilute Species application is used. The mesh is default (not refined).

The water content in dough/bread is approximately 40 % by weight (Czuchajowska et al, 1988, Thorvaldsson & Janestad, 1999). This means that for 100 kg of dough/bread, 40 kg of it will be water. COMSOL's default units for *c* (concentration) are mol/m^3, so the conversion is calculated as follows:

$$\frac{40\ \text{kg water}}{100\ \text{kg bread}} \times \frac{\frac{1000\ \text{g water}}{1\ \text{kg water}}}{\frac{1\ \text{m}^3\ \text{bread}}{380\ \text{kg bread}}} \times \frac{\frac{1\ \text{mol water}}{18.015\ \text{g water}}}{1} = \frac{8437.4\ \text{mol water}}{\text{m}^3\ \text{bread}} \qquad (6-4)$$

Table 6.13 shows the domain initial concentration and diffusion coefficients for the COMSOL model without heat transfer and convection. The diffusion coefficient is obtained from a similar diffusion coefficient in Table 6.14.

Table 6.13: Domain initial concentration and diffusion coefficients

Domain	Initial concentration (mol/m^3)	Diffusion coefficient (m^2/s)
1	0 (default)	1×10^{-9}, then 1×10^{-10}
6	8437.4 (from Eqn. 6-4)	1×10^{-9} , then 1×10^{-10}

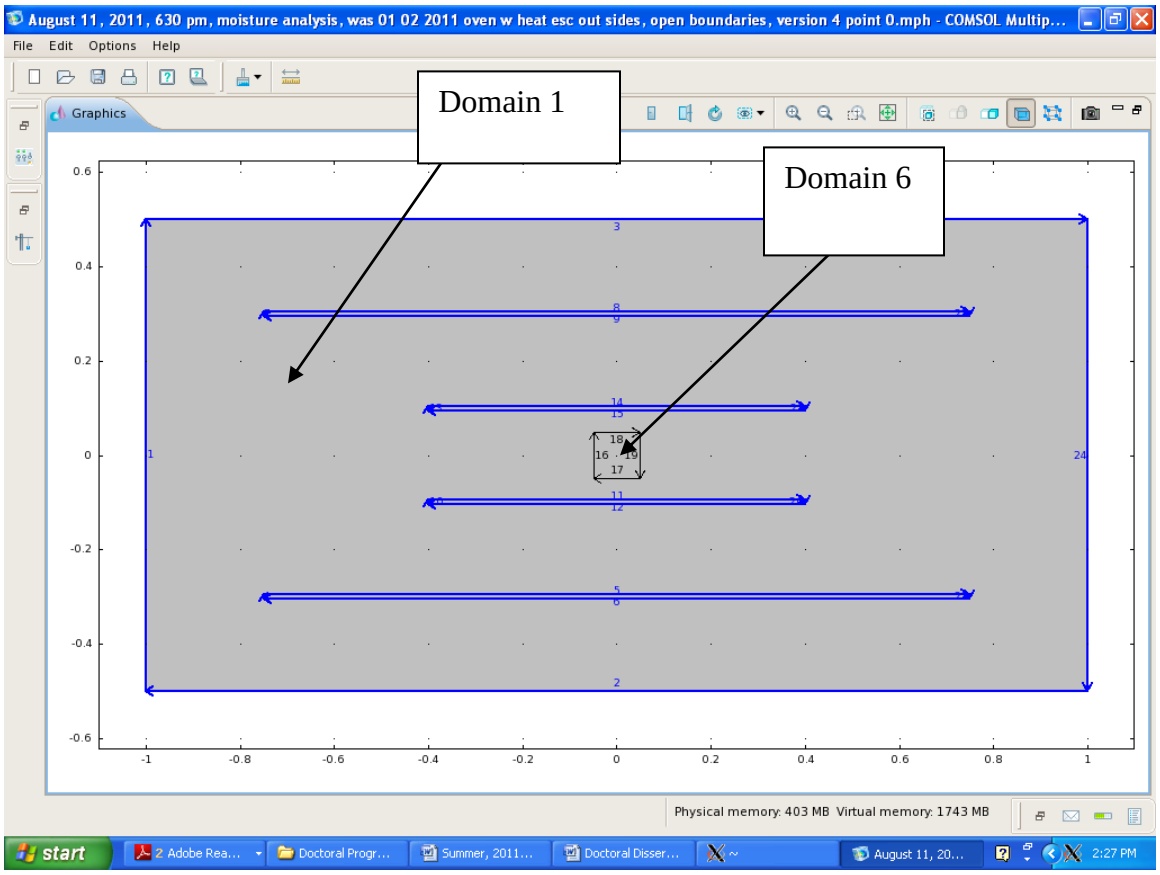

Figure 6.16: Oven with dough/bread within heating elements inside room, COMSOL model

6.3.2 Moisture loss with heat transfer and convection

Figure 6.17 shows the geometry for the moisture loss with heat transfer and convection; this 2-D geometry is 0.1 m by 0.1 m. The base COMSOL Multiphysics license is used; the Transport of Dilute Species and Heat Transfer Applications are employed. The mesh used is default (not refined).

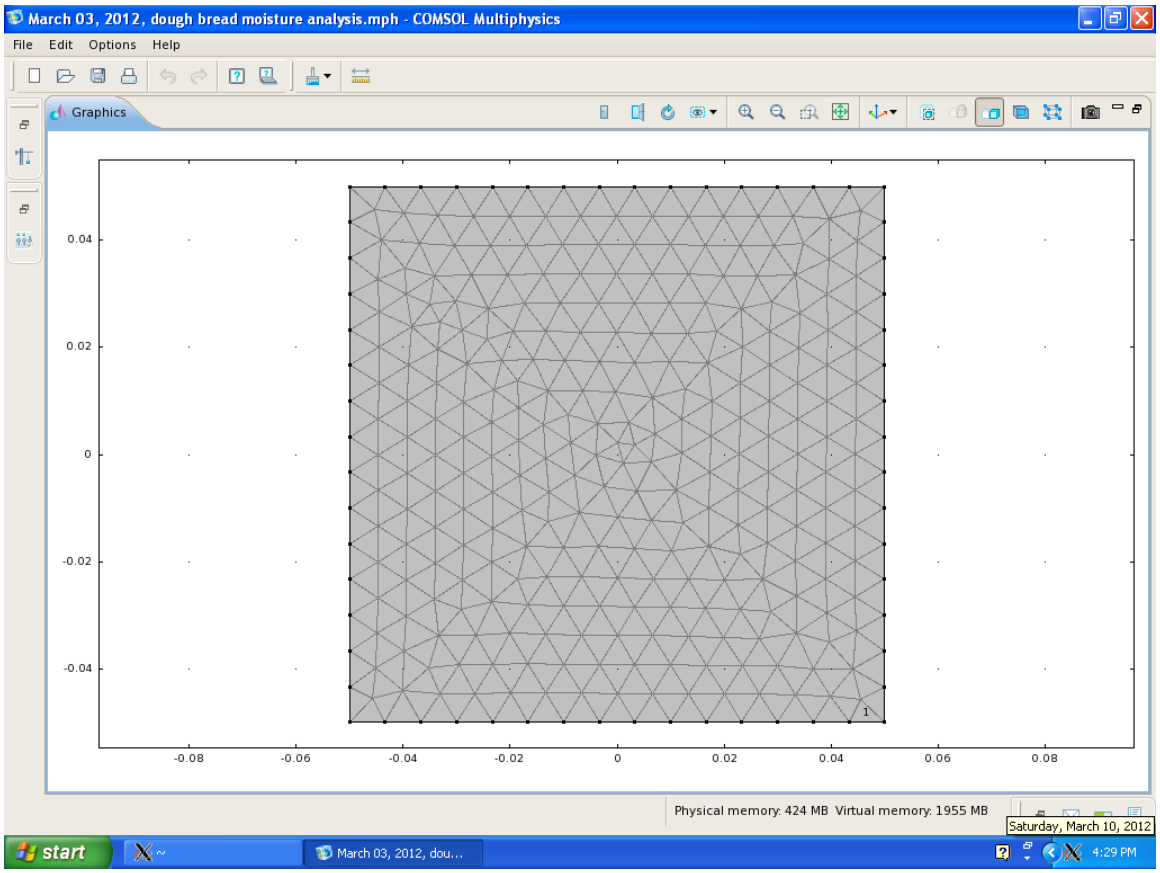

Figure 6.17: COMSOL moisture with heat transfer and convection, mesh

Table 6.14 shows the properties, expressions, values, and descriptions of the dough/bread for the moisture loss initial COMSOL model. The oven air temperature is obtained from Section 3.4 (to correspond to the analytical calculation), the initial dough temperature is at room temperature, the density of the dough is from Table 6.3, the heat transfer coefficient is from the addition of Equations (3-82) and (3-87); the initial dough moisture concentration, air moisture concentration, specific moisture capacity, moisture conductivity, mass transfer coefficient in mass units, surface moisture diffusivity, and latent heat of vaporization are from Chen et al (1999).

Table 6.14: Properties, expressions, values and descriptions of dough/bread for moisture loss initial COMSOL model

Property	expression	value	description
T_air	120[degC]	393.2 K	Oven air temperature
T0	20[degC]	293.2 K	Initial dough temperature
rho_d	380[kg/m^3]	380 kg/m^3	density of dough
h_T	28[W/(m^2*s)]	28 $W/(m^2 \cdot K)$	heat transfer coefficient
c0	0.78*rho_d	296.4 kg/m^3	initial dough moisture concentration
c_b	0.02*rho_d	7.6 kg/m^3	air moisture concentration
C_m	0.003	0.003	specific moisture capacity (kg moisture/kg dough bread)
k_m	1.29e-09[kg/(m*s)]	1.29E-09 kg/(m*s)	moisture conductivity
h_m	1.67e-06[kg/m^2*s]	1.67E-06 $kg/(m^2*s)$	mass transfer coefficient in mass units
D	k_m/(rho_d*C_m)	1.132E-9 m^2/s	diffusion coefficient
k_c	h_m/(rho_d*C_m)	1.465E-6 m/s	mass transfer coefficient
D_m	5e-10[m^2/s]	5.0E-10 m^2/s	surface moisture diffusivity
lda	2.3e06 J/kg	2300000 J/kg	latent heat of vaporization

Later in this research, better values for the dough/bread moisture loss model were obtained. Table 6.15 shows the properties, expressions, values, and descriptions of the dough/bread for the moisture loss final COMSOL model. The oven air temperature, the initial dough temperature, the density of the dough, and the heat transfer coefficient are

the same as in Table 6.14; air moisture concentration is from Equation (6-5); the initial dough moisture concentration, specific moisture capacity, moisture conductivity, mass transfer coefficient in mass units, surface moisture diffusivity and latent heat of vaporization are from Mondal et al (2010).

Table 6.15: Properties, expressions, values and descriptions of dough/bread for moisture loss final COMSOL model

Property	Expression	Value	Description
T_air	120 °C	393.2 K	oven air temperature
T0	20 °C	293.2 K	initial dough/bread temperature
rho_d	$380\ \frac{\mathrm{kg}}{\mathrm{m}^3}$	$380\ \frac{\mathrm{kg}}{\mathrm{m}^3}$	dough/bread density
h_T	$28\frac{\mathrm{W}}{\mathrm{m}^2\cdot\mathrm{K}}$	$28\frac{\mathrm{W}}{\mathrm{m}^2\cdot\mathrm{K}}$	heat transfer coefficient
c0	0.574* rho_d	$218.26\ \frac{\mathrm{kg}}{\mathrm{m}^3}$	initial dough moisture concentration
c_b	8.95×10^{-5} * rho_d	$0.034\frac{\mathrm{kg}}{\mathrm{m}^3}$	air moisture concentration
C_m	0.7373	0.7373	specific moisture capacity (kg moisture/kg dough bread)
k_m	$1.53\times10^{-6}\ \frac{\mathrm{kg}}{(\mathrm{m}\cdot\mathrm{s})}$	$1.53\times10^{-6}\ \frac{\mathrm{kg}}{(\mathrm{m}\cdot\mathrm{s})}$	Moisture conductivity
h_m	$5.09\times10^{-4}\ \frac{\mathrm{kg}}{(\mathrm{m}^2\cdot\mathrm{s})}$	$5.09\times10^{-4}\ \frac{\mathrm{kg}}{(\mathrm{m}^2\cdot\mathrm{s})}$	mass transfer coefficient in mass units
D	k_m/(rho_d* C_m)	$5.50\times10^{-9}\frac{\mathrm{m}^2}{\mathrm{s}}$	diffusion coefficient
k_c	h_m/(rho_d* C_m)	$1.82\times10^{-6}\ \mathrm{m/s}$	mass transfer coefficient
D_m	$5\times10^{-10}\frac{\mathrm{m}^2}{\mathrm{s}}$	$5\times10^{-10}\frac{\mathrm{m}^2}{\mathrm{s}}$	surface moisture diffusivity
lda	$2.3\times10^{6}\frac{\mathrm{J}}{\mathrm{kg}}$	$2.3\times10^{6}\frac{\mathrm{J}}{\mathrm{kg}}$	latent heat of vaporization

To find out if the value of air moisture concentration in Table 6.15 (which is the humidity (0.05 kg H_2O/kg dry air) from Section 3.4) is similar to Mondal et al (2010), a calculation is effected. From "Air- Density and Specific Weight" (2012), At 100 degrees C, density of air is 0.9461 kg/m^3; at 200 degrees C, density of air is 0.7461 kg/m^3. By interpolation density of air at 120 degrees C is 0.906 kg/m^3.

$$\frac{0.05 \text{ kg water}}{\text{kg dry air}} \times \frac{0.906 \text{ kg dry air}}{1 \text{ m}^3 \text{dry air}} \times \frac{1 \text{ m}^3 \text{dry air}}{1 \text{ m}^3 \text{ air-water vapor}} = \frac{0.0453 \text{ kg water}}{1 \text{ m}^3 \text{ air-water vapor}} \qquad (6\text{-}5)$$

Therefore, one can compare 0.034 kg/m^3 to 0.0453 kg/m^3, and see that they are similar.

CHAPTER VII

COMSOL MODELS, THREE-DIMENSIONAL

In this chapter, the three dimensional COMSOL models will be shown. First the dough/bread model with a volumetric heat source is shown, followed by a model of the dough/bread with heat fluxes imposed upon it. Finally, the 3-D model of the radiation effect upon the dough/bread with closely-spaced heating elements is presented. The results of the simulation of these models will be shown in Chapter IX.

7.1 Dough/bread as volumetric heat source

As a result of the MATLAB simulation in Section 10.3.1 closely correlating with the analytical simulation of Section 3.2.2, a simulation (that had a mesh refined twice) in COMSOL that corresponded to those two simulations was completed. The domain initial conditions are the same as in Table 6.3. This model uses only the base COMSOL Multiphysics license. Figure 7.1 shows the geometry of the COMSOL simulation; Table 11.4 shows the similarity of results of these four simulations.

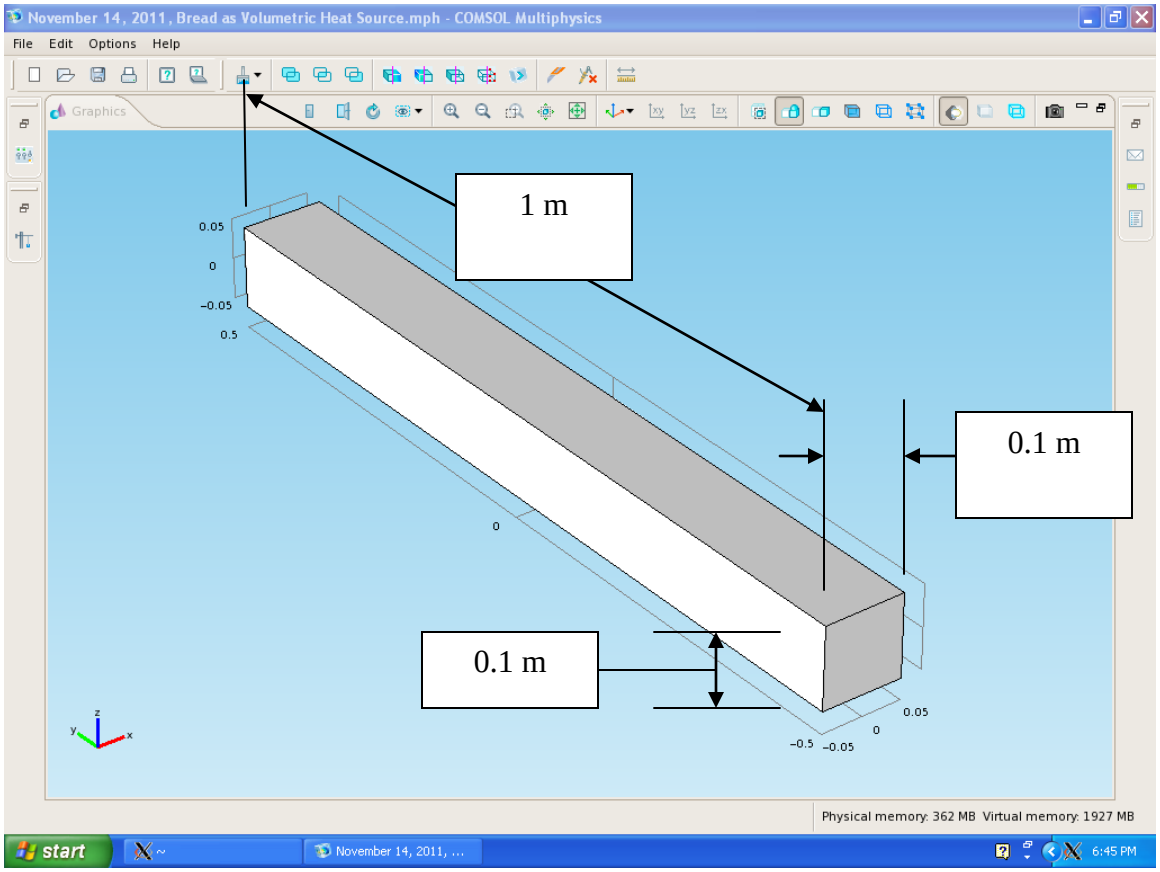

Figure 7.1: Dough/bread as volumetric heat source, COMSOL geometry

The volumetric heat source is calculated by using the values from Section 3.1.2 as follows:

$$\frac{-535.1\ \mathrm{W}}{(0.1\ \mathrm{m})(0.1\ \mathrm{m})(1\ \mathrm{m})} - \frac{738.5\ \mathrm{W}}{(0.1\ \mathrm{m})(0.1\ \mathrm{m})(1\ \mathrm{m})} = -127360\ \frac{\mathrm{W}}{\mathrm{m}^3} \qquad (7-1)$$

All of the six boundaries are chosen to be insulated.

7.2 Dough/bread with heat fluxes

Because of the discrepancy of the simulations that modeled the dough/bread as a volumetric heat source and the 2-D simulations that model radiative heat flux upon the dough/bread, a three dimensional simulation of dough/bread with boundary conditions of heat fluxes was completed. Figure 7.2 shows this three dimensional simulation; the heat fluxes are obtained from Section 3.1.2. This model uses only the base COMSOL Multiphysics license. The domain initial conditions are the same as in Table 6.3. The mesh was refined twice. The geometry is the same as Figure 7.1.

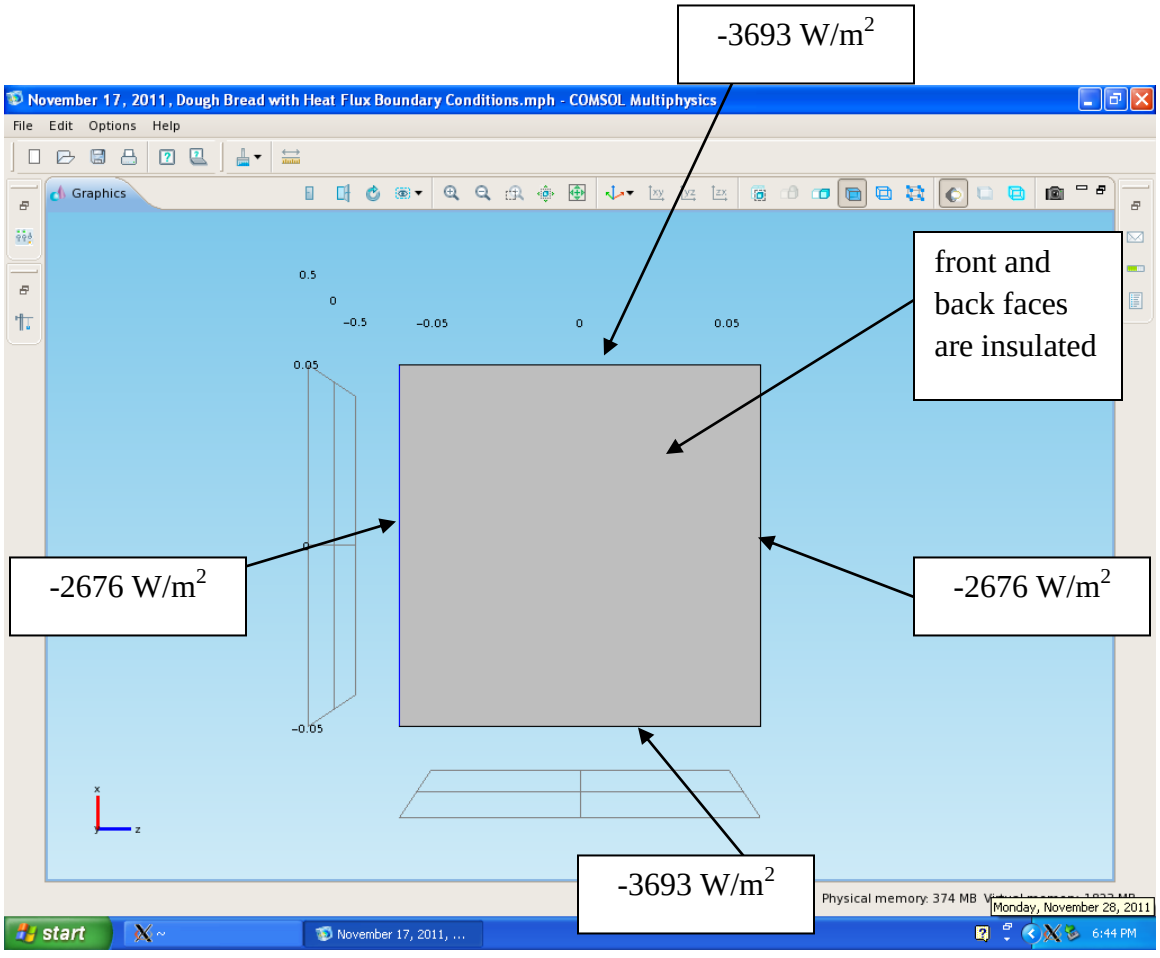

Figure 7.2: Dough/bread with heat fluxes, COMSOL model

7.3 Radiation upon dough/bread using closely-spaced heating elements

This model uses COMSOL's Multiphysics license and Heat Transfer Module. The mesh of all domains is default (not refined). At first, models with a 1 meter depth for the dough/bread and heating elements (with and without side boundaries) were created. Figure 7.3 shows the model without side boundaries and Figure 7.4 shows the model with side boundaries. Only the simulation of the model with side boundaries was first attempted on the OSC computer interactively; the computer ran out of memory for this serial computation. Therefore, the model had to be simulated in parallel on the OSC computer; Figure 7.5 shows the output file for this simulation. More information about this type of file can be found in Ohio Supercomputer Center (2010 b) (when running this model interactively, this file can be found in the log tab under the progress tab in the COMSOL Graphical User Interface (GUI) Results window). This simulation had a requested wall time of only 15 minutes, so after that time had elapsed, the job was terminated (before the solution was found). In order to run a similar 3-D model interactively on the OSC computer, the side boundaries were eliminated, and the depth of the model was reduced to 10 cm; this is shown in Figure 7.6. The rest of the geometry of this model is the same as Figure 6.4.

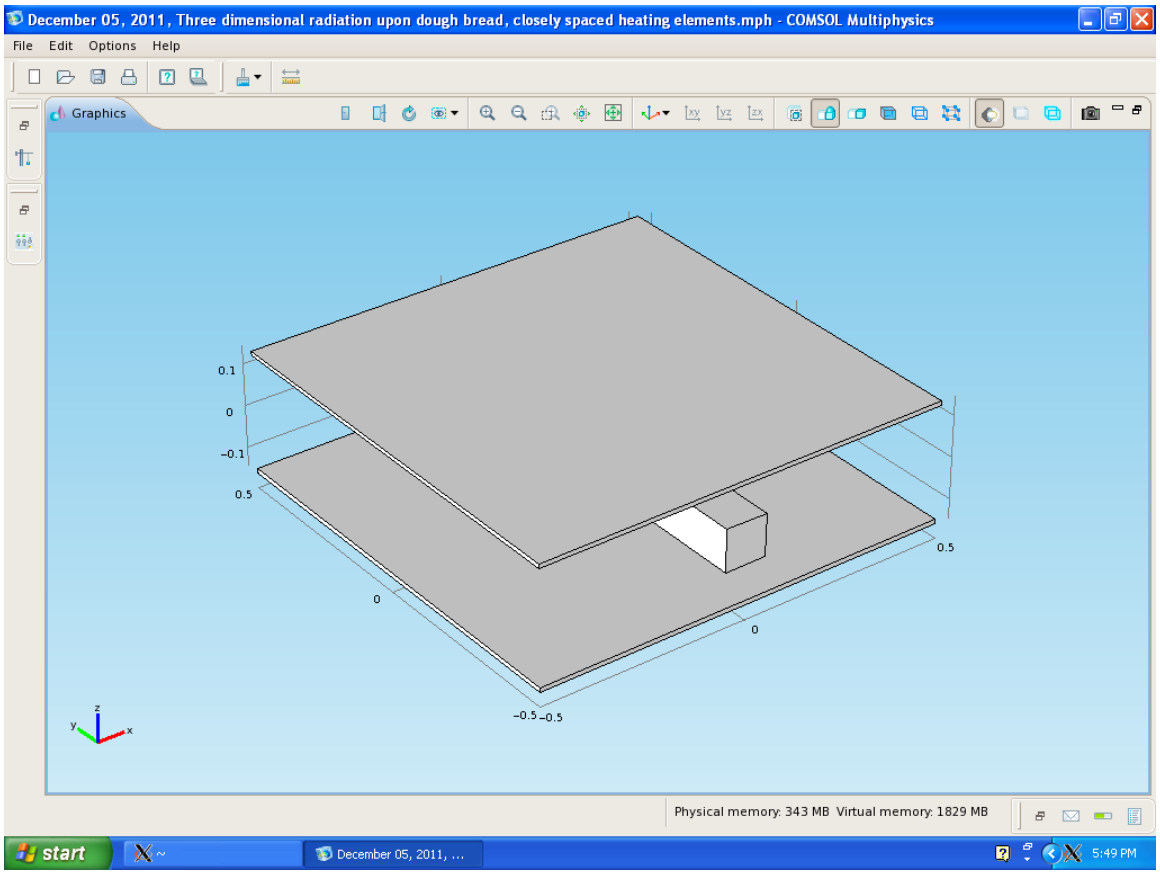

Figure 7.3: Radiation upon dough/bread using closely-spaced heating elements, COMSOL geometry

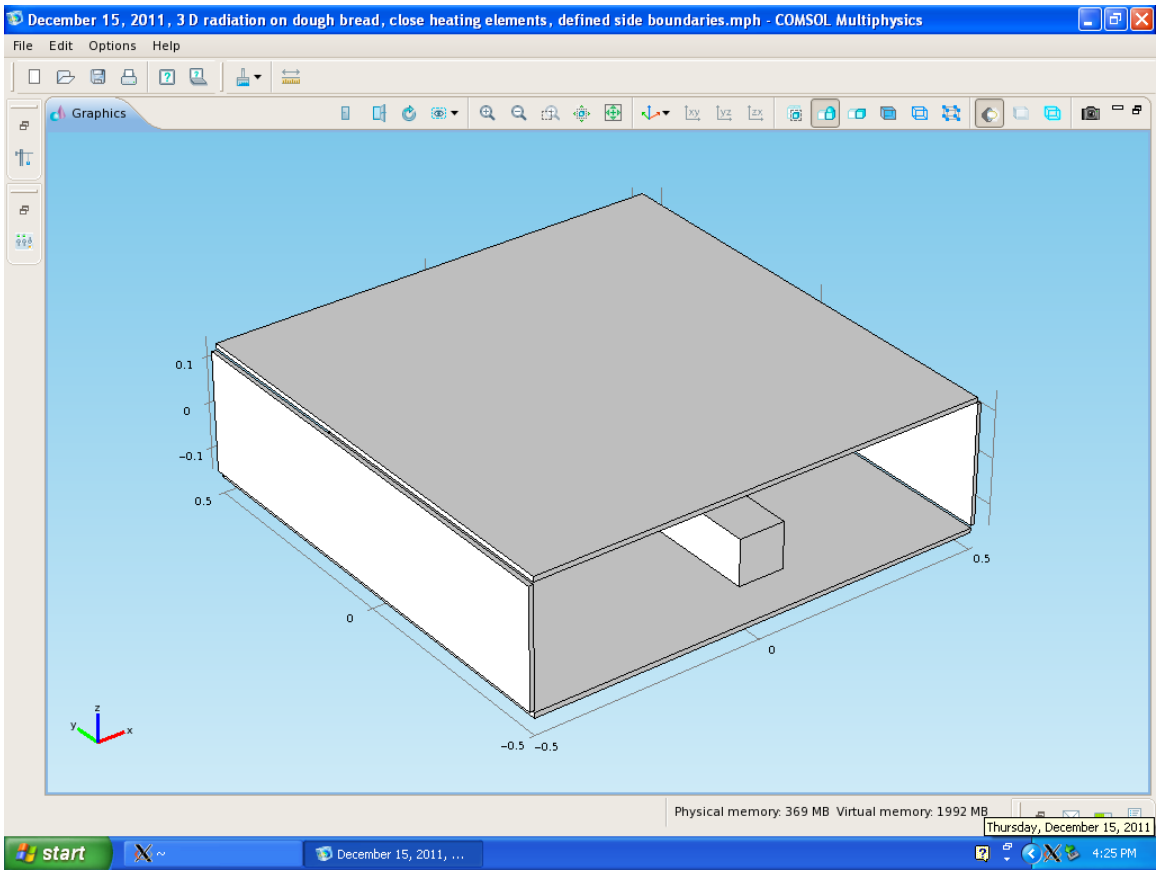

Figure 7.4: Radiation upon dough/bread using closely-spaced heating elements and side boundaries, COMSOL geometry

```
****************************************
********COMSOL progress output file********
****************************************
Mon Dec 19 16:31:53 EST 2011
Running: Study 1
---------- Current Progress: 100 %
Memory: 307/307 1532/1532
          Current Progress:   0 %
Memory: 333/333 1597/1597
---------- Current Progress: 100 %
Memory: 348/348 1605/1605
Time-dependent solver (Generalized-alpha)
Number of degrees of freedom solved for: 53479.
          Current Progress:   0 %
Memory: 398/398 1827/1827
Symmetric matrices found.
Symmetric matrices found.
Format not changed since SOR line uses nonsymmetric storage.
Nonsymmetric matrix found.
Step        Time    Stepsize      Res  Jac  Sol Order Tfail NLfail LinIt
LinErr   LinRes
Error estimate for segregated groups:
Error estimate for segregated groups:
Error estimate for segregated groups:
Error estimate for segregated groups:
Error estimate for segregated groups:
Error estimate for segregated groups:
Error estimate for segregated groups:
Error estimate for segregated groups:
   0           0             out   16    6   16                   0
                  Group #1:         8    3    8                        8
0.00087  2.2e-06
                  Group #2:         8    3    8                        8  3.8e-
13  9.5e-16
Error estimate for segregated groups:
Error estimate for segregated groups:
   1        0.24        0.24       20    8   20     2     0      0
                  Group #1:        10    4   10                       10
0.00087  2.2e-06
                  Group #2:        10    4   10                       10  2.9e-
13  7.4e-16
Error estimate for segregated groups:
Error estimate for segregated groups:
   2        0.72        0.48       24   10   24     2     0      0
                  Group #1:        12    5   12                       12
0.00087  2.2e-06
                  Group #2:        12    5   12                       12  1.8e-
13  4.5e-16
Error estimate for segregated groups:
=>> PBS: job killed: walltime 909 exceeded limit 900
```

Figure 7.5: Radiation upon dough/bread using closely-spaced heating elements and side boundaries, output file

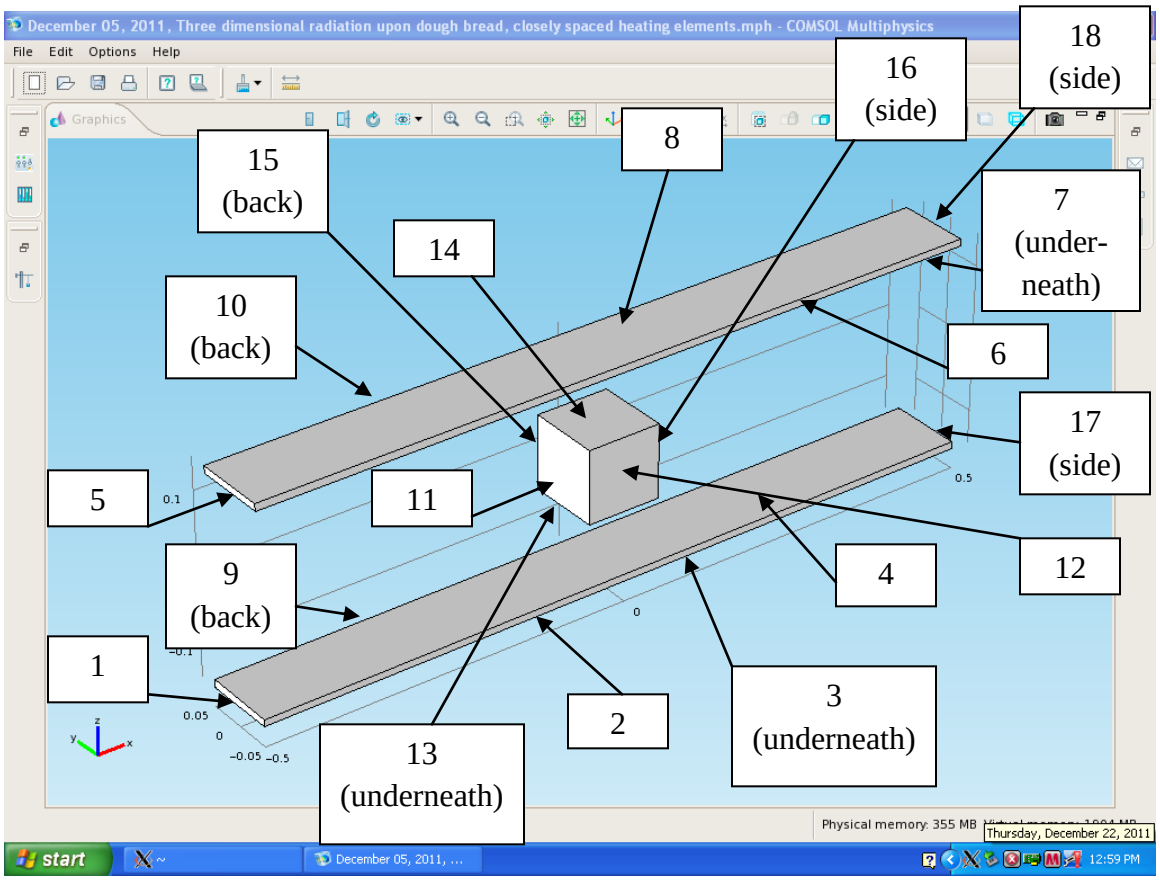

Figure 7.6: Radiation upon dough/bread using closely-spaced reduced width heating elements, COMSOL geometry and boundaries

Table 7.1: Boundary conditions, 3-D radiation effect on dough/bread, COMSOL model

Emissivity of Boundaries 4,7	Emissivity of Boundaries 11,13,14,16	Temperature of Boundaries 4,7	Condition of Boundaries 1,2,3,5,6,8,9,10,17,18 (default)	Condition of Boundaries 12,15
1	0.9	533.15 K	insulated	1st model: 298.825K; 2nd model: $\varepsilon = 0$; 3rd model: $\varepsilon = 0$; 4th model: $\varepsilon = 0.9$

The boundary conditions for the 3-D radiation effect on dough/bread COMSOL model are shown in Table 7.1. The emissivities and/or temperatures of boundaries 4, 7, 11, 13, 14 and 16 correspond to values in Section 3.1.2. The condition of boundaries 1, 2, 3, 5, 6, 8, 9, 10, 17, 18 are attempted to be modeled as in reality. The conditions of the boundaries 12 and 15 were attempted to be modeled as in reality, or as in Section 6.1.3.

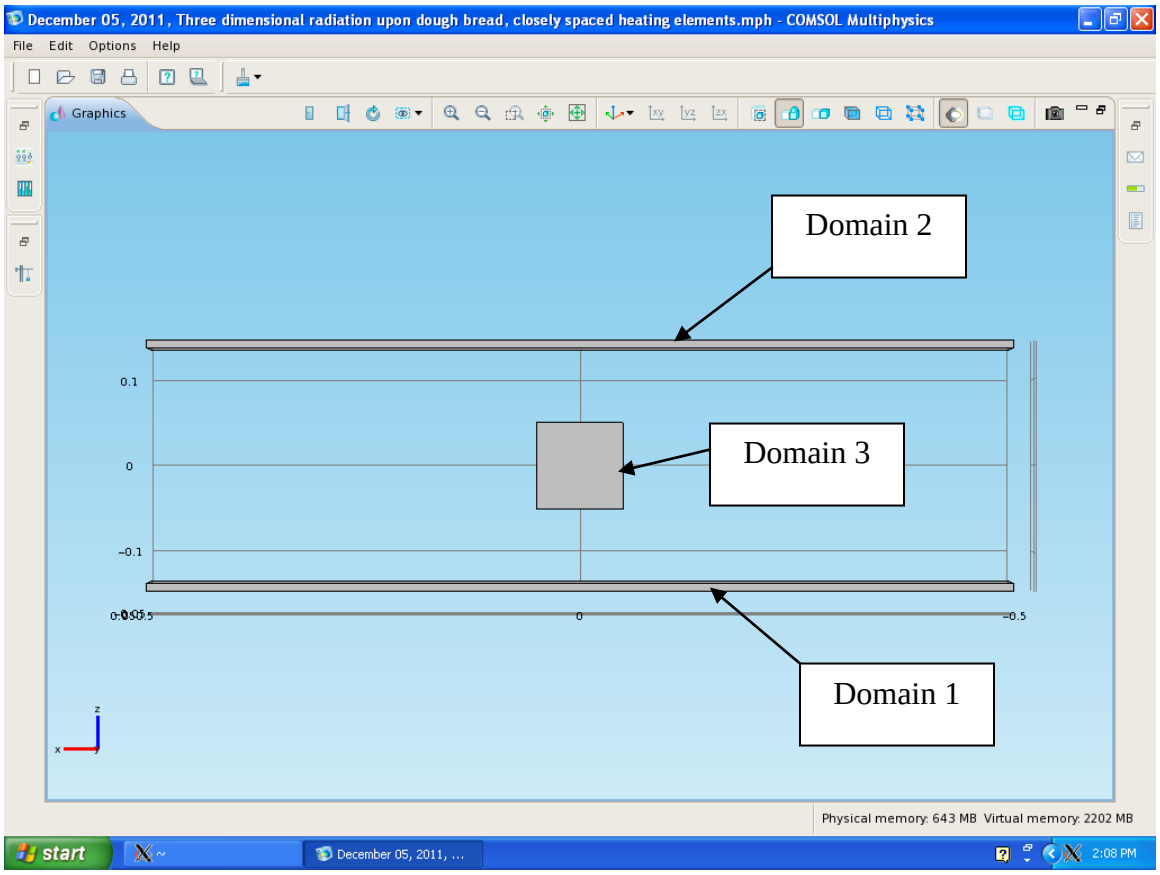

Figure 7.7: Radiation upon dough/bread using closely-spaced reduced width heating elements, COMSOL geometry "ZX" view showing domains

Domain 3 has the specifications of Table 6.3. Domains 1 and 2 were not specified.

CHAPTER VIII

COMSOL SIMULATIONS, TWO-DIMENSIONAL RESULTS AND DISCUSSIONS

The results and discussions for the two-dimensional COMSOL simulations are presented in this chapter; these simulations correspond to the COMSOL models in Chapter VI.

8.1 Radiation and conduction COMSOL simulations

In this section, the radiation and conduction COMSOL simulations are presented.

8.1.1 Distantly-spaced heating elements, steel container

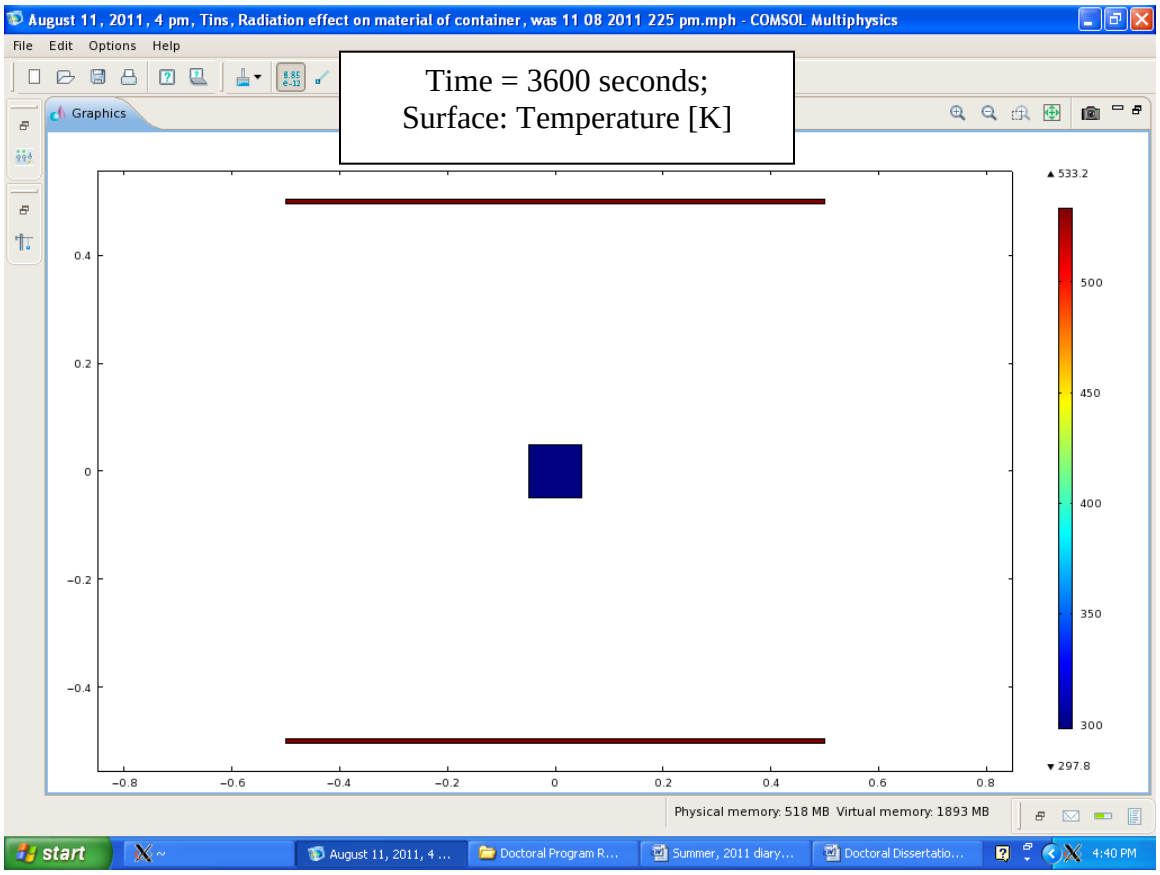

Figure 8.1: Radiation effect on surface of container, COMSOL solution

Figure 8.1 shows the radiation effect on the container for a COMSOL solution after 3600 seconds. A surface integration on the dough/bread domain yielded a value of 2.9785 $m^2 \cdot K$, which when divided by the area of the surface $(0.1\ m)^2$ yields an average surface temperature of 297.85 K. This shows an increase in temperature from the initial temperature calculated as: 297.85 K-293.15 = 4.70 K.

Table 8.1: Results of radiation effect on surface of containers, COMSOL solution

Emissivity of Container Surface	Type of Simulation	Temperature of Container (K)
0.1	Stationary	458.1
	Transient (3600 s)	297.85
0.8	Stationary	458.5
	Transient (3600 s)	329.9

Looking at Table 8.1, one can see that for a container surface emissivity of 0.1, the stationary simulation yielded a greater "Temperature of Container" (458.1 K) than the corresponding transient simulation (297.85 K). It might be determined from this observation that this simulation takes longer than 3600 seconds to reach steady state. A similar observation can be made for the simulation where the emissivity of the container surface is 0.8: for the stationary case, the "Temperature of Container" was 458.5 K, whereas the "Temperature of Container" was 329.9 K for the transient case. This means that the steady-state simulation takes longer than 3600 seconds to be reached.

As expected, the "Temperature of Container" was greater for the surface emissivity of 0.8 (versus the surface emissivity of 0.1) for each of the stationary and transient simulations. When the container surface emissivity was 0.8 for the stationary case, the "Temperature of Container" was 458.5 K (versus 458.1 for the emissivity of 0.1); the "Temperatures of Container" for the transient case were 329.9 K and 297.85 K for the surface emissivities of 0.8 and 0.1, respectively. These results are expected since the greater the emissivity of the container surface, the greater the absorptivity of the surface;

the greater the absorptivity of the surface, the more radiant energy will be absorbed by that surface. This is due to Kirchoff's law (Incropera & DeWitt, 1990) which states that the emissivity of a surface is equal to its absorptivity if the surface emission or irradiation is diffuse.

8.1.2 Distantly-spaced heating elements, food with constant properties

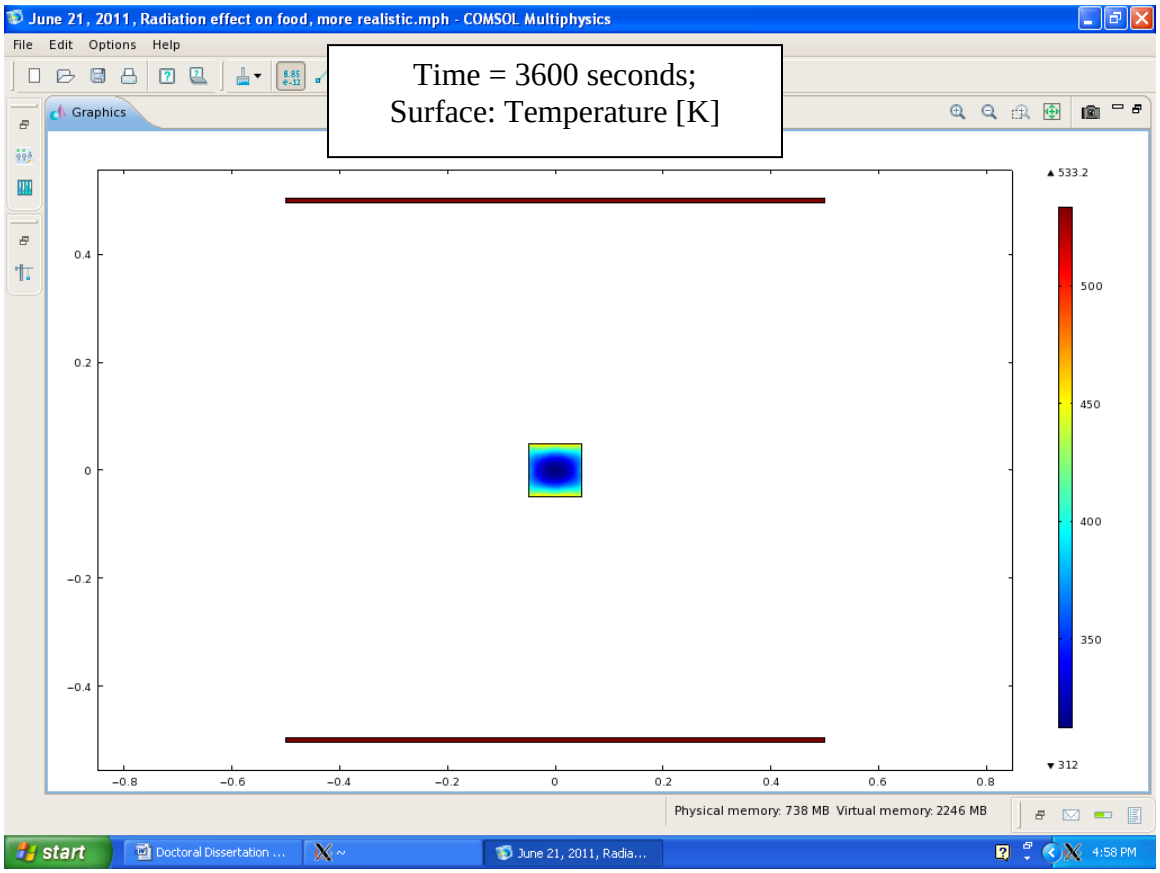

Figure 8.2: Radiation effect on dough/bread, COMSOL solution at 3600 seconds

Figure 8.2 shows the radiation effect on the dough/bread for a COMSOL solution after 3600 seconds. A surface integration on the dough/bread domain yielded a value of 3.7436 $m^2 \cdot K$, which when divided by the area of the surface $(0.1\ m)^2$ yields an average surface temperature of 374.36 K. This shows an increase in temperature from the initial temperature calculated as: 374.36 K – 293.15 K = 81.21 K.

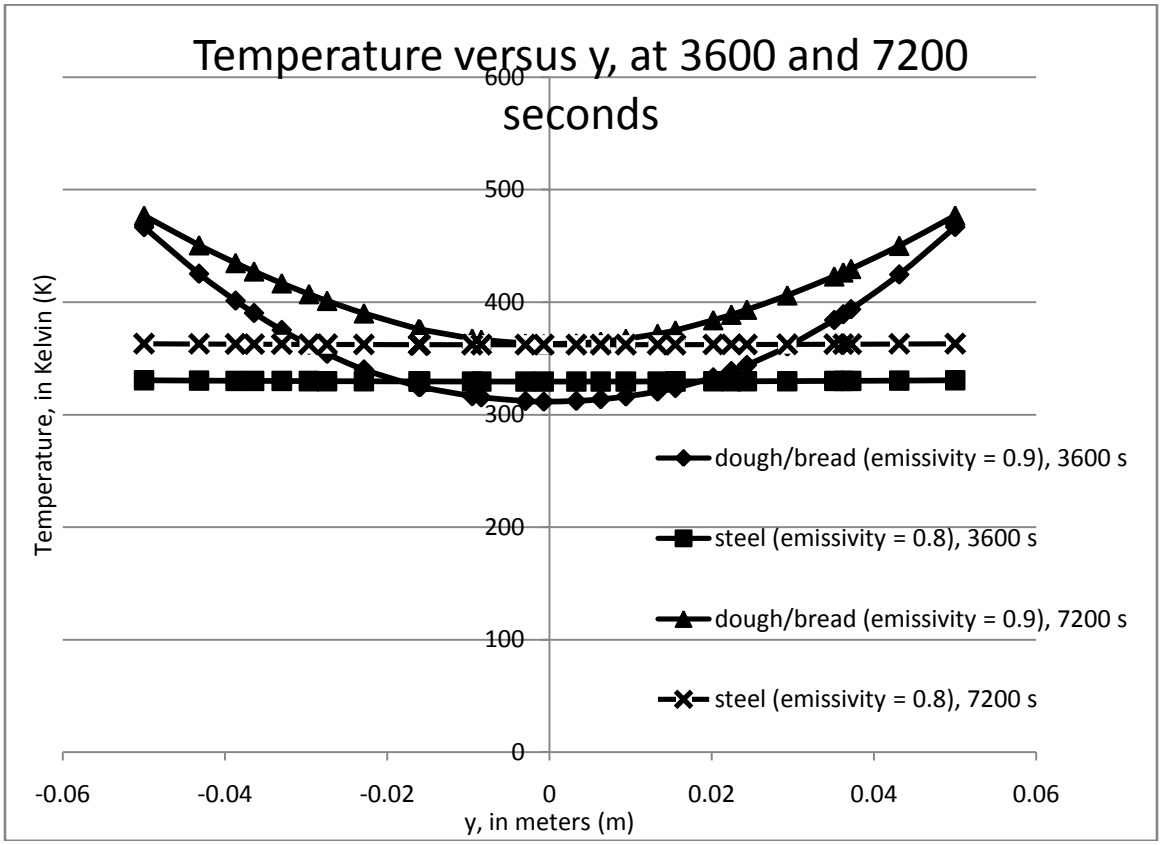

Figure 8.3 Temperature versus *y*, COMSOL solutions at 3600 and 7200 seconds

Figure 8.3 shows the graph of temperature versus *y* (at x = 0) of dough/bread and steel for the COMSOL solutions at 3600 and 7200 seconds. Looking at the 3600 second simulations first, the higher temperature at the bottom and top of the dough/bread with respect to the bottom and top of the steel is thought to be due to the fact that the surface of the dough/bread has a higher emissivity than the steel. Although the emissivity of each material is slightly different, it is believed that the more uniform plot (less variation of temperature versus *y*) for steel is due to steel's higher thermal diffusivity with respect to dough/bread. The thermal diffusivity is a measure of how fast heat travels through a material, and is defined (Incropera & Dewitt, 1990) as follows:

$$\alpha = \frac{k}{C_p \rho} \qquad (8-1)$$

where k is the thermal conductivity of the material, C_p is the specific heat of the material, and ρ is the density of the material. For dough/bread (using values from Table 6.3), the thermal diffusivity is:

$$\alpha_{\text{dough/bread}} = \frac{\left(0.1133 \frac{\text{W}}{\text{m}\cdot\text{K}}\right)}{\left(1941 \frac{\text{J}}{\text{kg}\cdot\text{K}}\right)\left(380 \frac{\text{kg}}{\text{m}^3}\right)} = 1.54 \times 10^{-7} \frac{\text{m}^2}{\text{s}} \qquad (8-2)$$

and for steel (using values from Table 3.1), the thermal diffusivity is:

$$\alpha_{\text{steel}} = \frac{\left(52 \frac{\text{W}}{\text{m}\cdot\text{K}}\right)}{\left(7800 \frac{\text{J}}{\text{kg}\cdot\text{K}}\right)\left(465 \frac{\text{kg}}{\text{m}^3}\right)} = 1.43 \times 10^{-5} \frac{\text{m}^2}{\text{s}} \qquad (8-3)$$

Comparing the thermal diffusivities of steel versus dough/bread:

$$\frac{1.43 \times 10^{-5} \frac{\mathrm{m}^2}{\mathrm{s}}}{1.54 \times 10^{-7} \frac{\mathrm{m}^2}{\mathrm{s}}} = 93.1 \qquad (8-4)$$

The thermal diffusivity of steel is 93.1 times greater than the thermal diffusivity of dough/bread. Now looking the 7200 second simulations, it can be seen that all locations of the dough/bread and steel have risen in temperature; this means that at 3600 seconds, neither the dough/bread nor the steel has reached steady state.

It must be stated that when the steel is graphed by itself, the temperature profile shows a prominent U-shape; this is due to the fact that the temperatures range (for the 7200 second simulation, for example) from 363.13 K at the bottom , to 362.15 K in the middle, then back to 363.13 K at the top.

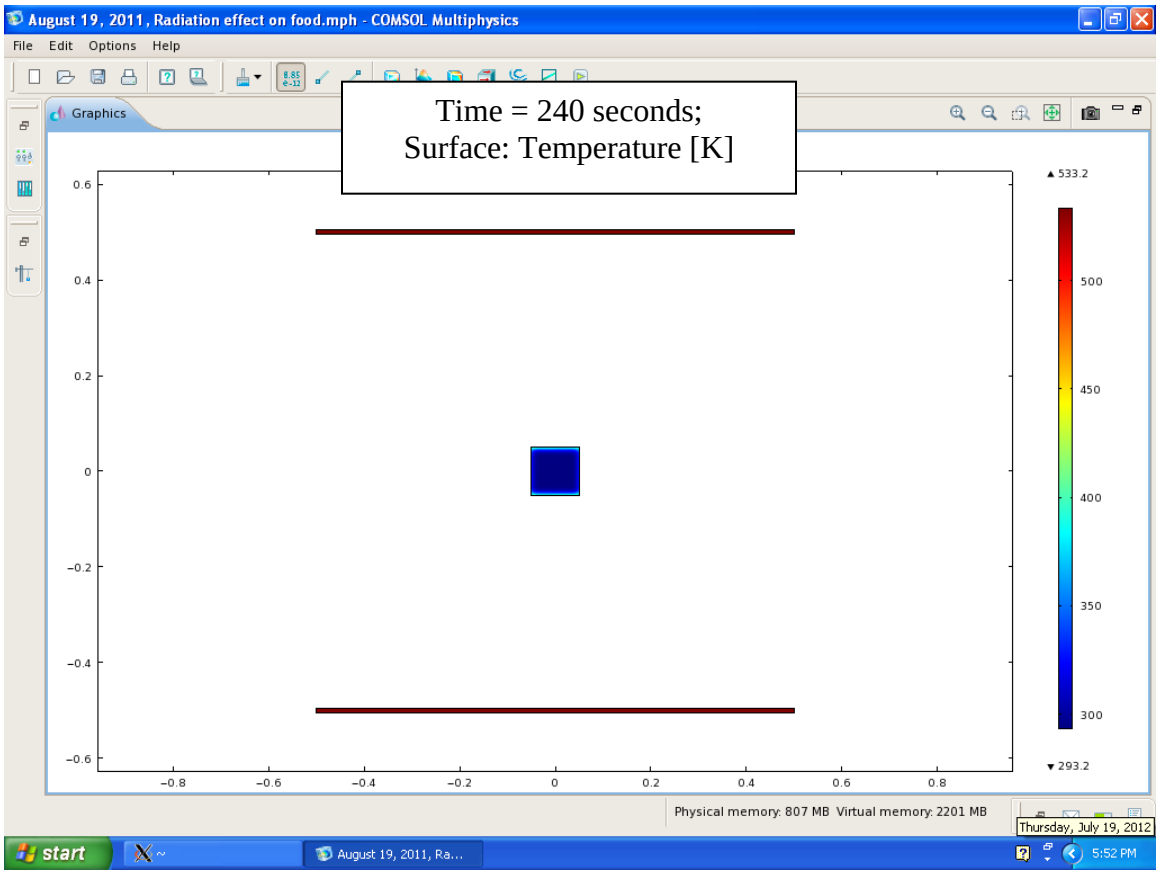

Figure 8.4: Radiation effect on dough/bread: COMSOL solution at 240 seconds

Figure 8.4 shows the COMSOL solution at 240 seconds for the radiation effect on dough/bread. A surface integration performed on the dough/bread domain yielded 3.0819 $m^2 \cdot K$, which when divided by the area of the surface $(0.1\ m)^2$ yields an average temperature of 308.19 K. This shows an increase in temperature from the initial temperature calculated as 308.19K – 293.15 K = 15.04 K.

8.1.3 Closely-spaced heating elements, food with constant properties

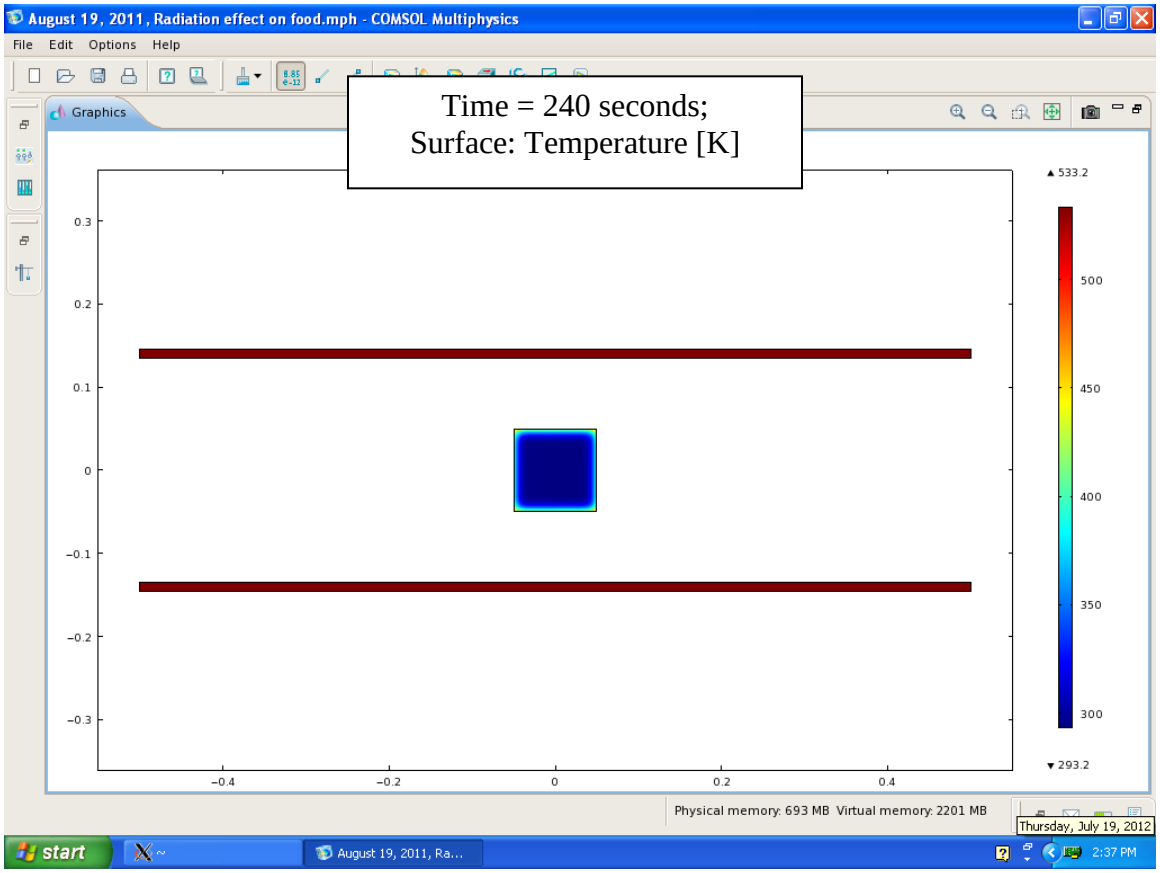

Figure 8.5: Radiation effect on dough/bread for closely-spaced heating elements, COMSOL solution at 240 seconds

Figure 8.5 shows the heating elements placed 14 cm above and below the center of the food. A surface integration performed on the dough/bread domain yielded 3.1854 $m^2 \cdot K$, which when divided by the area of the surface $(0.1\ m)^2$ yields an average temperature of 318.54 K. This shows an increase in temperature from the initial temperature calculated as 318.54 K – 293.15 K = 25.39 K. The increase in temperature here is higher than the corresponding COMSOL simulation with distantly-spaced heating elements (Section 8.1.2), which is expected (see Table 8.2). This temperature increase is lower than the

volumetric analytical simulation (Section 3.2.2), and the volumetric MATLAB simulation (Section 10.3.1); this is also expected, since those analytical and MATLAB simulations have a volumetric heat source, whereas this COMSOL simulation has radiation impinging upon the surface of the dough/bread.

Table 8.2 Comparison of distantly- and closely-spaced heating elements, COMSOL simulations

Dough/bread simulation with heating elements	Temperature rise of dough/bread (K)	Percent difference (see Eqn (11-1)) from Distantly-Spaced
Distantly-spaced	15.04	- -
Closely-spaced	25.39	51.29

Later, because of the discrepancy between the temperature rise (25.39 K) determined by COMSOL in this section and the temperature rise (41.46 K) calculated by the COMSOL simulation in Section 9.2 (using heat fluxes calculated from Section 3.1.2), an investigation was undertaken to find the radiative heat fluxes calculated by COMSOL for the results of Figure 8.5.

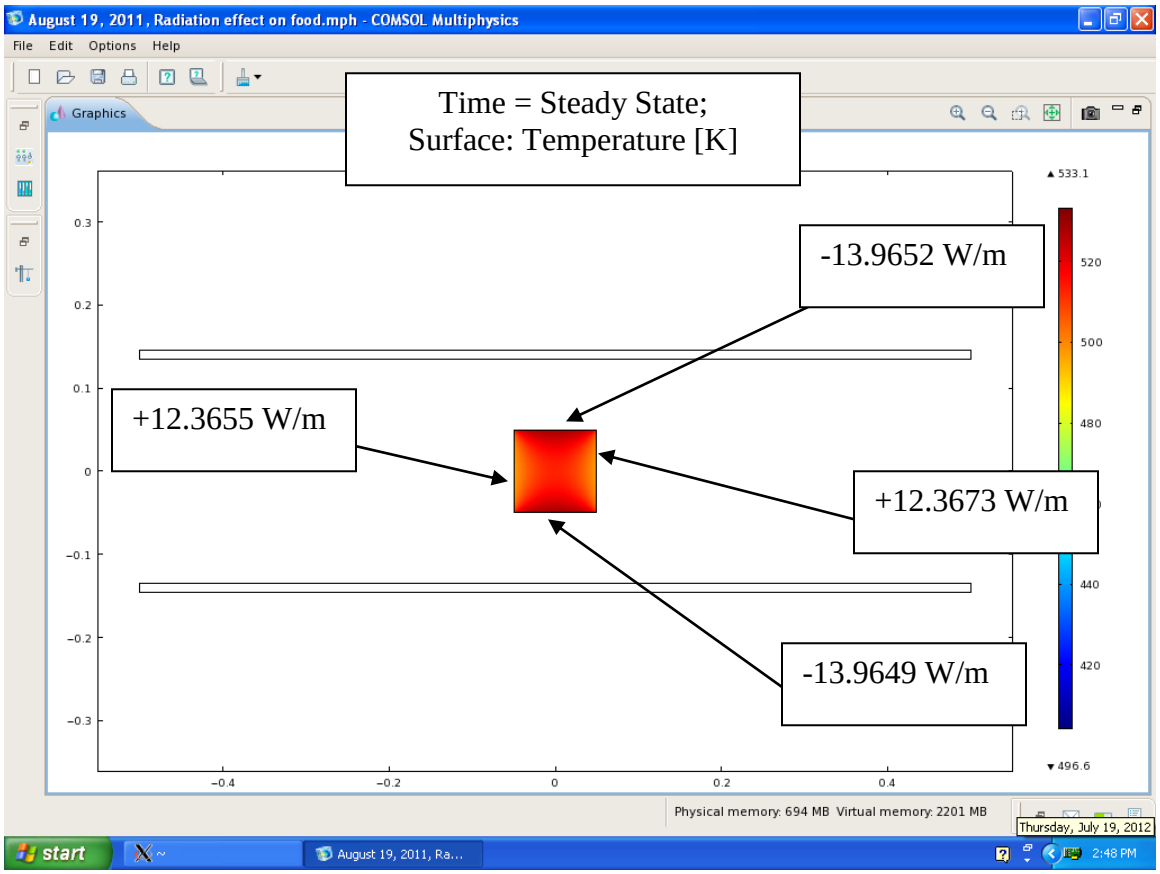

Figure 8.6: Radiation effect on dough/bread for closely-spaced heating elements, radiative heat fluxes at steady state

The heat fluxes in Figure 8.6 were determined using the stationary simulation. The first step in correlating the heat fluxes (W/m) in Figure 8.6 with the heat fluxes (W/m^2) in Section 3.1.2 is to make all the heat fluxes dimensionally consistent. For example, if the radiative heat flux is -13.9652 W/m, and the x-length of the surface is 0.1 m, then the total radiative heat on the length is -1.39652 W. From Section 3.1.2, conversely, if the radiative heat on a surface is -267.6 W and the surface area is 0.1 m^2, then the total radiative heat flux on the surface is -2676 W/m^2.

At this point it was decided to do a two-dimensional simulation with defined side boundaries (see Figure 6.6), as well as a three-dimensional simulation of the dough/bread with closely-spaced heating elements (see Section 7.3).

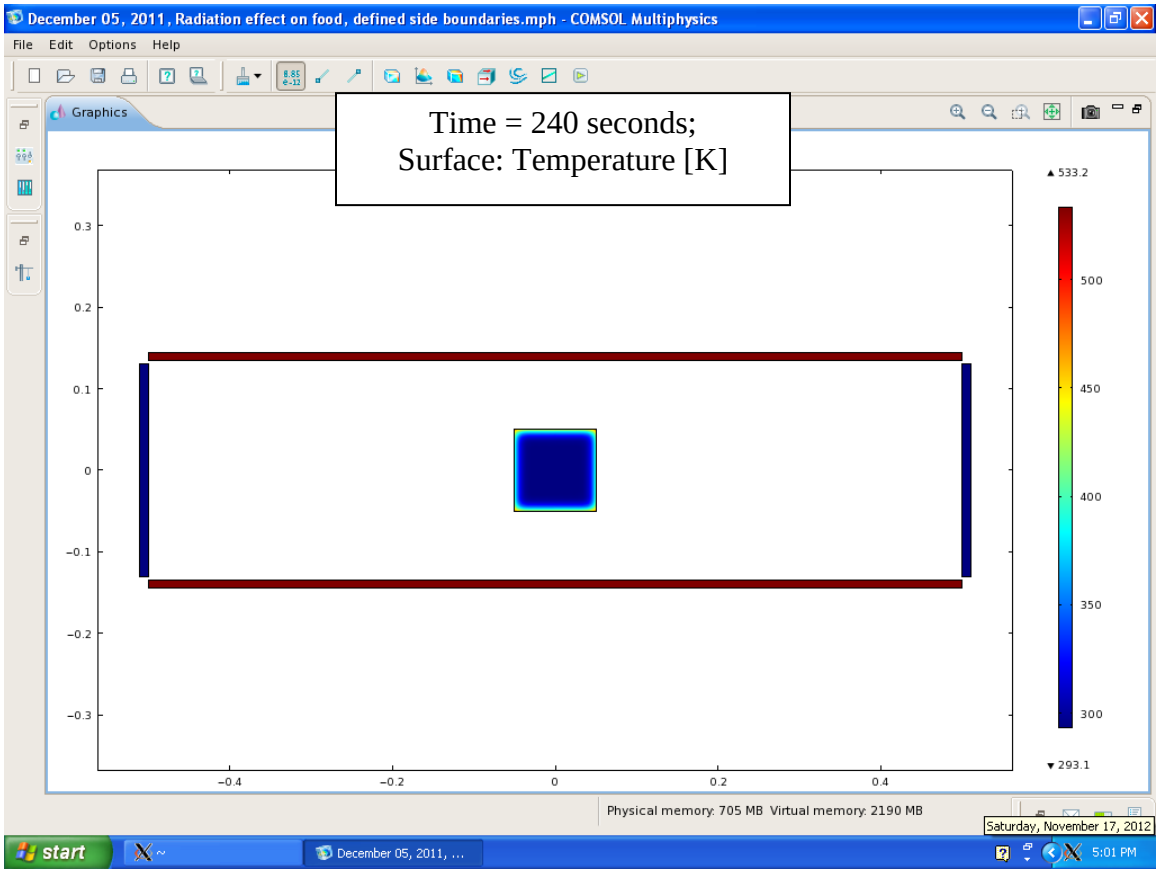

Figure 8.7 Radiation effect on dough/bread for closely-spaced heating elements, defined side boundaries, at 240 seconds

A surface integration performed on the unrefined dough/bread domain yielded 3.1642 $m^2 \cdot K$, which when divided by the area of the surface $(0.1\ m)^2$ yields an average temperature of 316.42 K. This shows an increase in temperature from the initial temperature calculated as 316.42 K – 293.15 K = 23.27 K. This result is somewhat less than is the temperature increase earlier (25.39 K) in Section 8.1.3 (where the side

boundaries of the oven where not defined). A mesh refinement (twice) on the dough/bread domain showed a temperature increase of 24.03 K (Figure 8.7).

Table 8.3 shows a comparison of the temperature rise of the COMSOL radiation effect on dough/bread for closely-spaced heating elements with and without defined side boundaries. The simulation with defined side boundaries resulted in a temperature rise slightly lower than the simulation without side boundaries. This comparison shows that specifying a value for T_{amb} alone produces slightly different results than explicitly modeling side boundaries and specifying a value for T_{amb}. Having side boundaries may result in a model where the colder surfaces are computationally closer to the dough/bread than the "far-away" (the term used in the documentation of COMSOL, 2010 c) temperature of T_{amb}.

Table 8.3: Comparison of temperature rise of COMSOL radiation effect on dough/bread for closely spaced heating elements, with and without defined side boundaries

Simulation	Temperature Rise	% difference with respect to without side boundaries
without side boundaries	25.39 K	- -
defined side boundaries	24.03 K	-5.50

Finally, a simulation was completed that calculated the temperature rise of the dough bread as a function of dough/bread height. As expected, the taller the dough/bread, the less the temperature rise.

Table 8.4: Comparison of different dough/bread height, COMSOL simulations

Dough/Bread height	Temperature rise
2"=0.0508 m	38.39 K
4"=0.1016 m	25.17 K
6"=0.1524 m	20.64 K

8.1.4 Distantly-spaced heating elements, food with varying properties

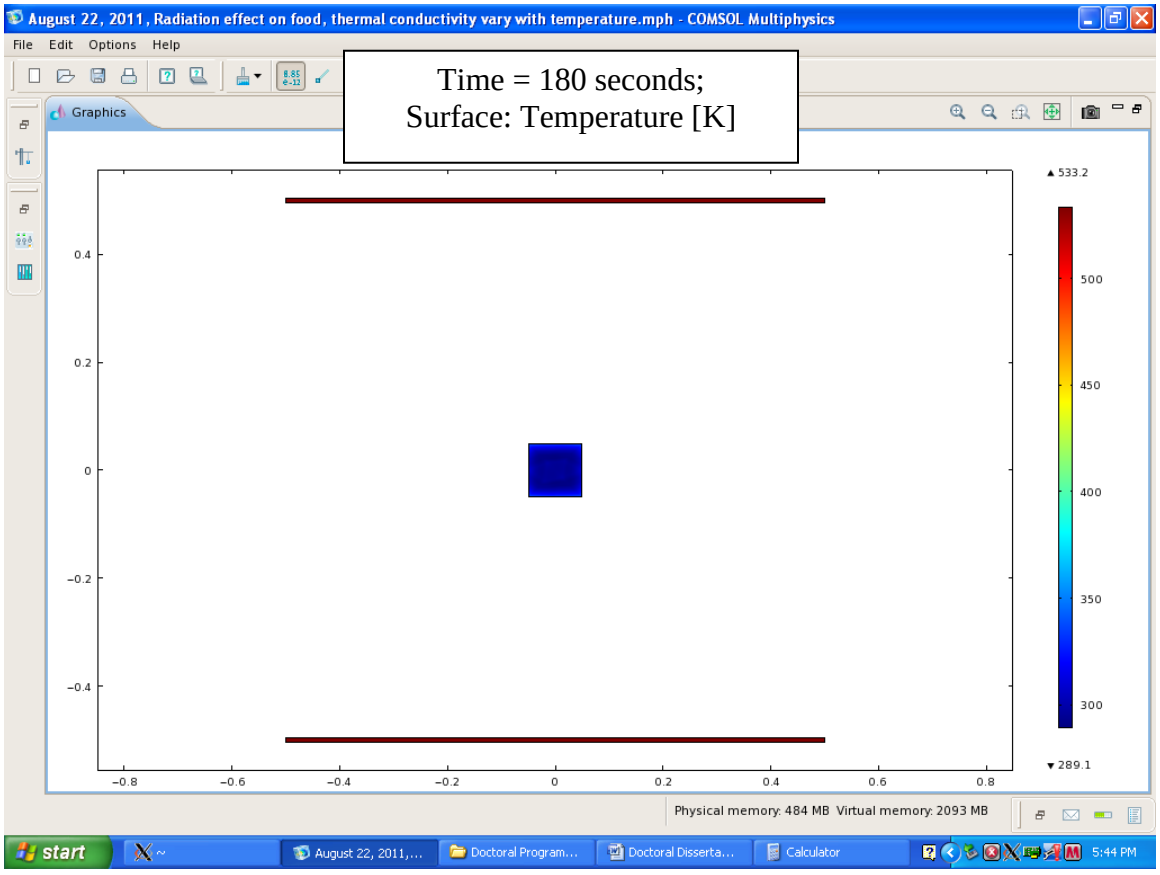

Figure 8.8: Dough/bread with temperature-varying thermal conductivity, COMSOL solution at 180 seconds

Figure 8.8 shows the temperature profile of the dough/bread at 180 seconds (3 minutes). A surface integration performed on the dough/bread domain yielded 3.0223 $m^2 \cdot K$, which when divided by the area of the surface $(0.1\ m)^2$ yields an average temperature of 302.23 K. This shows an increase in temperature from the initial temperature calculated as 302.23 – 293.15 K = 9.08 K.

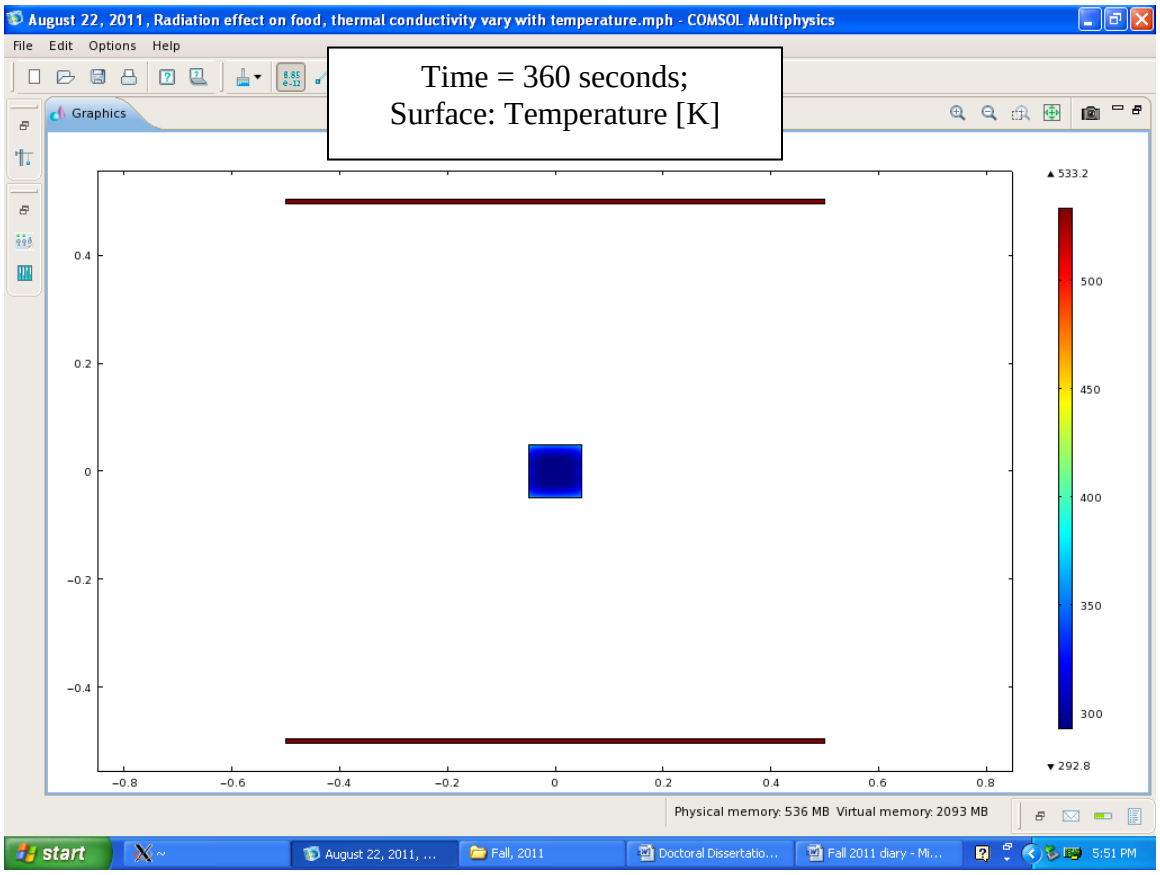

Figure 8.9: Dough/bread with temperature-varying thermal conductivity, COMSOL solution at 360 seconds

Figure 8.9 shows the temperature profile of the dough/bread at 360 seconds (6 minutes). A surface integration performed on the dough/bread domain yielded 3.1124 $m^2 \cdot K$, which when divided by the area of the surface $(0.1\ m)^2$ yields an average temperature of 311.24 K. This shows an increase in temperature from the initial temperature calculated as 311.24 – 293.15 K = 18.09 K.

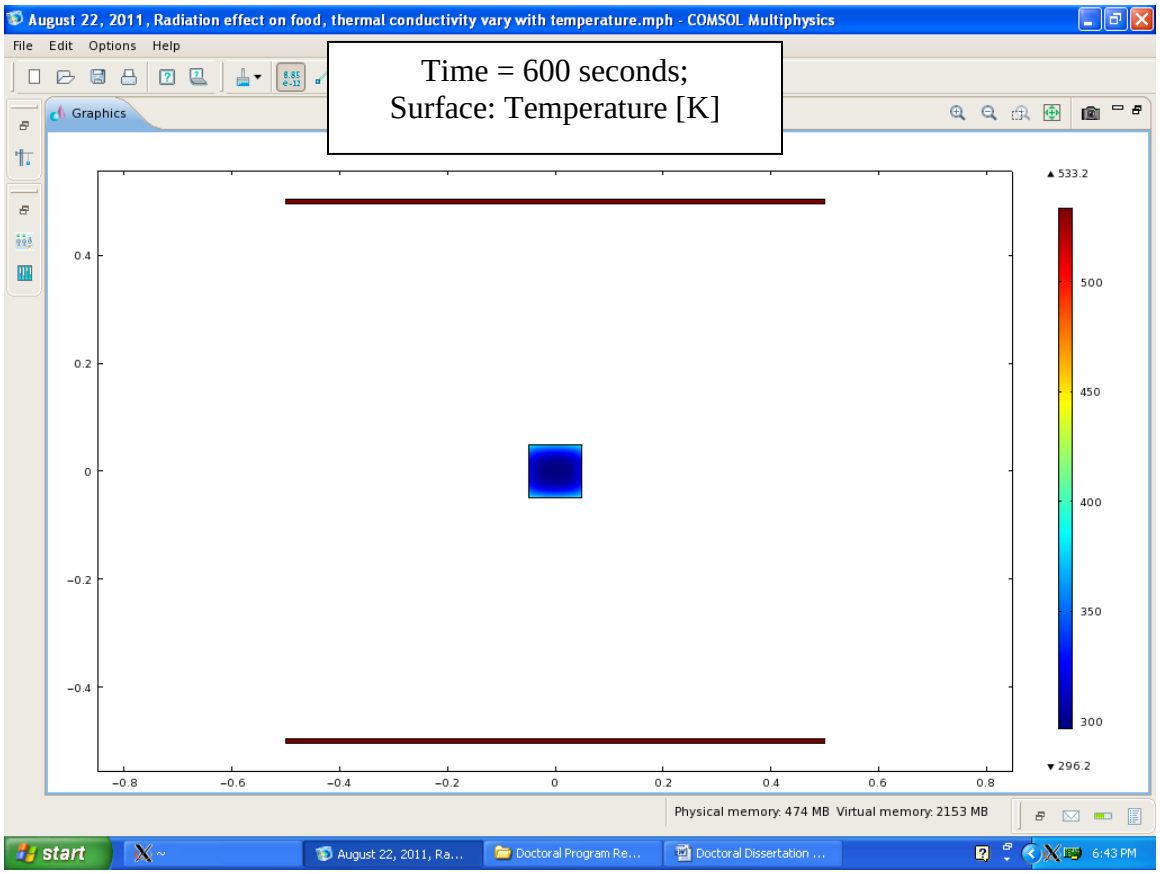

Figure 8.10: Dough/bread with temperature-varying thermal conductivity, COMSOL solution at 600 seconds

Figure 8.10 shows the temperature profile of the dough/bread at 600 seconds (10 minutes). A surface integration performed on the dough/bread domain yielded 3.2397 $m^2 \cdot K$, which when divided by the area of the surface $(0.1\ m)^2$ yields an average temperature of 323.97 K. This shows an increase in temperature from the initial temperature calculated as 323.97 – 293.15 K = 30.82 K.

Figure 8.11 shows a graph of temperature versus time at the center of the dough bread for when the properties of the dough/bread are constant, versus temperature-varying properties. It can be seen from this figure that specifying constant properties for the dough/bread results in a different temperature profile at the center of the dough/bread over time versus the temperature-dependent properties; but also, varying thermal conductivity, density and specific heat with temperature results in different profiles among themselves.

For the constant property simulation, the temperature of the center of the dough/bread first decreases, then increases; this is thought to be due to the fact that the initial radiosities of all the surfaces (dough/bread and heating elements) are specified as zero, and all of the domains (dough/bread and heating elements) initial temperatures are specified as 293.15 K. In other words, it takes some time for the dough/bread to start having realistic values for its increase in temperature as the simulation converges.

For the temperature-varying density simulation, the temperature at the center of the dough/bread first decreases in temperature, then increases. The reason for this is thought to be because as can be seen from Figure 8.12, the density first rises with respect to time, then decreases with respect to time; therefore, the initial temperature drop of the dough/bread is due to the higher density, and the temperature rise is due to the decreasing density. For the temperature-varying property simulations, the initial radiosities of all surfaces were calculated as 729.3 W/m^2, as shown in Appendix C. This calculation was made before the analytical simulation was performed for this model, so the values (such as view factors) for closest model to it (distantly-spaced heating elements) were used. Also in contrast to the constant-property simulation, the initial temperature of the heating

elements for the temperature-varying models is 533.15 K. The initial conditions were changed with respect to the temperature constant property simulation, due to the increased nonlinearity of the temperature-dependent property simulations; it is known that the closer the initial conditions are to the final solution, the better the convergence (COMSOL, 2010 b). From Figure 8.11, the temperature of the dough/bread for the density-varying simulation is in general less than the constant property simulation, which is expected due to the fact that the density of the bread in the density-varying simulation is always higher (roughly 423 kg/m^3 on the average) than the constant property simulation density (380 kg/m^3). A higher density means more energy is required to heat the dough/bread (shown in Wong et al, 2006), which is the same as stating that a higher-density dough/bread has a lower temperature for a given amount of energy.

For the simulation where the specific heat varies with temperature, the curve is qualitatively similar to the constant properties simulation curve. The temperature at the center of the dough/bread for the temperature-varying specific heat simulation is mostly below the curve for the constant property simulation. This is expected as the specific heat (an average of roughly 3030 J/kg·K, as seen in Figure 8.13) in the temperature-varying simulation is always more than the that (1941 J/kg·K) of the constant property simulation; more energy is required to heat the dough/bread with a higher specific heat, as shown in Wong et al (2006).

For the temperature-varying thermal conductivity simulation, the temperature at the center of the dough/bread was at first higher than the constant property simulation, then fell below the constant property simulation. The fact that the temperature is initially higher for the conductivity-varying simulation is expected due to the fact that the thermal

conductivity (roughly an average of 0.4665 W/m·C, as seen in Figure 8.14) for this simulation is always higher than the thermal conductivity (0.1133 W/m·C) of the constant-property simulation; the heat will travel faster to the interior of the dough/bread for a higher thermal conductivity as shown in Wong et al (2006). The fact that the temperature for the thermal conductivity-varying simulation fell below the temperature of the constant property simulation is not expected; it is possible that if the simulation was extended for a greater time period, the temperature of the dough bread for the temperature-varying conductivity simulation might become greater than the constant property simulation later in time (instead of only at the beginning). But it is also expected that when the thermal conductivity of the dough/bread (for the temperature-varying simulation) falls below the thermal conductivity of the dough/bread for the constant property simulation, the temperature of the dough bread with the temperature-dependent conductivity will fall below the temperature of constant property dough/bread. Also, there are different ways to model the dough/bread as having such a temperature-varying property, such as having a variable of thermal conductivity in a more global node, instead of within the material node. The way the temperature of the dough/bread increases in time in Figure 8.11 qualitatively follows the graph of Figure 8.14 (values change, then level, then change). In summary, Figure 8.11 proves that the settings in the physical properties can significantly affect the simulated temperature profiles, as stated in Wong et al (2006).

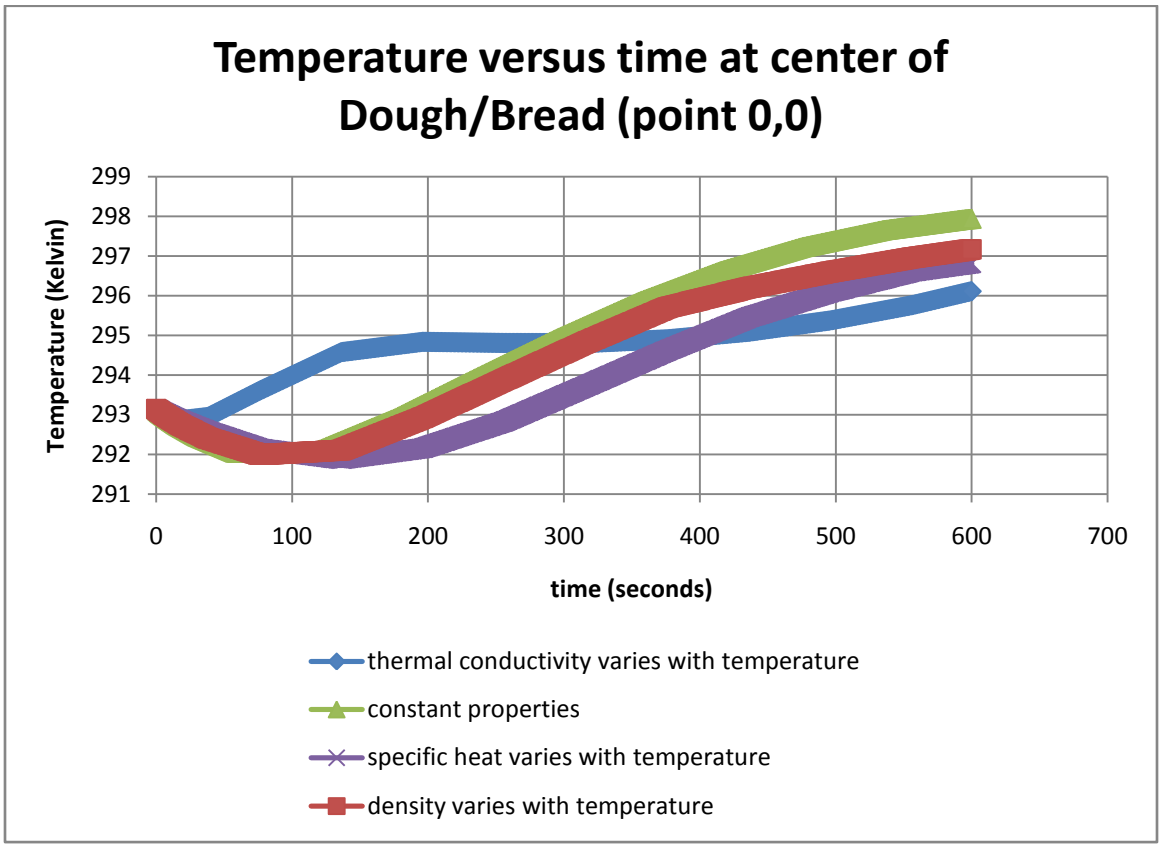

Figure 8.11: Temperature versus time at center of dough/bread, radiation effect on dough/bread with temperature-varying properties versus constant properties, COMSOL

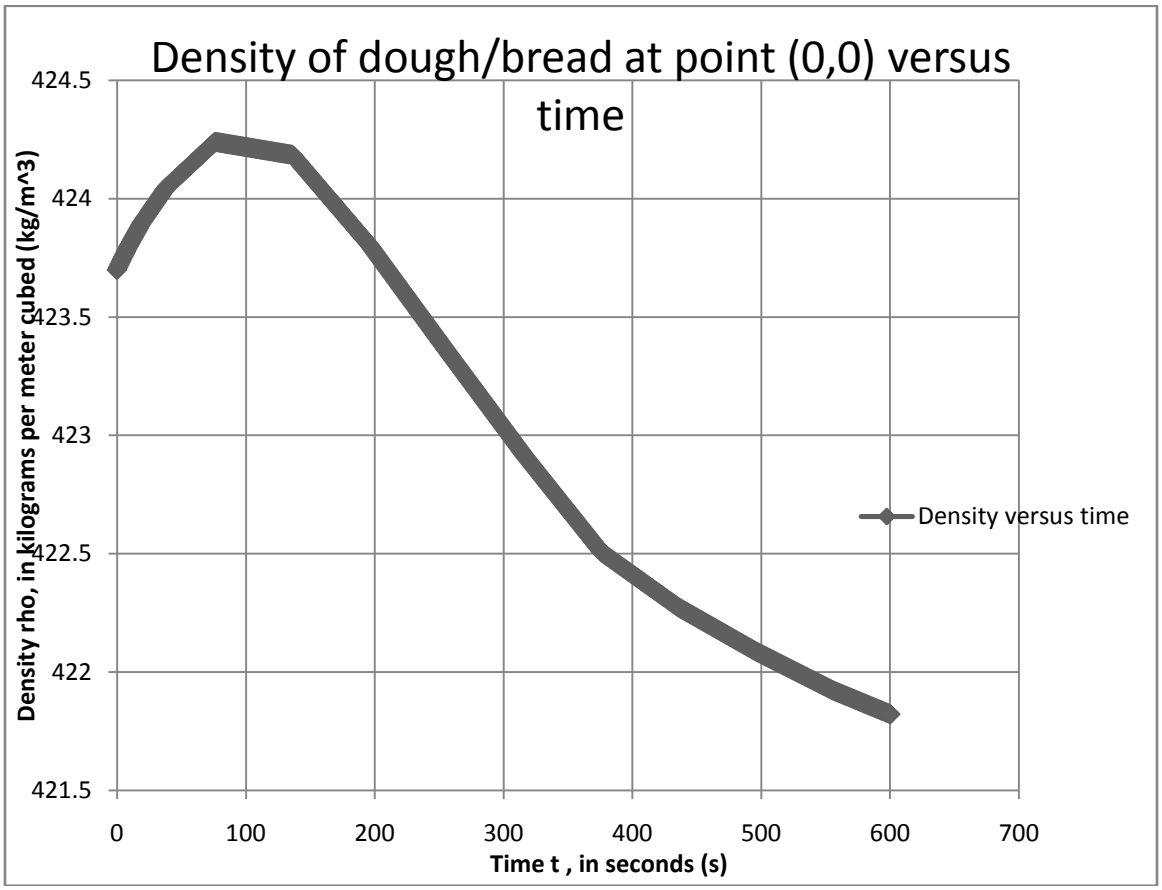

Figure 8.12: Density of dough/bread at point (0,0) versus time

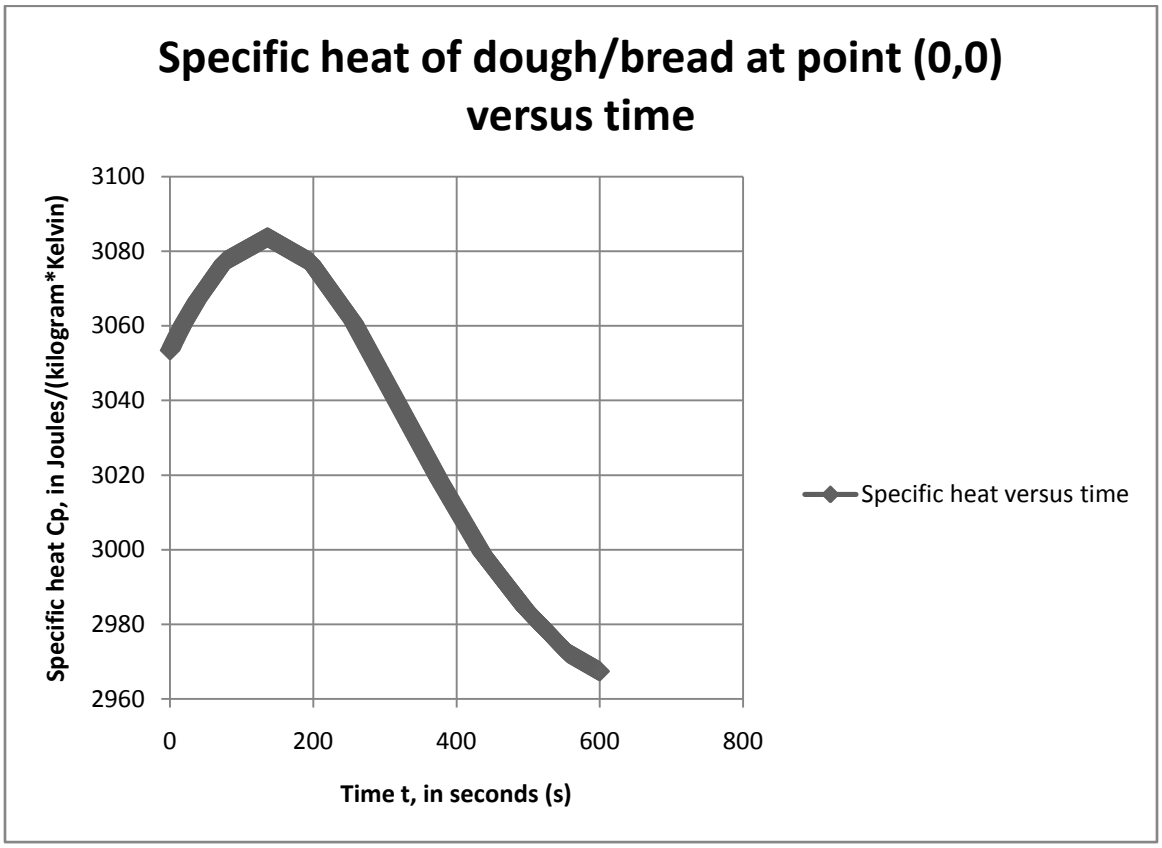

Figure 8.13: Specific heat of dough/bread at point (0,0) versus time

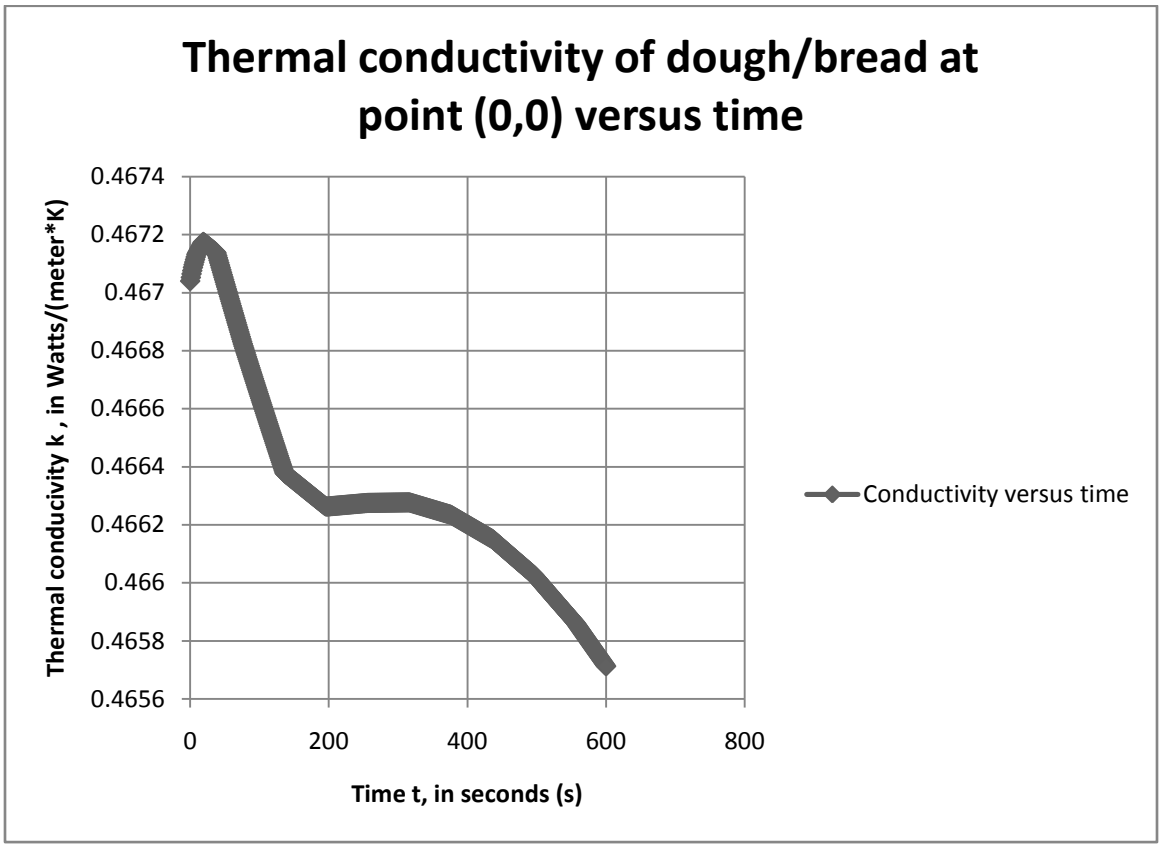

Figure 8.14: Thermal conductivity of dough/bread at point (0,0) versus time

8.2 Convection COMSOL simulations

The free and forced convection COMSOL simulations are presented in this section.

8.2.1 Dimensional free (natural) convection

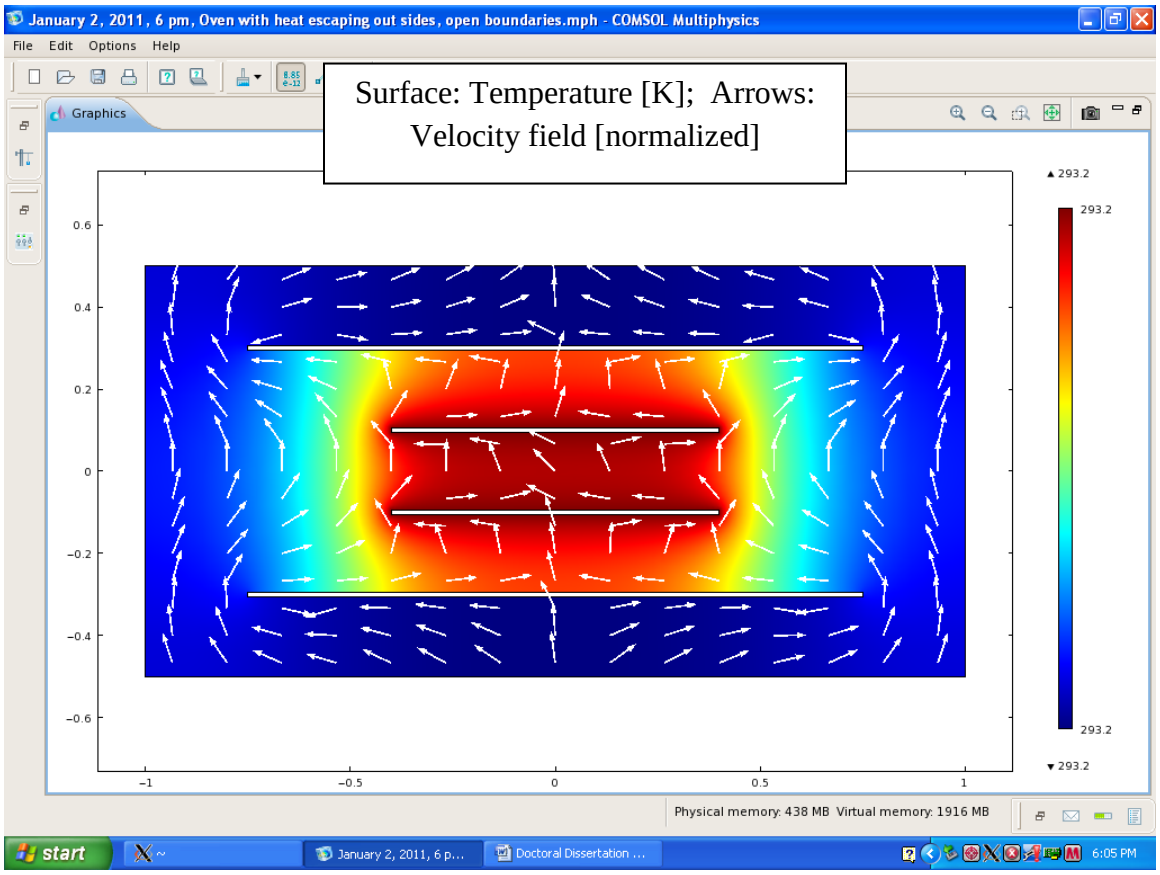

Figure 8.15: Oven with heating elements inside room, COMSOL solution

Figure 8.15 shows the room with open boundaries, and the oven with heating elements (solution). The air heated by the elements rises to the top of the oven, then out of the oven to the room. This solution did not converge, and the cause of this must be determined; the pressure was set to 1 atm initially and afterwards, and this may be a partial contributor to the lack of convergence.

8.2.2 Nondimensional free (natural) convection

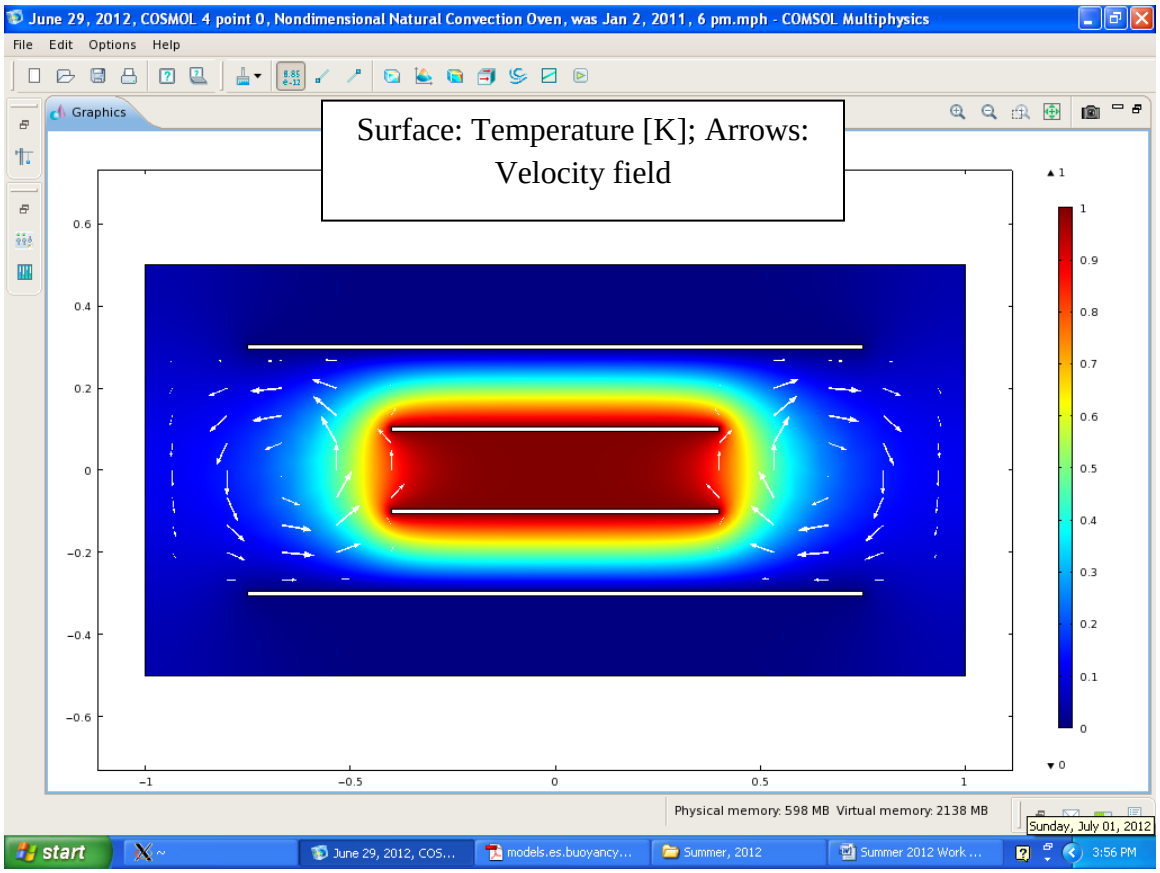

Figure 8.16: Temperature and velocity fields, nondimensional free convection COMSOL simulation, *Ra*=1

Figure 8.16 shows the temperature and velocity fields for the nondimensional free convection COMSOL simulation when the Raleigh number is equal to one. It can be seen from this figure that there are two distinct regions of cellular fluid flow: at the right side of the oven, there is a region of clockwise cellular flow, and at the left side of the oven, a region of counterclockwise cellular flow. These cellular flows are expected, given the locations of the hot and cold areas of the temperature distribution. Compared to the dimensional free convection simulation the nondimensional simulation converged, and

given the inputs of each model, the temperature and velocity distributions are qualitatively as expected. Both the dimensional are nondimensional simulations are laminar (see Section 3.3.1).

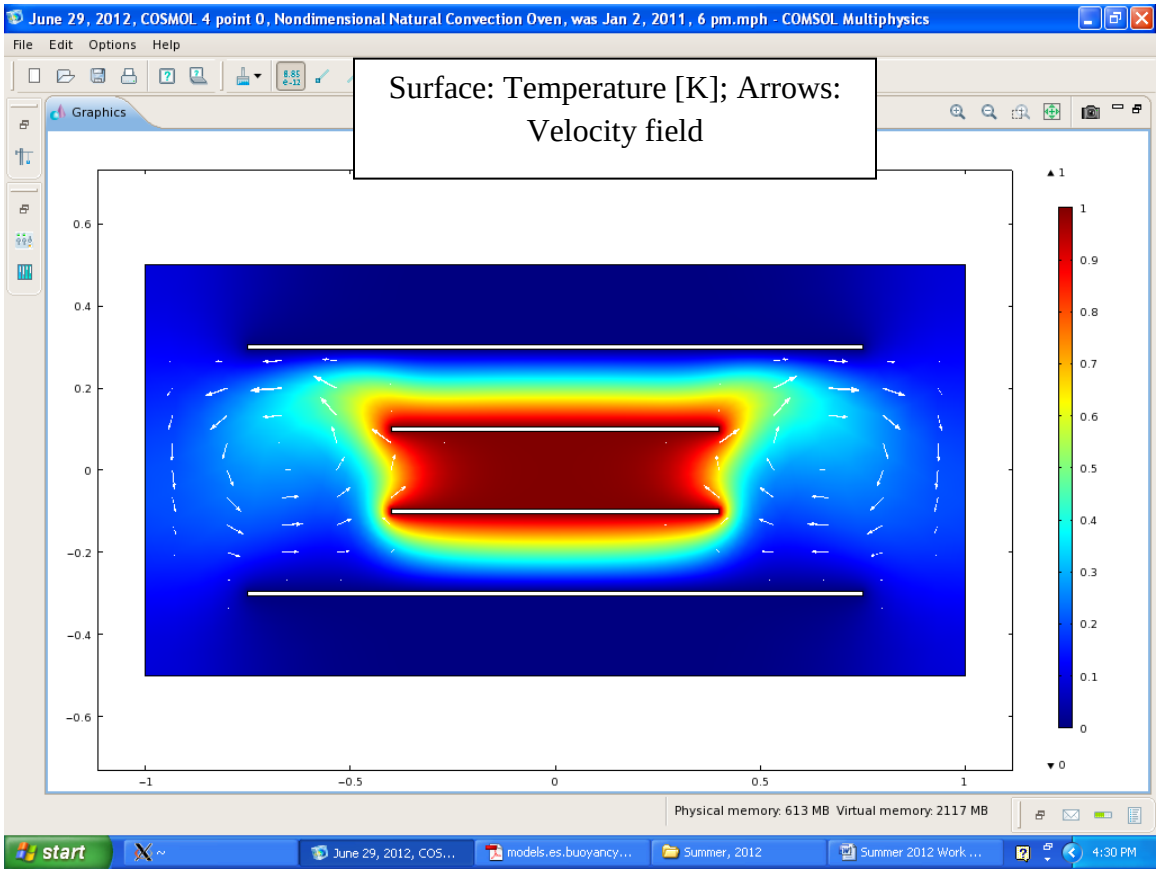

Figure 8.17: Temperature and velocity fields, nondimensional free convection COMSOL simulation, *Ra*=1e5

Figure 8.17 shows the temperature and velocity fields of the nondimensional free convection COMSOL simulation when Rayleigh number is equal to 1e05. Here the shape of the temperature distribution in the vicinity of the heating elements is more of a "butterfly" shape, compared to the when the Rayleigh number is equal to one, where the temperature distribution is more of an "oval" shape. This is expected since the higher the Rayleigh number the more disordered will be the temperature distribution and fluid flow.

Table 8.4 shows the dimensionless temperatures and velocity magnitudes versus Rayleigh numbers for the nondimensional free convection simulations. As expected (COMSOL 2010, e) with increasing the Rayleigh number, temperature increases, resulting in increased velocity magnitudes. The first three entries in the *T* column are all the same with the shown number of significant digits; it is possible that with a greater number of significant digits, the numbers may be different.

Table 8.5 Dimensionless temperatures and velocity magnitudes versus Rayleigh number

Rayleigh Number (*Ra*)	Temperature	Velocity magnitude
1	0.4e522	5.0236×10^{-4}
1e1	0.4522	0.005
1e2	0.4522	0.0502
1e3	0.4523	0.5019
1e4	0.4556	4.7042
1e5	0.4842	24.3723

8.2.3 Forced Convection

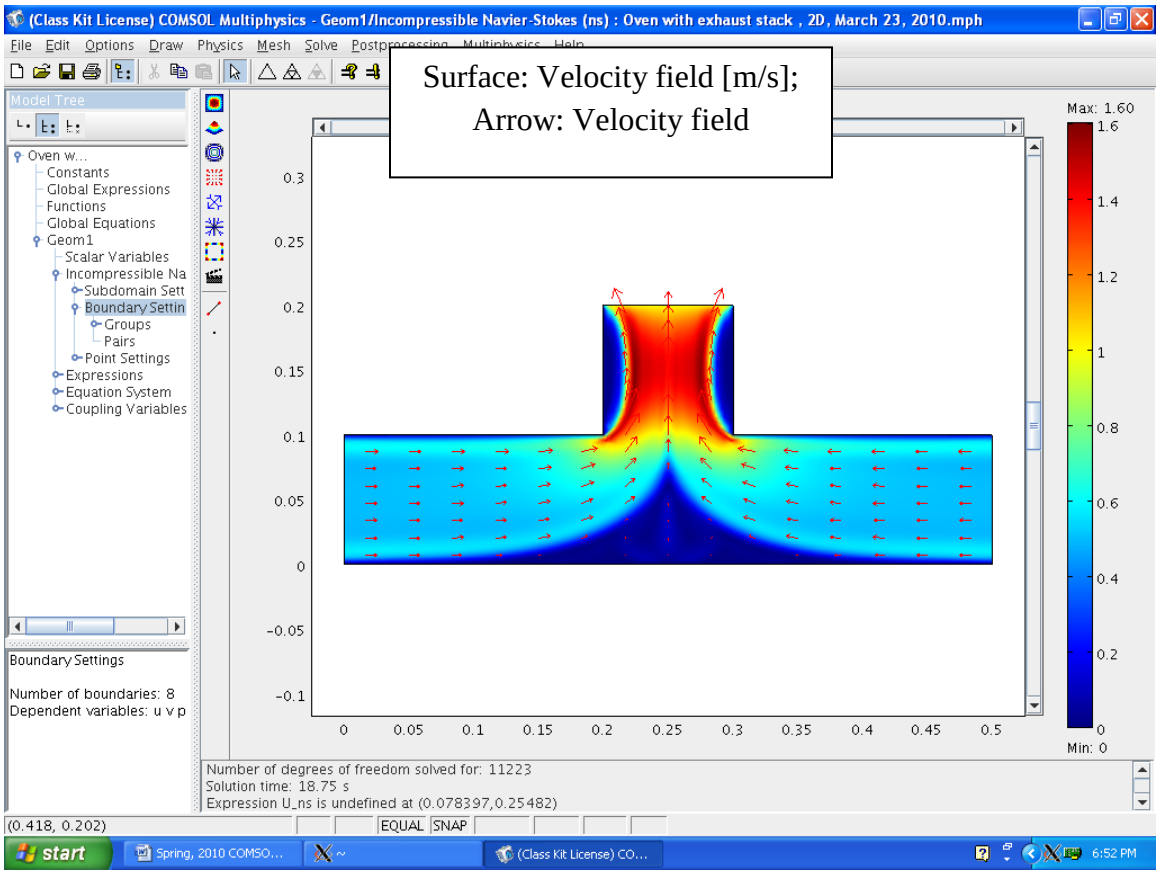

Figure 8.18: Oven with exhaust stack, COMSOL solution

Figure 8.18 shows the COMSOL solution of the oven with exhaust stack. This simulation did converge.

8.3 Moisture COMSOL simulations

The moisture COMSOL simulations are presented in this section.

8.3.1 Moisture loss without heat transfer and convection

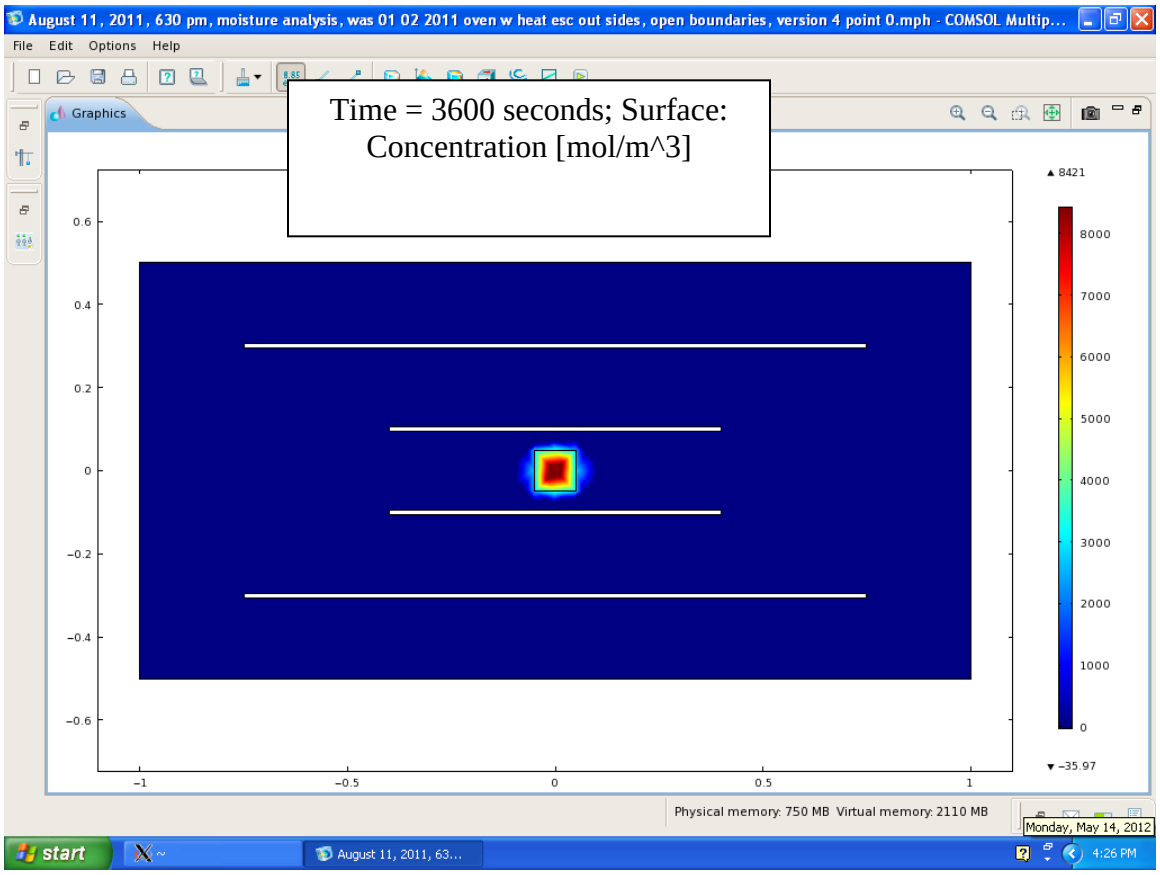

Figure 8.19: Oven with dough/bread within heating elements inside room, COMSOL solution

Figure 8.19 shows the COMSOL result of the oven with dough/bread within heating elements inside the room. It appears as though the moisture is leaving the dough/bread, and diffusing to the room; this can be seen by observing that the moisture concentration is decreasing within the bread, and increasing in the room. A surface integration on the dough bread domain at 3600 seconds resulted in a value of 55.6752 mol/m; this value

divided by the area of the domain $(0.1\ \text{m})^2$ =5567.52 (mol/m^3). The loss of moisture from the dough bread is calculated as follows:

$$\frac{8437.4\ \text{mol water}}{\text{m}^3\ \text{bread}} - \frac{5567.52\ \text{mol water}}{\text{m}^3\ \text{bread}} = \frac{2869.88\ \text{mol water}}{\text{m}^3\ \text{bread} \cdot \text{hr}} \qquad (8-5)$$

Now find kg water lost per m^3.

$$\frac{2869.88\ \text{mol water}}{\text{m}^3\ \text{bread} \cdot \text{hr}} \times \frac{18.015\ \text{g water}}{1\ \text{mol water}} \times \frac{1\ \text{kg water}}{1000\ \text{g water}} = 51.7009\ \frac{\text{kg}}{\text{m}^3 \cdot \text{hr}} \qquad (8-6)$$

$$51.7\ \frac{\text{kg}}{\text{m}^3 \cdot \text{hr}} \times 0.1\ \text{m} \times 0.1\ \text{m} \times 0.2\ \text{m} = 0.1034018\ \frac{\text{kg}}{\text{hr}} \qquad (8-7)$$

For a diffusion coefficient of 1×10^{-10} m^2/s, a surface integration on the dough/bread domain yielded a value of 5567.53 (mol/m^3). This result is used to calculate the moisture loss of the dough/bread as above. Table 8.5 shows the results of the two simulations; as expected, a lower diffusion coefficient resulted in a lower moisture loss from the dough/bread.

Table 8.6: COMSOL moisture simulations without convection and without heat transfer

Diffusion coefficient (m^2/s)	kg water lost /hour
1×10^{-9}	0.1034018
1×10^{-10}	0.1034014

8.3.2 Moisture loss with heat transfer and convection

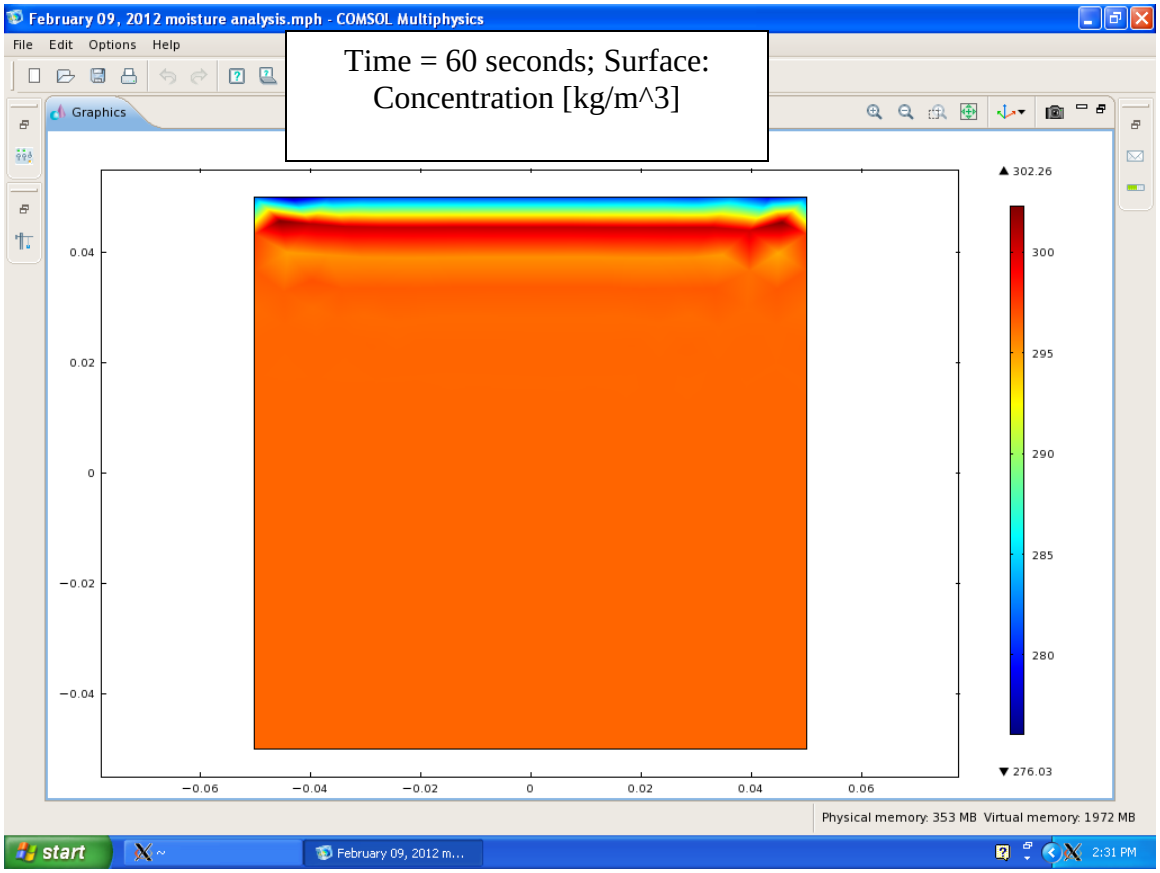

Figure 8.20: Moisture concentration at 60 seconds, COMSOL, using values from Table 6.14

The water loss per hour for Figure 8.20 is calculated as follows: at time 0, the moisture concentration in the dough is 296.4 kg/m^3. At time 60 seconds, the moisture concentration in the dough is 296.15 kg/m^3. The amount of water lost from the dough/bread is:

$$296.4\ \frac{\text{kg water}}{\text{m}^3\text{dough bread}} - 296.15\ \frac{\text{kg water}}{\text{m}^3\text{dough bread}} = 0.25\frac{\text{kg water lost}}{\text{m}^3\ \text{dough bread}} \qquad (8-8)$$

The amount of water lost from the dough bread is (using dimensions from this section and Section 3.4):

$$0.25\frac{\text{kg water lost}}{\text{m}^3\ \text{dough bread}} \times 0.2\ \text{m} \times 0.1\ \text{m} \times 0.1\ \text{m} = 5 \times 10^{-4}\ \frac{\text{kg water lost}}{60\ \text{seconds}} \qquad (8-9)$$

$$5 \times 10^{-4}\ \frac{\text{kg water lost}}{60\ \text{seconds}}\ \times \frac{3600\ \text{seconds}}{\text{hour}} = 0.03\ \ \frac{\text{kg water lost}}{\text{hour}} \qquad (8-10)$$

Table 8.6 shows the results of changes made in the transition from the initial to final COMSOL moisture simulation. When the initial moisture content of the dough/bread (c0) was changed from 0.78*rho_d to 0.57437*rho_d, the moisture loss decreased; this is expected because the difference between the initial moisture content of the dough/bread and the moisture content of the air decreased. When the moisture concentration of the air (c_b) was decreased, the moisture loss of the dough/bread increased; this is expected because the difference between the moisture content of the air and the initial moisture content of the dough/bread increased. When the specific moisture capacity of the dough/bread (C_m) was increased, the moisture loss decreased; this is expected because it is believed that specific moisture capacity in similar to the specific heat capacity of a

substance. The amount of energy required to increase the temperature of a substance is directly related to the magnitude of its specific heat, and this is analogous to the amount of energy required to reduce the moisture content of a substance being directly related to its specific moisture capacity. When the moisture conductivity (k_m) was increased, the moisture loss of the dough/bread did not appear to change; this is somewhat unexpected because it is thought that the moisture would travel faster to the surface, therefore increasing moisture loss. However, increasing k_m resulted in a more uniform moisture distribution throughout the dough/bread: for k_m= 1.29e-09[kg/(m*s)] the low and high moisture concentrations in the dough bread were 214.37 and 219.4 kg/m^3, respectively, whereas for k_m= 1.53e-06 [kg/(m*s)] the low and high moisture concentrations in the dough/bread were 217.1 and 218.27 kg/m^3, respectively. This is expected, and is analogous to the graph shown in Figure 8.3, where the steel being of higher (thermal) conductivity than dough/bread shows a more uniform temperature distribution. Finally, when the mass transfer coefficient in mass units (h_m) was increased, the moisture loss of the dough/bread increased; this is expected since the mass transfer coefficient is directly related to the moisture loss from the dough bread.

Table 8.7: Initial to final COMSOL moisture simulation

Previous Value	Final Value	Previous Moisture Loss $\left(\frac{\text{kg water lost}}{\text{hour}}\right)$	Final Moisture Loss $\left(\frac{\text{kg water lost}}{\text{hour}}\right)$	% differ-ence from previous value
c0: 0.78*rho_d	0.57437*rho_d	0.03	0.0216	-32.56
c_b: 0.02*rho_d	1.192e-04* rho_d	0.0216	0.0228	5.40
C_m: 0.003	0.7373	0.0228	0.0001	-198.25
k_m: 1.29e-09 [kg/(m*s)]	1.53e-06 [kg/(m*s)]	0.0001	0.0001	0
h_m: 1.67e-06 [kg/m^2*s]	5.09e-04 [kg/m^2*s]	0.0001	0.01342	197.04

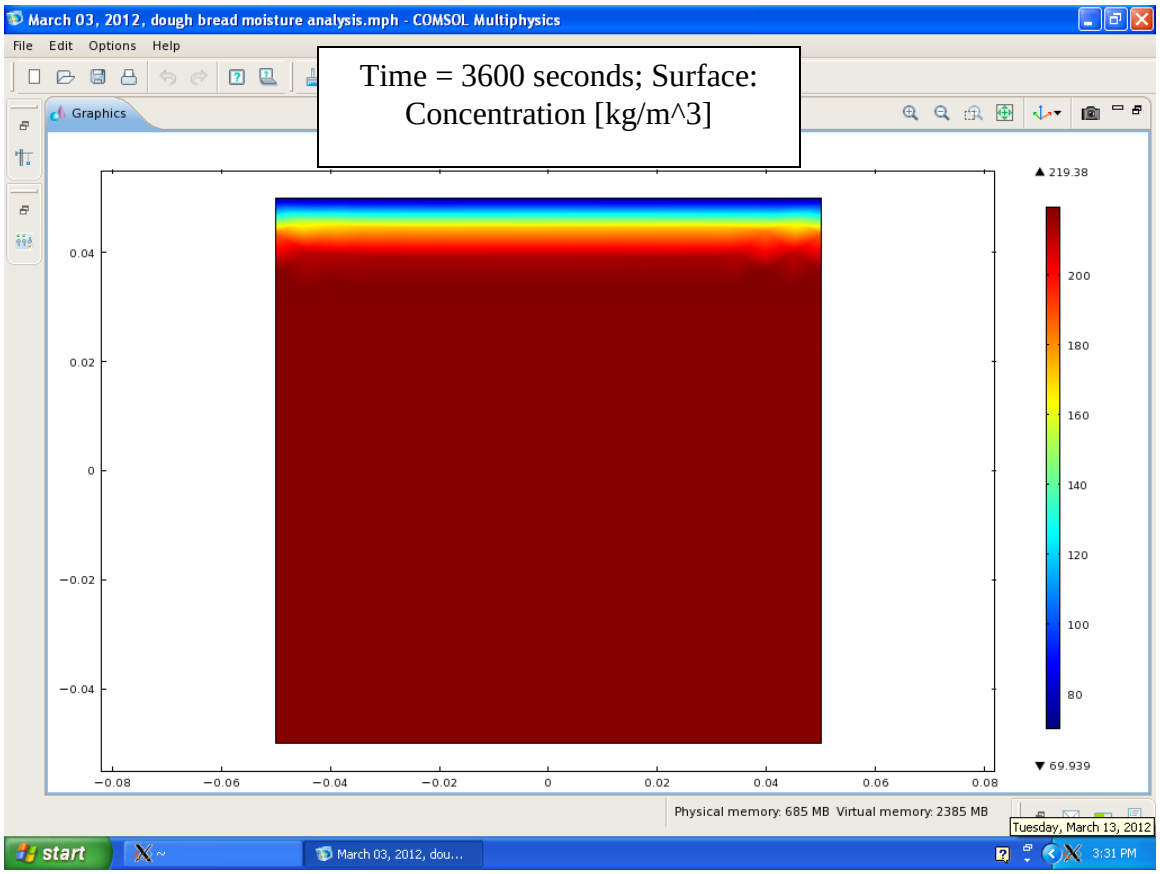

Figure 8.21: Moisture concentration at 3600 seconds, COMSOL, using values from Table 6.15

Following the same procedure for Figure 8.21 as for Figure 8.20:

$$218.26\ \frac{\text{kg water}}{\text{m}^3\text{dough bread}} - 211.55\ \frac{\text{kg water}}{\text{m}^3\text{dough bread}} = 6.71\ \frac{\text{kg water lost}}{\text{m}^3\ \text{dough bread}\ \cdot \text{hour}} \qquad (8-11)$$

$$6.71\ \frac{\text{kg water lost}}{\text{m}^3\ \text{dough bread} \cdot \text{hr}} \times 0.2\ \text{m} \times 0.1\ \text{m} \times 0.1 = 0.01342\ \frac{\text{kg water lost}}{3600\ \text{seconds}} \qquad (8-12)$$

CHAPTER IX

COMSOL SIMULATIONS, THREE-DIMENSIONAL RESULTS AND DISCUSSIONS

This chapter shows the three-dimensional results corresponding to the COMSOL models in Chapter VII.

9.1 Dough/bread as volumetric heat source

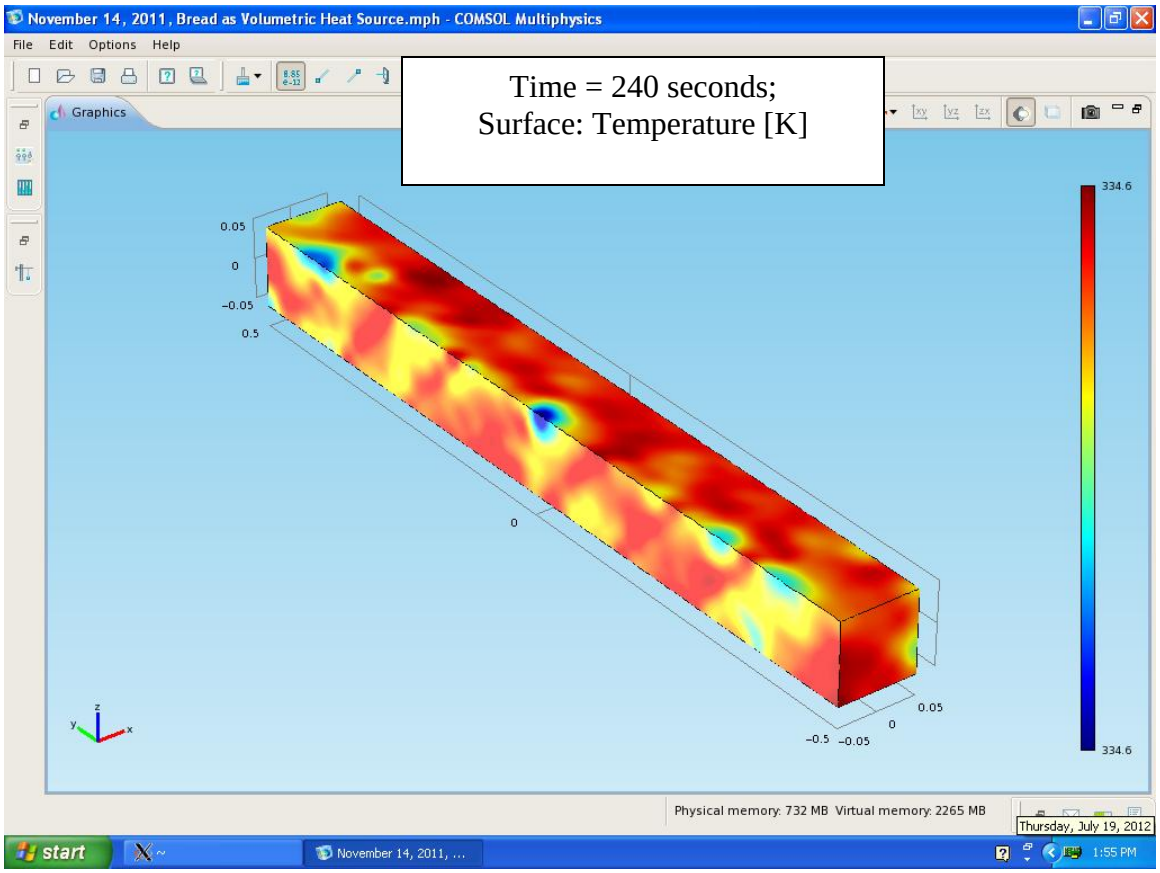

Figure 9.1: Dough/bread as volumetric heat source, COMSOL solution at 240 seconds

Figure 9.1 shows the temperature profile of the dough/bread at 240 seconds (4 minutes). A volume integration performed on the dough/bread domain yielded 3.346 $m^3 \cdot K$, which when divided by the volume (1 m)(0.1 m)^2 yields an average temperature of 334.6 K. This shows an increase in temperature from the initial temperature calculated as 334.6 – 293.15 K = 41.45 K.

9.2 Dough/bread with heat fluxes

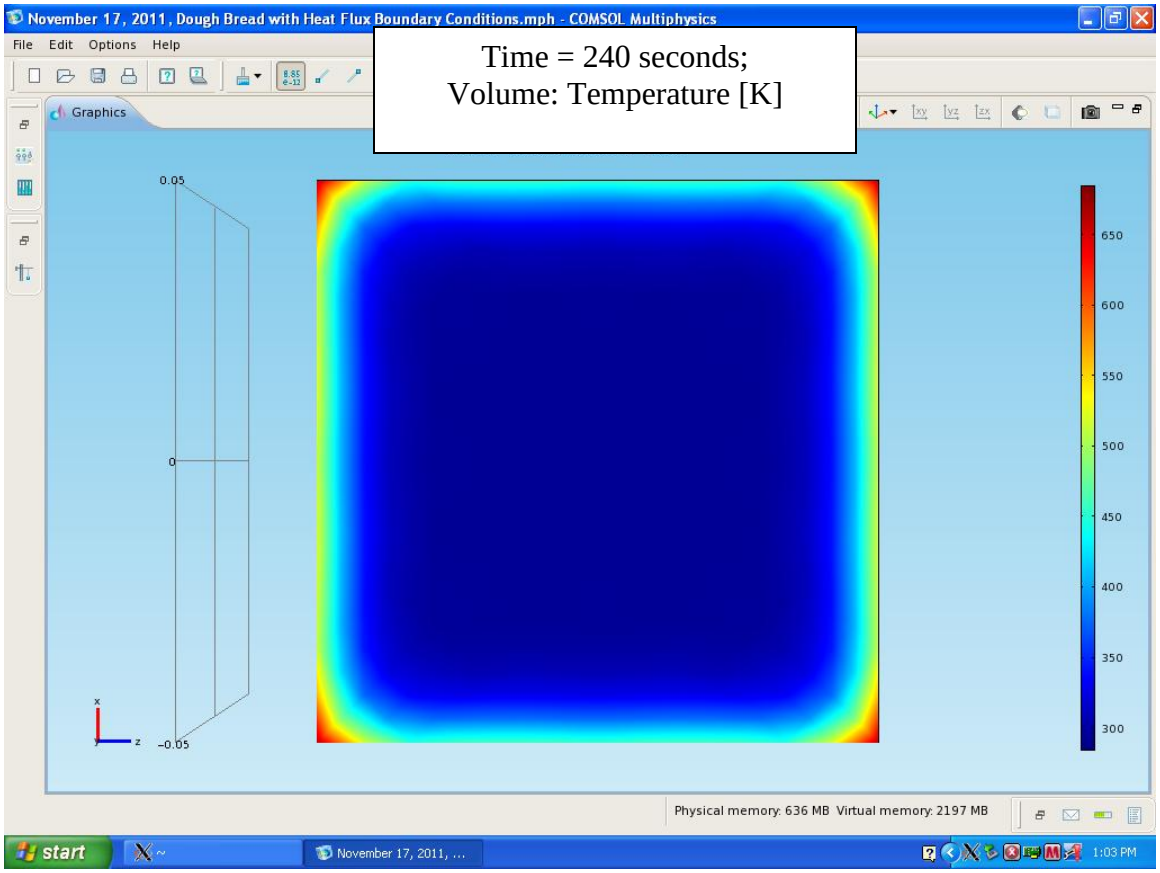

Figure 9.2: Dough/bread with heat fluxes, COMSOL solution

Figure 9.2 shows the temperature profile of the dough/bread at 240 seconds (4 minutes). A volume integration performed on the dough/bread domain yielded 3.3461 $m^3 \cdot K$, which when divided by the volume (1 m)(0.1 m)^2 yields an average temperature of

334.61 K. This shows an increase in temperature from the initial temperature calculated as 334.61 – 293.15 K = 41.46 K.

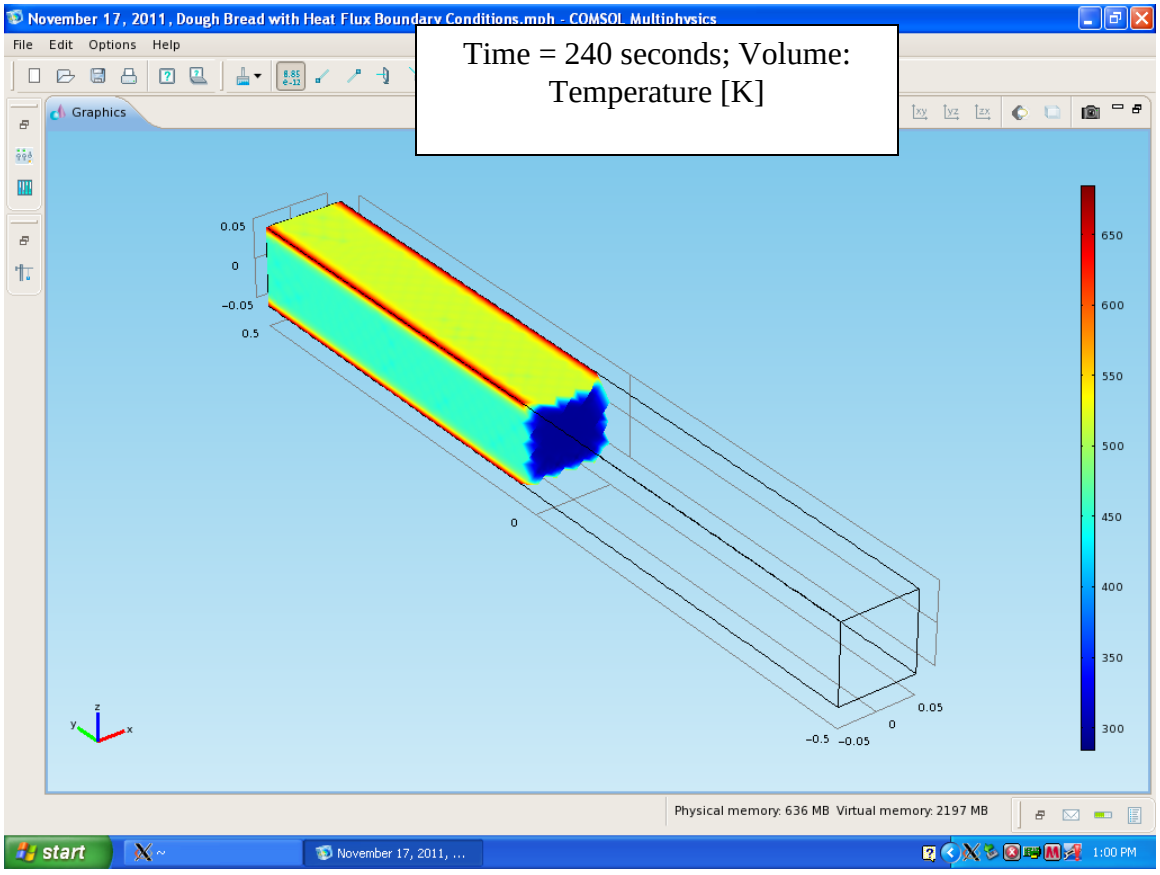

Figure 9.3: Mesh elements y>0.05 m

Figure 9.3 shows the dough/bread having the mesh elements for y values greater than 0.5 m. This is one way of looking at the inside and outside of the dough/bread simultaneously.

9.3 Radiation upon dough/bread using closely-spaced heating elements

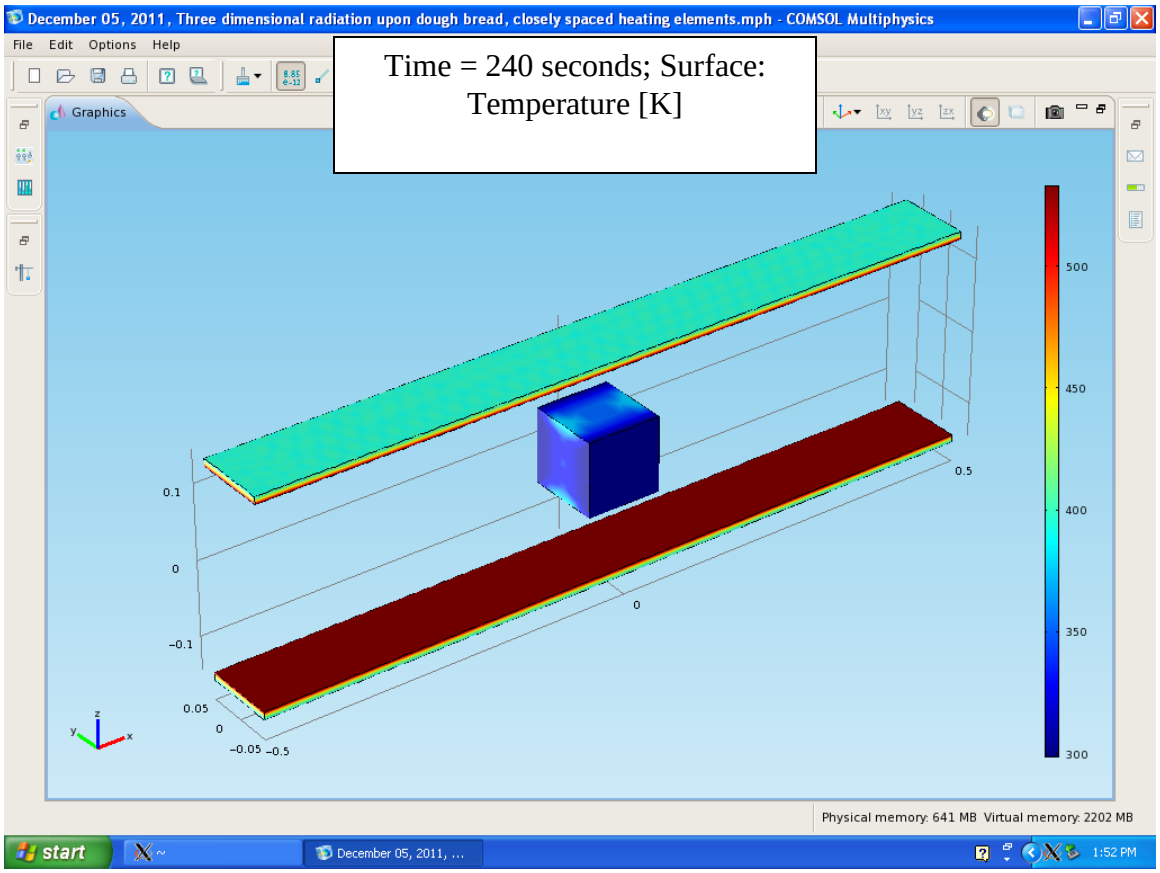

Figure 9.4: 3-D radiation upon dough/bread, closely-spaced heating elements, COMSOL solution at 240 seconds, 1st simulation

Figure 9.4 shows the temperature profile of the dough/bread at 240 seconds (4 minutes). A volume integration performed on the dough/bread domain yielded 0.3045 $m^3 \cdot K$, which when divided by the volume $(0.1\ m)^3$ yields an average temperature of 304.5 K. This shows an increase in temperature from the initial temperature calculated as 304.5 – 293.15 K = 11.35 K. This simulation's average (between intial and final) temperature is used to arrive at an input temperature for the side boundaries 12 and 15. Table 9.1 was constructed by running a simulation with a certain temperature for boundaries 12 and 15, then calculating the average temperature of the dough/bread domain over 240 seconds. The temperature of boundaries 12 and 15 were then adjusted to be closer to the previous average temperature, until the dough/bread average temperature was the same as the inputted temperatures for boundaries 12 and 15.

Table 9.1: Convergence of boundary temperature with average temperature

Initial Temperature	Boundary Temperature (B.T.)	Final Temperature	Average (between initial and final) Temperature (A.T.)	% difference between B.T. and A.T
293.15 K	413.15 K	326.1 K	309.625 K	28.65
293.15 K	313.15 K	307.3 K	300.225 K	4.21
293.15 K	300.15 K	304.8 K	298.975 K	0.392
293.15 K	298.975 K	304.6 K	298.875 K	0.0335
293.15 K	298.875 K	304.5 K	298.825 K	0.0167
293.15 K	298.825 K	304.5 K	298.825 K	0

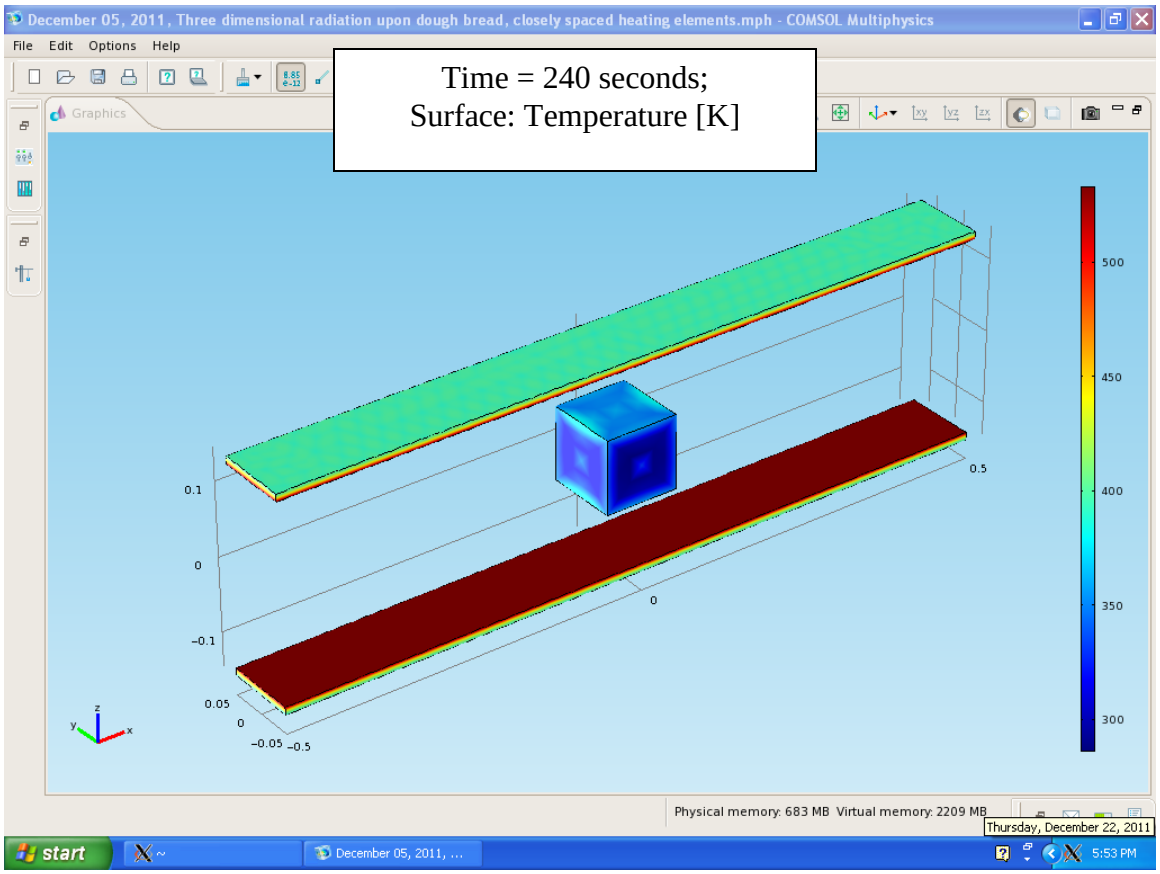

Figure 9.5: 3-D radiation upon dough/bread, closely-spaced heating elements, COMSOL solution at 240 seconds, 2nd simulation

Figure 9.5 shows the temperature profile of the dough/bread at 240 seconds (4 minutes). This simulation uses an emissivity of zero for side boundaries, and an ambient temperature of 293.15 K. A volume integration performed on the dough/bread domain yielded 0.3053 $m^3 \cdot K$, which when divided by the volume $(0.1\ m)^3$ yields an average temperature of 305.3 K. This shows an increase in temperature from the initial temperature calculated as 305.3 – 293.15 K = 12.15 K.

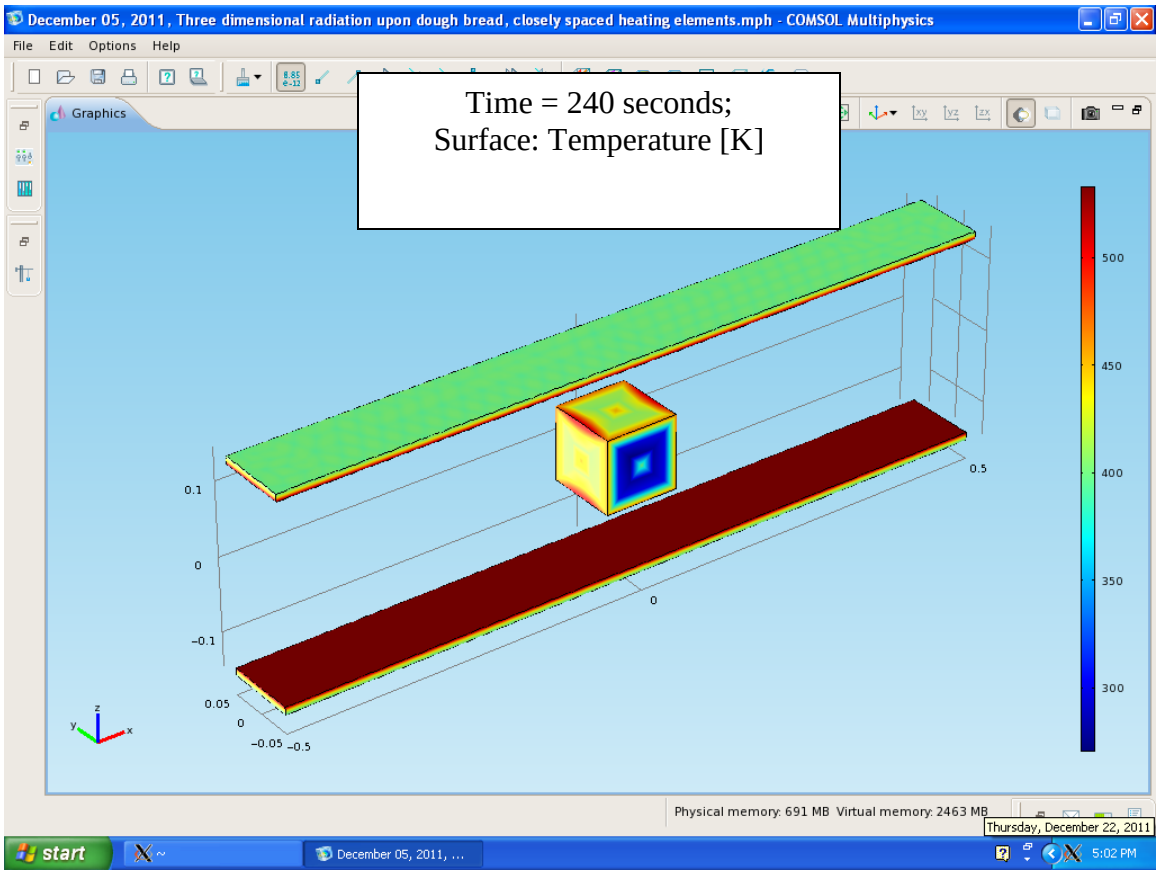

Figure 9.6: 3-D radiation upon dough/bread, closely-spaced heating elements, COMSOL solution at 240 seconds, 3rd simulation

Figure 9.6 shows the temperature profile of the dough/bread at 240 seconds (4 minutes). This simulation uses an emissivity of zero for side boundaries, and an ambient temperature of 533.15 K. A volume integration performed on the dough/bread domain yielded 0.3281 $m^3 \cdot K$, which when divided by the volume $(0.1\ m)^3$ yields an average temperature of 328.1 K. This shows an increase in temperature from the initial temperature calculated as 328.1 – 293.15 K = 34.95 K.

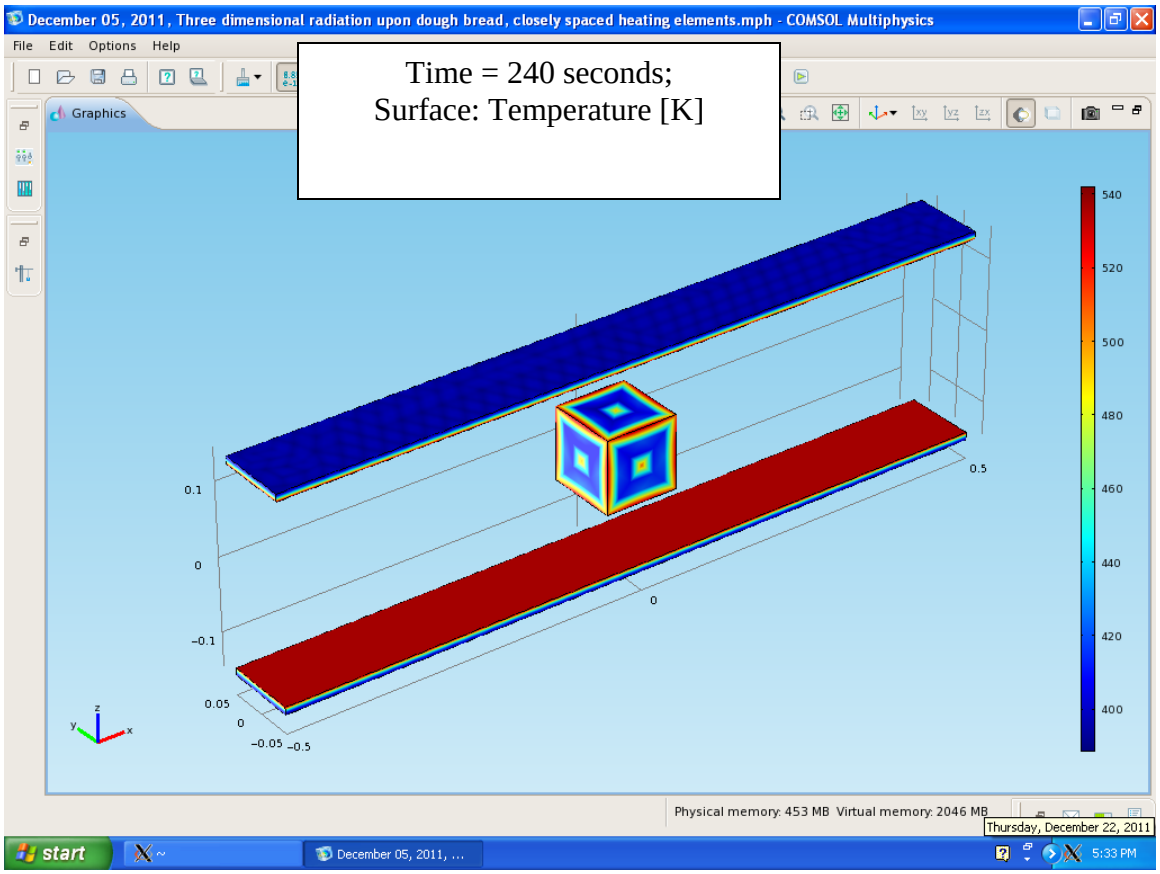

Figure 9.7: 3-D radiation upon dough/bread, closely-spaced heating elements, COMSOL solution at 240 seconds, 4th simulation

Figure 9.7 shows the temperature profile of the dough/bread at 240 seconds (4 minutes). This simulation uses an emissivity of 0.9 for side boundaries, and an ambient temperature of 533.15 K. A volume integration performed on the dough/bread domain yielded 0.3421 $m^3 \cdot K$, which when divided by the volume $(0.1\ m)^3$ yields an average temperature of 342.1 K. This shows an increase in temperature from the initial temperature calculated as 342.1 – 293.15 K = 48.95 K.

CHAPTER X

DESCRIPTION OF MATLAB CODE, MATLAB MODELS, AND MATLAB SIMULATIONS

10.1 Description of MATLAB code

MATLAB is a high-level language and interactive environment that may enable one to perform computationally intensive tasks easier than with traditional programming languages such as C, C++, and FORTRAN ("MATLAB-the Language of Technical Computing", 2011). One example where using MATLAB is more efficient in this research is the "solve" function, which automatically solves for the desired variable in a given equation (see Appendix C).

10.2 MATLAB models

The MATLAB models are discussed in this section. These are the inputs for the corresponding simulations.

10.2.1 Radiation (with conduction) MATLAB models

A MATLAB model (transient) is coded that corresponds to the analytical calculations (stationary) in Sections 3.1.2 and 3.2.2. The code for this model in shown in Appendix A.

10.2.2 Conduction MATLAB models

A MATLAB model is coded that corresponds to the analytical calculations in Section 3.2.3. The program is shown in Appendix D.

10.2.3 Moisture MATLAB models

A MATLAB model is coded that corresponds to the analytical calculations in Section 3.4. This program is shown in Appendix F.

10.3 MATLAB simulations

This section describes the MATLAB simulations corresponding to the MATLAB models. The simulations are the outputs of the programs.

10.3.1 Radiation (with conduction) MATLAB simulations

A simulation was performed that modeled a transient analysis of the closely-spaced heating elements heating food with constant properties. The MATLAB output is given in Appendix “B”. This simulation was performed after it was found that there was a significant discrepancy in the results of the corresponding analytical (Section 3.2.2) and COMSOL (Section 8.1.3, without side boundaries) simulations. As shown before, the analytical simulation showed a change in food temperature 41.4 K whereas the COMSOL simulation showed a food temperature change of 25.39 K. The MATLAB simulation

showed a food temperature change of 39.90 K, which shows that the analytical simulation may be similar in physics to the MATLAB simulation.

10.3.2 Conduction MATLAB simulations

The conduction MATLAB output is shown in Appendix E. This simulation shows a temperature increase of the dough/bread to be 22.73 K.

10.3.3 Moisture MATLAB simulations

The moisture MATLAB output is shown in Appendix G. This simulation shows a drying rate of 2.1150 kg/(hour *m^2), which is exactly the same as in Section 3.4.

CHAPTER XI

COMPARISONS, RECOMMENDATIONS AND CONCLUSIONS

11.1 Comparisons

Comparisons between the radiation and conduction simulations, and then the moisture simulations, are discussed in this section.

11.1.1 Radiation and conduction simulations

Figure 8.1 in Section 8.1.1 is compared to the results from the analytical simulation in Sections 3.1.1 and 3.2.1. The analytical simulation shows a temperature increase of 6.2 K, whereas the COMSOL simulation shows a temperature increase of 4.70 K.

The results shown in Table 11.1 are compared using a percent difference. The percent difference is the difference between two values divided by the average of the two values. The equation for this research is shown as follows:

$$\%\ \text{difference with respect to reference value} = \left(\frac{\text{value under inspection} - \text{reference value}}{\left(\frac{\text{reference value} + \text{value under inspection}}{2} \right)} \right) \times 100 \qquad (11-1)$$

Table 11.1: Results from section 8.1.1 versus sections 3.1.1 and 3.2.1, radiation effect upon container material

Section(s)	Temperature Increase (K)	% difference with respect to Analytical
3.1.1 and 3.2.1 (Analytical)	6.2	- -
8.1.1 (COMSOL)	4.70	-27.52 %

The ΔT = 6.2 K corresponds to the emissivity of 0.1, for the 3600 second simulation in Table 8.1 in the COMSOL simulation (where ΔT =297.85 K-293.15 = 4.70 K). The value for the analytical solution is greater due to the fact of the (steady-state) assumption that the container remains at 293.15 K during the entire simulation, so it gains more radiation (heat) from the heated plate (which is fixed at 533.15 K), and loses less radiation (heat) to the environment (which is fixed at 293.15 K). Or, one could say that with respect to the COMSOL simulation, the temperature differential between the container material and the heating elements decreases with time (resulting in less heat transfer from the heating elements to the container surface), and the temperature differential between the container surface and the surroundings increases with time (resulting in more heat transfer from the container material to the surroundings). Probably another reason that the ΔT for the analytical simulation is greater than for the COMSOL simulation is that for the analytical simulation, the heat source is assumed to be from within the entire container (volumetric), whereas for the COMSOL simulation the heat source is actually only from the heating elements radiating heat upon the upper and lower surfaces of the container material.

Table 11.2 shows the results of the volumetric MATLAB, 1-D MATLAB, and Analytical Simulations versus the COMSOL simulation. All of the simulations in this table are compared to the MATLAB simulation of Section 10.3.1. It is apparent that the MATLAB simulation of Section 10.3.1 and the Analytical simulation of Section 3.2.2 are calculating similar physical phenomena. The COMSOL simulation of Section 8.1.3, however, shows a much lower temperature increase for the dough bread than those first two simulations in the table. From Figure 8.6, it can be seen that the amount of radiative heat flux upon the dough/ bread in the COMSOL simulation is much less than that calculated in the Analytical simulation. For the COMSOL simulation, the steady-state radiative heat flux upon the dough bread is:

$$\left(-13.9652\,\frac{\mathrm{W}}{\mathrm{m}}\right)(0.1\ \mathrm{m}) + \left(12.3655\,\frac{\mathrm{W}}{\mathrm{m}}\right)(0.1\ \mathrm{m}) + \left(-13.9649\,\frac{\mathrm{W}}{\mathrm{m}}\right)(0.1\ \mathrm{m}) + \left(12.3673\,\frac{\mathrm{W}}{\mathrm{m}}\right)(0.1\ \mathrm{m}) = -0.31973\ \mathrm{W} \qquad (11-2)$$

For the Analytical simulation the steady-state radiative heat flux upon the dough/bread is:

$$-535.1\ \frac{\mathrm{J}}{\mathrm{s}} + \left(-738.5\ \frac{\mathrm{J}}{\mathrm{s}}\right) = -535.1\ \mathrm{W} + (-738.5\ \mathrm{W}) = -1273.6\ \mathrm{W} \qquad (11-3)$$

The fact that less radiative heat flux (energy) is impinging upon the dough/bread in the COMSOL simulation compared to the Analytical simulation may be a clue as to why the temperature is less in the COMSOL simulation (though the Analytical simulation has a 3-D dough/bread). The value for the temperature increase in the 1-D MATLAB simulation is significantly less the value for the volumetric MATLAB simulation. This may be partly due to the fact that the 1-D MATLAB simulation only models one heating element

impinging upon the dough/bread, although the other side of the dough bread is being heated by the oven air (the average of room temperature and heating element temperature). The dough/bread temperature rise in the MATLAB 1-D simulation is slightly less than the 2-D COMSOL simulation, and this is due at least to the same reasons that the MATLAB 1-D simulation is lower than the volumetric MATLAB simulation.

Table 11.2 Results of volumetric MATLAB and analytical simulations versus surface COMSOL and MATLAB 1-D simulations, for dough/bread

Simulation	Temperature rise (stationary or transient)	% difference with respect to Volumetric MATLAB
Volumetric MATLAB (Section 10.3.1)	39.90 K (transient)	--
Volumetric Analytical (Section 3.2.2)	41.4 K (stationary)	3.70 %
2-D COMSOL (Section 8.1.3)	25.39 K (transient)	-44.4 %
MATLAB 1-D (Section 10.3.2)	22.73 K (transient)	-54.8 %

Table 11.3 shows a comparison between the 2-D and 3-D COMSOL simulations for the radiation effect on dough/bread. One of the challenges of the 3-D model is to specify an appropriate boundary condition for the faces (named 12 and 15) of the dough/bread that do not "see" the heating elements (the faces that do not exchange heat with the heating elements). The boundary conditions on these faces may be specified to correspond to the 2-D model or reality, or both. For the 1st 3-D COMSOL simulation (Figure 9.4), the temperature rise is seen to be less than the 2-D COMSOL simulation (Figure 8.5). For the 2nd 3-D COMSOL simulation (Figure 9.5), it is seen that the temperature rise is closer than the 1st simulation in magnitude to the 2-D simulation; this shows that changing the side boundaries 12 and 15 to an emissivity of zero rather than at an average temperature of 298.25 K better corresponds to the 2-D simulation.

For the 3rd 3-D COMSOL simulation (Figure 9.6) the temperature rise is greater than the preceding simulations in the table (due to the increase in T_{amb}), as expected. Changing the emissivity to 0.9 in the 4th 3-D simulation results in a greater temperature rise than the 3rd simulation; this suggests that specifying an emissivity for the 2nd 3-D simulation (Figure 9.5) might result in a greater temperature increase within the simulation, leading to a value closer to the 2-D COMSOL simulation.

Table 11.3: Comparison between 2-D and 1st, 2nd, 3rd and 4th 3-D COMSOL simulations, radiation effect on dough/bread

Simulation	Temperature rise	% difference with respect to Figure 8.5 (Section 8.1.3)
Figure 8.5 (Section 8.1.3)	25.39 K	--
Figure 9.4 (Section 9.3): Sides 12 and 15 T = 298.825 K; T_{amb} = 293.15 K	11.35 K	- 76.4 %
Figure 9.5 (Section 9.3): Sides 12 and 15 ε = 0; T_{amb} = 293.15 K	12.15 K	- 69.1 %
Figure 9.6 (Section 9.3): Sides 12 and 15 ε = 0; T_{amb} = 533.15 K	34.95 K	31.7 %
Figure 9.7 (Section 9.3): Sides 12 and 15 ε = 0.9; T_{amb} = 533.15 K	48.95 K	63.4 %

Looking at Table 11.4, one can see the comparison of the volumetric heat source results for the MATLAB, Analytical, and COMSOL simulations, along with the COMSOL 3-D heat flux simulation. It is apparent from this table that the same (or very nearly the same) phenomena are being simulated. Essentially, whether the energy is being generated within the dough/bread or is impinging upon it, the temperature rise of the dough/bread is very similar.

Table 11.4: Comparison of volumetric heat source results for MATLAB, analytical, and COMSOL simulations, along with COMSOL 3-D heat flux simulation

Simulation	Temperature rise (stationary or transient)	% difference with respect to MATLAB
MATLAB (Section 10.3.1)	39.90 K (transient)	--
Analytical (Section 3.2.2)	41.4 K (stationary)	3.70 %
COMSOL (Section 9.1)	41.45 K (transient)	3.82 %
COMSOL (Section 9.2)	41.46 K (transient)	3.84 %

11.1.2 Moisture simulations

Table 11.5 shows the moisture model comparisons (with the literature values) for the analytical (and MATLAB) and COSMOL simulations. The analytical (and MATLAB) simulations yielded a moisture loss that is within the range of the literature values. The

analytical (and MATLAB) simulations show a value of 0.0423 kg water lost per hour, which is closer to the low value shown in Baik et al (2000, b); this is thought to be possibly because the analytical (and MATLAB) simulations only model one heating element. Undoubtedly, modeling more than one heating element analytically and in MATLAB would cause a greater loss of moisture from the dough/bread. The COMSOL simulation with convection and heat transfer resulted in a value that was less than the low value of Baik et al (2000 b), and this might be due to any number of reasons. Baik et al (2000 b) cited another work by Hasatani et al (1991), and the article by Hasatani et al (1991) was not available on the internet, nor available to be borrowed. The work in Hasatani et al (1991) is only known to have the inputs of a temperature of 200°C in an electric batch oven, but the size of the bread in that article is not known, nor the exact physical properties, etc.; so the similarity of the COMSOL simulation with the results of Hasatani et al (1991) is not expected to be exact. The value for the heat transfer coefficient in the COMSOL simulation was based on the analytical simulation, so a higher heat transfer coefficient would probably lead to a higher moisture loss from the dough/bread. The properties in the COMSOL simulation do not depend on temperature, and temperature-dependent properties can improve the accuracy of this type of simulation (Haiqing et al, 1999). Finally, the mesh of the COMSOL simulation was rather coarse, and a refinement in the mesh might improve the accuracy of the results.

The COMSOL simulation without convection and without heat transfer yielded a value that is in between the low and high values from Baik et al (2000 b). It is expected that this COMSOL simulation value (0.103 kg water lost/hour) is less than the high value from Baik et al (2000 b), because the COMSOL simulation has no heat transfer, whereas

the value from Baik et al (2000 b) undoubtedly has heat transfer. This simulation is thought to be higher than the COMSOL (with convection and heat transfer) and the Analytical and MATLAB simulations because the dough/bread is losing moisture from all four sides (it is not in a container), whereas the other simulations involve a container.

Table 11.5: Moisture model comparisons

Simulation or Literature	kg water lost /hour	% difference with respect to (w.r.t.) Baik et al (2000, b) low value or high value
Baik et al (2000, b), low value	0.030	0 (w.r.t.) low value --
Baik et al (2000, b), high value	0.25488	0 (w.r.t) high value --
Analytical (and MATLAB)	0.0423	34.02 (w.r.t) low value
Analytical (and MATLAB)	0.0423	-143.065 (w.r.t) high value
COMSOL (with convection and heat transfer)	0.01342	-76.37(w.r.t.) low value
COMSOL (no convection and no heat transfer)	0.103	-84.88 (w.r.t.) high value

11.2 Recommendations

In this research, a number of recommendations can be made with respect to the various relevant physics.

11.2.1 Radiation and conduction recommendations

To advance the content of this research, workers in this field may want to calculate the view factor for the three-dimensional geometry of Figure 7.6 (Howell, 2012). This can be done as a step toward comparing the COMSOL 3-D radiation models with analytical solutions.

Participating media may be added to the radiation heat transfer models in COMSOL, thereby creating a more complete simulation of the oven; the participating media in this case is the humid air.

In the case of the 1-D MATLAB conduction model (which has radiation boundary conditions), the implicit method may be used instead of the explicit method. The implicit method is in general unconditionally stable, and may be more accurate, although possibly harder to code. The increase in coding difficulty is due to the method's requirement to solve simultaneous equations.

11.2.2 Convection recommendations

In the future, researchers may wish to model air curtains at the ends of a tunnel oven in order to minimize heat loss from the oven. An air curtain is a stream of air, usually blowing down from an overhead compartment; its purpose is to reduce heat transfer between hot and cold environments.

11.3 Conclusions

In this research a bread-baking oven, and the dough/bread within it, are successfully modeled and simulated. The bread baking process is proven to involve the physics of radiation, conduction, convection (both free and forced), and mass transfer (with respect to both the dough/bread and oven). This is a complex process that always warrants further improvements, and computational fluid dynamics can be the most effective method of modeling and simulating this process. However, researchers must always check their inputs and results with appropriate sources.

BIBLIOGRAPHY

Air-Density and Specific Weight. Retrieved on April 24, 2012 from http://www.engineeringtoolbox.com/air-desity-specific-weight-d_600.html

Amit, A (2012, January 12). What is the weak formulation of a differential equation? *Quora*. Retrieved July 12, 2012 from http://www.quora.com/What-is-the-weak-formulation-of-a-differential-equation

Aversa, M., Curcio, S., Calabro, V., & Iorio, G. (2007). An analysis of the transport phenomenon occurring during food drying process. *Journal of Food Engineering, 78,* 922-932.

Baik. O.D., Marcotte, M.., & Castiagne, F. (2000 a). Cake baking in tunnel type multi-zone industrial ovens. Part I. Characterization of baking conditions. *Food Research International, 33,* 587-598.

Baik. O.D., Marcotte, M.., & Castiagne, F. (2000 b). Cake baking in tunnel type multi-zone industrial ovens Part II. Evaluation of quality parameters. *Food Research International, 33,* 599-607.

Boulet, M., Marcos, B., Dostie, M., & Moresoli, C. (2010). CFD modeling of heat transfer and flow field in a bakery pilot oven. *Journal of Food Engineering, 97,* 393-402.

Broyart, B., & Trystram, G. (2003). Modelling of heat and mass transfer phenomena and quality changes during continuous biscuit baking using both deductive and inductive (neural network) modeling principles. *Food and Bioproducts Processing, 81,* 316-326.

Chen, H., Marks, B.P., & Murphy, R. Y. (1999). Modeling coupled heat and mass transfer for convection cooking of chicken patties. *Journal of Food Engineering, 42,* 139-146.

Chhanwal, N., Anishaparvin, A, Indrani, D., Raghavarao, K.S.M.S., Anandharamakrishnan, C. (2010). Computational fluid dynamics (CFD) modeling of an electrical heating oven for bread-baking process. *Journal of Food Engineering, 100,* 452-460.

COMSOL (2008) *COMSOL Multiphysics Heat Transfer Module Model Library* [computer software manual]. Burlington, Massachusetts.

COMSOL (2010 a) *COMSOL Multiphysics Reference guide* [computer software manual]. Burlington, Massachusetts.

COMSOL (2010 b). *COMSOL Multiphysics User's Guide* [computer software manual]. Burlington, Massachusetts.

COMSOL (2010 c) *Heat Transfer Module User's Guide* [computer software manual]. Burlington, Massachusetts.

COMSOL (2010 d). *LiveLink for MATLAB User's Guide* [computer software manual]. Burlington, Massachusetts.

COMSOL (2010 e) *Model Library* [computer software manual]. Burlington, Massachusetts.

Cortella, G. (2007). CFD Aided Retail Cabinets Design. In D. W. Sun (Ed.), *Computational Fluid Dynamics in Food Processing* (pp. 84-99). New York: CRC Press.

Curcio, S. (2006). A FEM analysis of transport phenomenon occurring during vegetables drying. *Proceedings from COMSOL Users Conference 2006 Milano*.

Czuchajowska, Z., Pomeranz, Y., & Jeffers, H.C. (1989). Water Activity and Moisture Content of Dough and Bread. *Cereal Chemistry*, *66*, 128-132.

Denys, S., Pieters, J., & Dewettinck, K. (2007). CFD analysis of thermal processing of eggs. In D.W. Sun (Ed.), *Computational Fluid Dynamics in Food Processing* (pp. 347-380). NewYork: CRC Press.

Dvorak, P. (2006, August 16). Air doors not just hot air, CFD shows. *Machine Design*.

Farlow, S.J. (1993). *Partial differential equations for scientists and engineers*. New York: Dover Publications, Inc.

Geankoplis, C.J. (2003). *Transport processes and separation process principles* (*includes unit operations*), (4th ed.). New Jersey: Prentice-Hall.

Ghani, A.G.A. & Farid, M.M. (2007). Thermal sterilization of food using CFD. In D. W. Sun (Ed.), *Computational Fluid Dynamics in Food Processing* (pp 331-345). New York: CRC Press.

Hasatani, M., Arai, N., Katsuyama, H. Harui, H., Itaya, Y., Fushida, N., & Tatsukawa, N. (1991). Heat and mass transfer in bread during baking in an electric oven. In A.S. Mujumdar & I. Filková (Ed.), *Drying '91* (pp. 385 – 393). Amsterdam: Elsevier Science.

Hassanien, I.A., Shamardan, A., Moursy, N.M., & Gorla, R. S. R. (1999). Flow and heat transfer in the boundary layer of a micropolar fluid on a continuous moving surface. *International Journal of Numerical Methods for Heat & Fluid Flow*, *9*, 643-659.

Hemicube (computer graphics). (2007). Retrieved September 24, 2012 from (http://en.wikipedia.org/wiki/File:Hemicube_Unfold.gif)

Holman, J.P. (1990) *Heat transfer*, (7th ed.). New York: McGraw-Hill.

Howell, J. R. (2010). Section C: Factors from finite areas to finite areas; C-13 Rectangle to rectangle in a parallel plane *A catalog of radiation heat transfer configuration factors*, (3rd ed). Retrieved January 12, 2012 from: http://www.engr.uky.edu/rtl/Catalog/sectionc/C-13.html

Incropera, F.P. & DeWitt, D.P. (1990) *Fundamentals of heat and mass transfer*, (3rd ed.). New York: John Wiley & Sons.

Larson, J. (2010, September 20). *Using COMSOL 4.0a at Ohio Super Computer Center*. Columbus, Ohio.

Marcotte, M. (2007, August/September). Virtual oven to assist baking industry. *Food Quality*.

MATLAB: The Language of Technical Computing. (2011). Retrieved October 15, 2011 from http://www.mathworks.com/products/matlab/

Mirade, P.S., Daudin, J.D., Ducept, F., Trystram, & Clement, J. (2004). Characterization and CFD modeling of air temperature and velocity profiles in an industrial biscuit baking tunnel oven. *Food Research International*, *37*, 1031- 1039.

Mirade, P.S. (2007). CFD Prediction of the air velocity field in modern meat dryers. In D. W. Sun (Ed.), *Computational Fluid Dynamics in Food Processing* (pp. 223-246). New York: CRC Press.

Mondal, A., & Datta, A.K. (2008). Bread baking-a review. *Journal of Food Engineering*, *86*, 465-474.

Ohio Supercomputer Center (2010 a). Using the IBM Opteron 1350 at OSC. Columbus, Ohio.

Ohio Supercomputer Center. (2010 b). Using the IBM Opteron 1350 at OSC- Batch Processing. Columbus, Ohio.

Ohio Supercomputer Center. (2011). OSC at a glance. Retrieved November 28, 2011, from http://www.osc.edu/about/

Ohio Supercomputer Center (2012 a). Job Submission. Retrieved November 01, 2012 from https://www.osc.edu/supercomputing/batch-processing-at-osc/job-submission

Ohio Supercomputer Center (2012 b). Monitor and managing your job. Retrieved November 01, 2012 from http://www.osc.edu/supercomputing/batch-processing-at-osc/monitoring-and-managing-your-job

Ogawa, A. (2007). Psychrometric chart. Retrieved on April 19, 2012 from http://en.m.wikipedia.org/wiki/File:PsychrometricChart-SeaLevel-SI.jpg

Piazza, L., & Masi, P. (1997). Development of crispness in cookies during baking in an industrial oven. *Cereal Chemistry*, *74*, 135-140.

Shelton, D.P. (April, 2008). Air properties: temperature and relative humidity. Retrieved on April 05, 2012 from http://www.ianrpubs.unl.edu/pages/publicationD.jsp?publicationId=1000

Siegel, R., & Howell, J.R. (1981). *Thermal Radiation Heat Transfer*, (2nd ed.). New York: Hemisphere Publishing Company.

Strauss, D, & Azevedo, J.L.F. (2003). On the Development of an Agglomeration Multigrid Solver for Turbulent Flows. *Journal of the Brazilian Society of Mechanical Scientists and Engineers*, *25*, 315-324.

Sun, Da-Wen. (Ed.). (2007). *Computational fluid dynamics in food processing*. New York: CRC Press.

Tatham, Simon (2011). WinSCP. Retrieved November 01, 2012 from: http://winscp.net/eng/download.php

Therdthai, N., Zhou, W., & Adamczak, T. (2003). Two-dimensional CFD modeling and simulation of an industrial continuous bread baking oven. *Journal of Food Engineering*, *60*, 211-217.

Therdthai, N., Zhou, W., & Adamczak, T. (2004 a). Three-dimensional CFD modelling and simulation of the temperature profiles and airflow patterns during a continuous industrial baking process. *Journal of Food Engineering*, *65*, 599-608.

Therdai, N., Zhou, W., & Adamczak, T (2004 b). Simulation of starch gelatinization During baking in a travelling-tray oven by integrating a three-dimensional CFD model with a kinetic model. *Journal of Food Engineering*, *65*, pp 543-550.

Thorvaldsson, K., & Janestad, H. (1999). A model for simultaneous heat, water, and vapour diffusion. *Journal of Food Engineering*, *40*, 167-172.

Wang, L., & Sun, D.W. (2006). Heat and Mass Transfer in Thermal Food Processing. In D. W. Sun (Ed.), *Thermal Food Processing: new technologies and quality issues*. (pp. 35-72). Boca Raton, FL: CRC Press.

Wang, N., and Brennan, J. G., (1995). A mathematical model of simultaneous heat and moisture transfer during drying of potato. *Journal of Food Engineering*, *24*, 47-60.

Weinhold, I. (2008, November 1). Embedded FloEFD puts food on the table. *Desktop Engineering*.

Wong, S. Y., Weibiao Z., & Jinsong, H. (2006). Robustness analysis of a CFD model to the uncertainties in its physical properties for a bread baking process. *Journal of Food Engineering*, *77*, 784-791.

White, F. M. (1986). *Fluid mechanics*, (2nd ed.). New York: McGraw-Hill.

White, F.M. (2006). *Viscous fluid flow*, (3rd ed.). New York: McGraw-Hill.

Zhou, W., & Therdthai, N. (2007). Three-dimensional CFD modeling of a continuous industrial baking process. In D.W. Sun (Ed.), *Computational fluid dynamics in food processing* (pp. 287-312). New York: CRC Press.

APPENDIX A (MATLAB program, transient radiation simulation)

```
% This MATLAB program calculates the temperature rise of the food
% due to the radiation exchange in an enclosure. This is a transient
% analysis.

% smdeltat is the sum of the change in temperatures.

smdeltat = 0;

% t2 is the initial temperature of Surface 2, which is the surface of
the
% food.

t2 = 293.15;

% lla is the distance between Surface 2 and Surface 3, which is the
% surface of the surroundings; this is for the first enclosure
% problem (denoted by letter "a").

lla = .5-.5*.1;

% w2a is the width of Surface 2.

w2a = .1;

% w3a is the width of Surface 3.

w3a = .28-.5*.01-.5*.01;

ww3a = w3a/lla;

ww2a = w2a/lla;

% f23a is the view factor between Surfaces 2 and 3 in the first
% enclosure problem.

f23a = (((ww2a+ww3a)^2+4)^(.5)-((ww3a-ww2a)^2+4)^(.5))/(2*ww2a);

% f21a is the view factor between Surfaces 2 and 1 in the first
% enclosure problem; Surface 1 is part of the top heating element.

f21a = (1-f23a)/2;

% f24a is the view factor between Surfaces 2 and 4 in the first
% enclosure problem; Surface 4 is part of the bottom heating
% element.

f24a = f21a;
```

```
% The "for" loop calculates the radiosity of Surface 2 in the first
% enclosure problem, then the heat transferred to Surface 2 in the
% first enclosure problem; it then calculates the radiosity of
% Surface 2 in the second enclosure problem, then the heat transferred
% to Surface 2 in the second enclosure problem. The change in
temperature
% of Surface 2 is then calculated, and this change is added to the
% preceding temperature of Surface 2. The increase in temperature is
% then added to the previous increase in temperature, to eventually
% arrive at a total sum increase in temperature. This loop runs from 1
% second to 240 seconds.

for time = 1: 1 : 240

% eb2 is the blackbody emmissive power of Surface 2.

eb2 = (5.67e-8)*(t2^4);


% j3 is the emmissive power of Surface 3, which is equal to that
% Surface's blackbody emissive power.

j3= (5.67e-8)*(293.15^4);

% j1 is the emissive power of Surface 1, which is equal to that
% Surfaces' blackbody emissive power.


j1= ( 5.67e-8)*(533.15^4);

% j4 is the emissive power of Surface 4.

j4 = j1;

% e2 is the emissivity of Surface 2.

e2 = .9;

% a2 is the area of Surface 2.

a2 = .1*1;

% j2a is the radiosity of Surface 2 for the current time step in the
% first enclosure problem.

j2a= -(e2*(eb2-f21a*j1-f23a*j3-
f24a*j4)+f21a*j1+f23a*j3+f24a*j4)/(e2*(f21a+f23a+f24a-1)-f21a-f23a-
f24a);
```

```
% halfq2a is half of the heat transferred to Surface 2 from the
% other surfaces in the first enclosure problem; the "half" stems
% from the fact that there are two such first enclosures.


halfq2a = -(eb2-j2a)/((1-e2)/(e2*a2));

% ------------------------------------------------------------------
----

% Now look at the second enclosure problem, denoted by "b" in its
% respective variables.


% 11b is the distance between Surface 1 (the heating element surface)
% and Surface 2 (the food surface) in the second enclosure problem.

l1b = .14-.05-.005;

% w2b is the width of Surface 2 in the second enclosure problem.

w2b = .1;

ww2b = w2b/l1b;

% w1b is the width of Surface 1 in the second enclosure problem.

w1b = 1;

ww1b = w1b/l1b;

% f21b is the view factor between Surfaces 1 and 2 in the second
% enclosure problem.


f21b = (((ww2b+ww1b)^2+4)^(.5)-((ww1b-ww2b)^2+4)^(.5))/(2*ww2b);

% f23b is the view factor between Surfaces 2 and 3 in the second
% enclosure problem.

f23b = 1-f21b;

% j2b is the radiosity of surface 2 for the current time step in the
% second enclosure problem.

j2b = -(e2*(eb2-f21b*j1-f23b*j3)+f21b*j1+f23b*j3)/(e2*(f21b+f23b-1)-
f21b-f23b);
```

```
% halfq2b is half of the heat transferred to Surface 2 from the
% other surfaces in the second enclosure problem; the "half" stems
% from the fact that there are two such second enclosures.

halfq2b = -(eb2-j2b)/((1-e2)/(e2*a2));

% end sub-analysis of second enclosure problem

% ------------------------------------------------------------------------
----


% deltat is the change in temperature of Surface 2; this corresponds
% to Equation (3-53).

deltat = 1*(halfq2b*2+halfq2a*2)/(380*.1*.1*1941);


% Display the time (in seconds) in the MATLAB Command Window.

disp ('For time (in seconds)')
disp (time)

% The value of the temperature of Surface 2 is updated in the next
line.

t2 = t2+deltat;

% Display the change in temperature (in Kelvin) of Surface 2 for the
% current time step in the MATLAB Command Window.

disp ('deltat (in Kelvin) is')
disp (deltat)

% The value of the sum of the changes in temperature of Surface 2 is
% updated in the next line.


smdeltat = deltat + smdeltat;

% Display the latest sum of changes in temperature (in Kelvin) of
Surface 2
% in the MATLAB Command Window.


disp ('sumdeltat (in Kelvin) is')
disp (smdeltat)


% End the "for" loop
```

```
end
% End of MATLAB Program
```

APPENDIX B (MATLAB output, transient radiation simulation)

(note: the nomenclature for this output is shown in APPENDIX A)

```
For time (in seconds)

     1


deltat (in Kelvin) is

    0.1727


sumdeltat (in Kelvin) is

    0.1727

.

.

.

For time (in seconds)

   240


deltat (in Kelvin) is

    0.1591


sumdeltat (in Kelvin) is

   39.8967


>>
```

APPENDIX C (MATLAB program and output, radiosity calculation)

```
This MATLAB program calculates the initial radiosity for the models in
Tables 6.6, 6.7, and 6.8. This program uses Equation (2-21) with view
factors, temperatures, and dimensions from Section 3.1.1, but with an
emissivity from Section 3.1.2.

syms j2;


solve ('(418.7-j2)/((1-0.9)/(0.9*0.1*1))=(j2-4581.2)/(1/0.07461)+(j2-
418.7)/(1/0.02539)', 'j2')
```

```
>> August_22_2011_Solve_for_Radiosity


ans =


729.264125
```

APPENDIX D (MATLAB program, conduction model)

```
% This MATLAB program calculates the temperature distribution
% in the dough/bread when radiation is present from a heating element.
% Heat travels through the dough/bread by conduction.
% This simulation is based on this dissertation's Section 3.2.3
% This is a one-dimensional numerical method, based on Holman (1990).

% t1p through t5p are the first the initial temperatures (in K) of the
% nodes one though five, then the previous temperatures of the nodes
% during the simulation. These nodes correspond to discrete locations
% within the dough/bread.
t1p=20+273.15;
t2p=20+273.15;
t3p=20+273.15;
t4p=20+273.15;
t5p=20+273.15;

% tsur is the temperature of the surroundings (the oven), in K
tsur=140+273.15;

% trad is the temperature of the heating element, in K
trad=260+273.15;

% sigma is the Stefan-Boltzmann constant, in W/((m^2)*(K^4))
sigma=5.67e-08;

% rho is the density of the dough/bread, in kg/m^3
rho=380;

% cp is the heat capacity at constant pressure of the dough/bread,
% in J/(kg*K)
cp=1941;

% deltax is the distance between nodes, in m
deltax=0.025;

% deltatau is the time step, in s
deltatau=10;

% time is the current time
time=10;

% k is the thermal conductivity of the dough/bread, in W/(m*K)
k=0.1133;


cc1=rho*cp*deltax/2;
cc5=rho*cp*deltax/2;
cc2=rho*cp*deltax;
```

```
cc3=rho*cp*deltax;
cc4=rho*cp*deltax;

% epsilon is the emissivity of the dough/bread
epsilon=0.9;

% in the while loop, the succeeding values (t1pplus1, etc.) of the
% temperatures of the
% five nodes are calculated. The nodes' values are updated, and the
% time is increased by 10 seconds. The simulation runs for a
% computational time of 240 seconds.
while time < 250

t1pplus1=deltatau/cc1*(sigma*epsilon*(tsur^2+t1p^2)*(tsur+t1p)*
tsur+k/deltax*t2p)+(1-
deltatau/cc1*(sigma*epsilon*(tsur^2+t1p^2)*(tsur+t1p)+k/deltax))*t1p;

t5pplus1=deltatau/cc5*(sigma*epsilon*(trad^2+t5p^2)*(trad+t5p)*trad+k/d
eltax*t4p)+(1-
deltatau/cc5*(sigma*epsilon*(trad^2+t5p^2)*(trad+t5p)+k/deltax))*t5p;

t2pplus1=deltatau/cc2*(k/deltax)*(t1p+t3p)+
(1-2*deltatau/cc2*(k/deltax))*t2p;

t3pplus1=deltatau/cc3*(k/deltax)*(t2p+t4p)+
(1-2*deltatau/cc2*(k/deltax))*t3p;

 t4pplus1=deltatau/cc4*(k/deltax)*(t3p+t5p)+
(1-2*deltatau/cc3*(k/deltax))*t4p;


disp('For time (in seconds) is')
disp(time)
disp('t1pplus1 (in Kelvin) is')
disp(t1pplus1)
disp('t2pplus1 (in Kelvin) is')
disp(t2pplus1)
disp('t3pplus1 (in Kelvin) is')
disp(t3pplus1)
disp('t4pplus1 (in Kelvin) is')
disp(t4pplus1)
disp('t5pplus1 (in Kelvin) is')
disp(t5pplus1)

    t1p=t1pplus1;
    t2p=t2pplus1;
    t3p=t3pplus1;
    t4p=t4pplus1;
    t5p=t5pplus1;

time=time+deltatau;
end

% the average of the final temperatures of the nodes is calculated
```

```
% as average_tplus1, in K
average_tplus1=(t1pplus1+t2pplus1+t3pplus1+t4pplus1+t5pplus1)/5;
disp('average tplus1 (in Kelvin) is')
disp(average_tplus1)


% the difference between the initial and average final temperature of
% the dough/bread is calculated as change_tplus1, in K
change_tplus1=average_tplus1-293.15;
disp('change in temperature plus1 (in Kelvin) is')
disp(change_tplus1)
```

APPENDIX E (MATLAB output, conduction simulation)

```
>> Conduction_program_July_15_2012

For time (in seconds) is

   10


t1pplus1 (in Kelvin) is

  294.3539


t2pplus1 (in Kelvin) is

  293.1500


t3pplus1 (in Kelvin) is

  293.1500


t4pplus1 (in Kelvin) is

  293.1500


t5pplus1 (in Kelvin) is

  297.2133


.

.

.

For time (in seconds) is

   240
```

t1pplus1 (in Kelvin) is

318.6887

t2pplus1 (in Kelvin) is

293.8790

t3pplus1 (in Kelvin) is

293.2077

t4pplus1 (in Kelvin) is

295.5911

t5pplus1 (in Kelvin) is

378.0162

average tplus1 (in Kelvin) is

315.8765

change in temperature plus1 (in Kelvin) is

22.7265

>>

APPENDIX F (MATLAB program, moisture model)

```
% This program calculates the rate of drying in the constant-rate
% period when convection, radiation, and conduction heat
% transfer are present.


% t is the temperature of the air stream in degrees Celsius
t=120;

% tr is the temperature of the heating element in degrees Celsius
tr=260;

% tsguess is the guess of the surface temperature in degrees Celsius
tsguess=55;

disp (t)

% hs is the saturation humidity (dimensionless)
hs=0.115;

% h is the humidity (dimensionless)
h=0.05;

% lambdas is the latent heat of vaporization at the saturation
% temperature, in J/kg
lambdas=2370700;

% cs is the humid heat of the air-water vapor mixture,
% in J/kg dry air * K
cs=(1.005+1.88*h)*1000;
disp(cs);

% vel is the air stream velocity, in m/s
vel=0.61;

% vh is the humid volume of the air-water vapor mixture,
% in m^3/kg dry air
vh=(0.00283+0.00456*h)*(t+273.15);

% rho is the density of the air and water vapor mixture
rho=1+h/vh;

% g is the mass velocity of the air-water vapor stream,
% in kg/h * m^2
g=vel*rho*3600;

% hc is the convective heat transfer coefficient, in W/ (m^2 * C),
% or W/ (m^2 * K)
hc=0.0204*g^0.8;
disp(hc);
```

```
% zm is the metal thickness in meters
zm=0.002;

% km is the thermal conductivity of the metal in W/(m * K)
km=52;

% zs is the solid thickness in meters
zs=0.10;

% ks is the thermal conductivity of the solid in W/(m * K)
ks=0.1133;

% uk is the overall heat transfer coefficient, in W/m^2 * K
uk=1/(1/hc+zm/km+zs/ks);

% emissivity is the emissivity (dimensionless) of the surface of the
solid
emissivity=0.9;

% hr is the radiation heat transfer coefficient, in W/(m^2 * K)
hr=emissivity*5.676*(((tr+273.15)/100)^4....
-((tsguess+273.15)/100)^4)....
/(tr+273.15-(tsguess+273.15));
disp(hr);

% ts is the saturation temperature, in degrees Celsius
ts=(cs*(hc*t+hr*tr+t*uk)...
+(h-hs)*hc*lambdas)/(cs*(hc+hr+uk));
disp(ts);

% rc is the rate of drying, in kg/h * m^2
rc=((hc+uk)*(t-ts)+hr*(tr-ts))*3600/lambdas;
disp(rc);
```

APPENDIX G (MATLAB output, moisture simulation)

(note: the nomenclature for this output is shown in APPENDIX F)

```
>> February_09_2012_moisture_analysis

    120 (this is the temperature of air stream in degrees C)

      1099 (this is the humid heat of the air-water vapor mixture, in J/kg dry air *C)

    9.9333 (this is the convective heat transfer coefficient, in W/m^2 *C)

   17.2444 (this is the radiation heat transfer coefficient, in W/m^2 *C)

  156.2279 (this is the saturation temperature in degrees C)

    2.1150 (this is the rate of drying, in kg/(hour *m^2)

>>
```